# Synthesis of Nitrogen Alloyed Steels by Arc Melting Technique for Improved Properties



**Zahra Nazar**

**Reg. # 00000172920**

A thesis submitted in the partial fulfillment of requirements for the degree of Master of Science in chemistry

Supervised by

**Dr Azhar Mahmood**

Department of Chemistry

School of Natural Sciences

National University of Sciences and Technology

Islamabad, Pakistan

**2018**

# National University of Sciences & Technology

## MS THESIS WORK

We hereby recommend that the dissertation prepared under our supervision by: <u>ZAHRA NAZAR</u>, Regn No. <u>00000172920</u> Titled: <u>Synthesis of Nitrogen alloyed Steels by Arc Melting Technique for improved properties</u> be accepted in partial fulfillment of the requirements for the award of **MS** degree.

### Examination Committee Members

1. Name: <u>Dr. Habib Nasir</u>                 Signature: _____

2. Name: <u>Dr. Zuhair S. Khan</u>                 Signature: _____

External Examiner: <u>Dr. Shafiq Ur Rehman Qureshi</u>  Signature: _____

Supervisor's Name: <u>Dr. Azhar Mahmood</u>      Signature: _____

Co-Supervisor's Name: <u>Dr. Zahida Malik</u>      Signature: _____

_____
Head of Department

17/09/18
Date

### COUNTERSINGED

Date: 17/09/18

_____
Dean/Principal

# THESIS ACCEPTANCE CERTIFICATE

Certified that final copy of MS thesis written by **Ms. Zahra Nazar,** (Registration No. **00000172920**), of **School of Natural Sciences** has been vetted by undersigned, found complete in all respects as per NUST statutes/regulations, is free of plagiarism, errors, and mistakes and is accepted as partial fulfillment for award of MS/M.Phil degree. It is further certified that necessary amendments as pointed out by GEC members and external examiner of the scholar have also been incorporated in the said thesis.

Signature: _____

Name of Supervisor:  Dr. Azhar Mahmood

Date: _____ 17/09/18 _____

Signature (HoD): _____

Date: _____ 17/09/18 _____

Signature (Dean/Principal): _____

Date: _____ 17/09/18 _____

*Dedicated*

*To*

*My parents*

*My Father for his encouragement, hard work and faith in me*

*My mother*

*For her love and prayers*

# Table of Contents

# List of Abbreviations

| | | | |
|---|---|---|---|
| Al | Aluminum | ESR | Electro slag remelting |
| AISI | American Iron and Steel Institute | EDX | Energy Dispersive X-ray Spectroscopy |
| Ar | Argon | EDM | Electro discharge machining |
| AE | Auger electrons | FCC | Face centered cubic |
| Agcl | Silver chloride | $Fe_2O_3$ | Iron Oxide |
| Au | Gold | Fe | Iron |
| $Al_2O_3$ | Alumina | g | grams |
| Ag | Silver | h | Hours |
| B | Boron | HNS | high nitrogen stainless steel |
| BSE | Back scattered electrons | Hv | Vickers Hardness |
| BOD | Ball on disk | HNAS | High nitrogen austenitic steels |
| BCC | Body centered cubic | IBAD | Ion assisted deposition beam |
| cm | Centi meter | kv | Kilovolt |
| Cr | Chromium | K | Kelvin |
| Cu | Copper | KW | Kilo watt |
| $CH_4$ | methane | ml | Mili litter |
| ºC | Degree Celsius | Mo | Molybdenum |
| $co_2$ | Carbon dioxide | Mpa | Mega Pascal |
| C | Carbon | Mg | Magnesium |

| | | | |
|---|---|---|---|
| min | minutes | ZRA | Zero Resistance Ammeter |
| mm | Milli meter | | |
| Ni | Nickel | | |
| N | Nitrogen | | |
| NaCl | Sodium chloride | | |
| P | Phosphorus | | |
| PECVD | Plasma enrich chemical vapor deposition method | | |
| Pt | Platinum | | |
| PACVD | Plasma-assisted chemical vapor deposition | | |
| SEM | Scanning Electron Microscopy | | |
| Sec | Seconds | | |
| sccm | Standard cubic centimeter per min | | |
| SE | Secondary electrons | | |
| SS | Stainless steel | | |
| SiC | Silicon Carbide | | |
| Si | Silicon | | |
| Ti | Titanium | | |
| TiN | Titanium nitride | | |
| Wt% | Weight Percentage | | |
| WHA | World Health Association | | |

# List of Figures

# List of Tables

# Acknowledgements

# Abstract

Incorporation of nitrogen into 30CrMnSiA and 316 Stainless Steel was executed by arc melting furnace at 3500ºC by altering the nitrogen pressure from 0.1bar to 0.3bar. Characterization techniques involved the optical microscopy (OM) for investigation of microstructure, X-ray diffraction and SEM (Scanning Electron Microscopy) with EDX (Energy Dispersive X-ray Spectroscopy).It was suggested that nitrogen incorporation into 30CrMnSiA and 316 stainless Steel was a favorable way to attain high hardness.Nitrogen comprising steel samples exhibited superior corrosion resistance as compared to the raw steel specimens when they are examined in electrolyte solution of 3.5wt% NaCl. Tafel plots and polarization resistance results revealed that the corrosion resistance from argon melted steel sample to high nitrogen incorporated samplewas improved from 14.13mpy to 6.70mpy, 0.06606mpy to 0.02677mpy and from 12.28 to 4.81, 0.02mpy to 0.010mpy for 30CrMnSiA and for 316ss respectively. These results suggest that nitrogen is beneficial for anticorrosion properties in different media.

By linking the benefits of nitrogen added 30CrMnSiA and for 316SS, low density, high hardness and more corrosion resistant steel as compared to presently used raw steel ,the recently developed nitrogen incorporated steel is a trustworthy substitute for marine application.

# Chapter 1

# Introduction

Henry Bessemer first invented steel in 1856.Steel is an iron and carbon alloy that contains lower than 2% C, 1% Mn and little amount of other elements like Si, P, S, Mo and Cr that control the properties of different grades of steels **[1]**. But some elements added are favorable and some are damaging the strength and properties of steel. According to WHA (World Health Association) steel have 3500 various grades on the basis of physical, chemical and environmental properties. Different grades of steels are present that differentiate them on the basis of their properties.

## 1.1 Steel and its types

According to AISI (American iron and steel institute), depending on the chemical composition there are following types of steel:

- Tool steel

- Alloy steel

- Carbon steel

- Stainless steel

**Tool steels** have Co, V and W in different quantities to enhance their heat resistance and durability. **Alloy steels** have different alloying elements like Cu, Al, Si, Ti, Cr and Ni in adjustable amounts for the purpose of enhancing steel properties like corrosion resistance, wear resistance, ductility and strength.

There are different groups of **carbon steel** depending on their carbon content:

- Low carbon (0.3% C)

- High carbon (0.6%C)

- Medium carbon (more than 0.6%C)

**Stainless steel**was first discovered by Harry Brearley while he was investigating various types of steels. He observed that steel with 13% Cr has not undergone corrosion after a time period of several months. Stainless steels have thousands of applications in our daily life for example domestic (microwave oven, razor blades, drums and cutlery), Oil and gas, transport, pharmaceutical, chemical, engineering, medical, water(hot water tanks) and food**[2].**
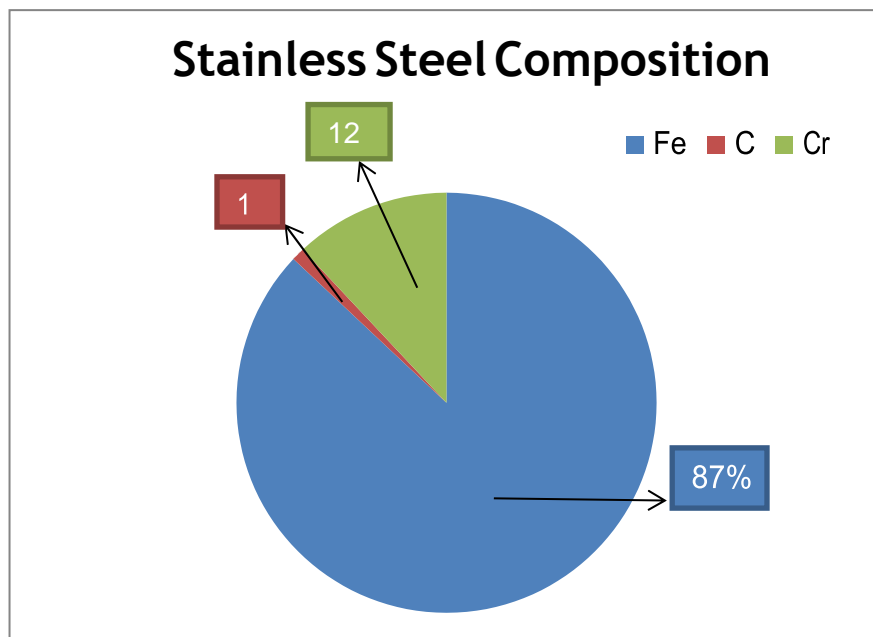


**Figure 1.1: Stainless steel composition**

Stainless steel contains iron as well as about 16% Cr; this chromium is significant for enhancing corrosion resistant property of stainless steel. Cr makes a thin layer of oxide on steel surface this layer is named as passive layer. This passive layer is the protection layer of steel from corrosion. Therefore we can say that steel with the high amount of Cr

has high corrosion resistant property. Stainless steel also contains various other elements added for the purpose of enhancing the other properties of stainless steels such as wear resistance, strength, formability and ductility.
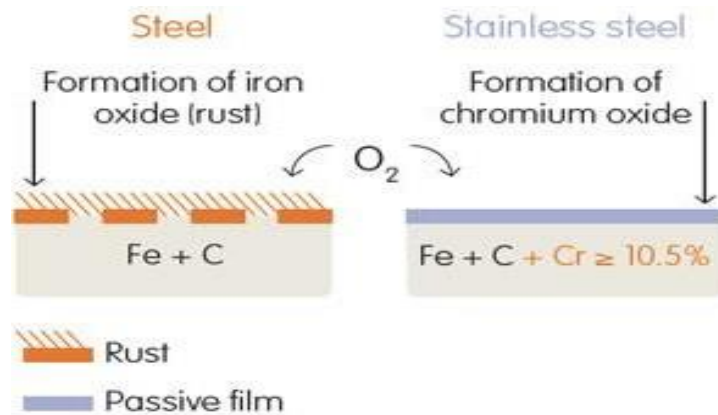


**Figure1.2 Demonstration of rust and passive film formation**

Three major types of microstructure exist in steel such as martensitic, austenitic and ferritic. The alloying elements are reason for the amendment in crystallographic arrangements such as BCC, FCC and stability of $\alpha$ and $\gamma$ phases. Some specific carbon steels find application in surgical tools which need high hardness and corrosion resistance. By the quenching method such steels are hardened that result in the alteration of austenite to martensite [3]. On the basis of crystalline structure stainless steel is divided into following types:

- Ferritic stainless steel
- Austenitic stainless steel
- Martensitic stainless steel
- Duplex stainless steel

**Table 1: List of types of steel**

| Type | Corrosion resistance | Hardness | Magnetism | Hardenable with thermal treatment | Weldability |
|------|----------------------|----------|-----------|-----------------------------------|-------------|
| Martensitic | Low | High | Yes | Yes | Poor |
| Ferritic | Good | Medium-Low | Yes | No | Limited |
| Austenitic | Excellent | High | No | No | Excellent |
| Duplex | Excellent | High | Yes | No | Good |

All these have various compositions (Table 2) and properties (Table 1). **Ferritic steels** have small amount of Ni, C(less than 0.1%) and Cr (12-17%) also with other alloying elements. These are magnetic steels. **Austenitic steels** are not magnetic in nature and have Cr, Ni and carbon. **Martensitic steel** have Cr (11-17%), Ni (0.4%) and carbon greater than 1.2%C. these steels are magnetic in nature.

**Table 2: Composition of various types of Steel**

| Types | Chromium | Nickel | Carbon |
|-------|----------|--------|--------|
| Ferritic | 11.5-27% | 0 | 0.2%Max |
| Austenitic | 16-26% | 7-22% | 0.25% |
| Martensitic | 11.5-27% | 0-2.5% | 0.15-1.2% |

Stainless steel is although very corrosive resistant as compared to the ordinary alloy steels. We can say that stainless steel is stain-less, it's not stain impossible. Thus it can undergo corrosion. Stainless steel in the normal environmental conditions will not

undergo corrosion for example in the domestic use. But in the harsh environmental conditions such as marine or acidic environment, stainless steel may undergo the process of corrosion.

## 1.1.2. Corrosion

The continuous deterioration of a metal by electrochemical or chemical reaction with the environments is corrosion. Corrosion affects the properties of material such as strength, mechanical properties and form. We though select stainless steel as stainless steel is resistant to corrosion but not immune to corrosion (Figure 1.3). But the anticorrosive property of stainless steel depends upon the harshness of the surroundings and the chemical composition.
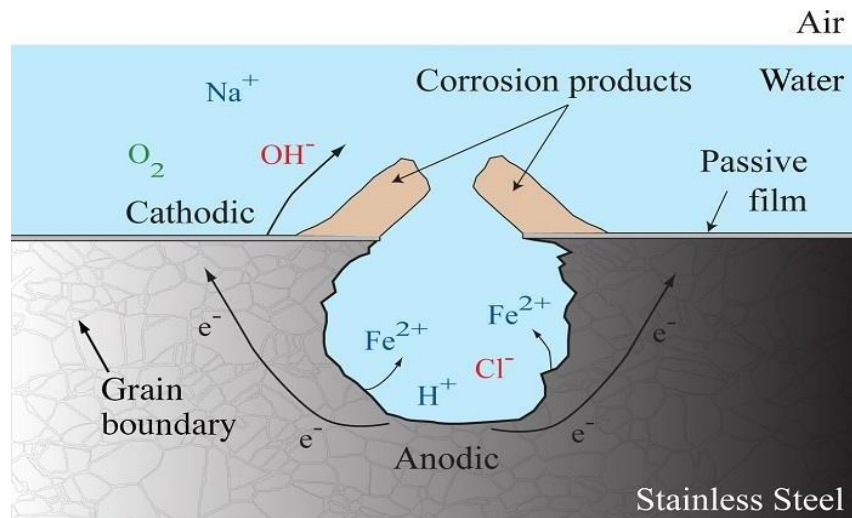


**Figure1. 3: Demonstration of corrosion in steel**

Thin passive film formed on the surface of stainless steel makes the stainless steel corrosion resistant in the presence of oxidizing environment. If the steel has minimum amount of 10.5% Cr, passive film sticks strongly to the surface of metal and halts the electrochemical reactions. These reactions are responsible for the corrosion and guard metal from the relating atmosphere. Many factors such as pH, fabrication method, temperature, chemical environment and impurity affect corrosion behavior of steel. A rod of iron undergoes corrosion more swiftly due to the absence of Cr passive layer and oxidation of iron in aquatic environment (Figure 1.4).
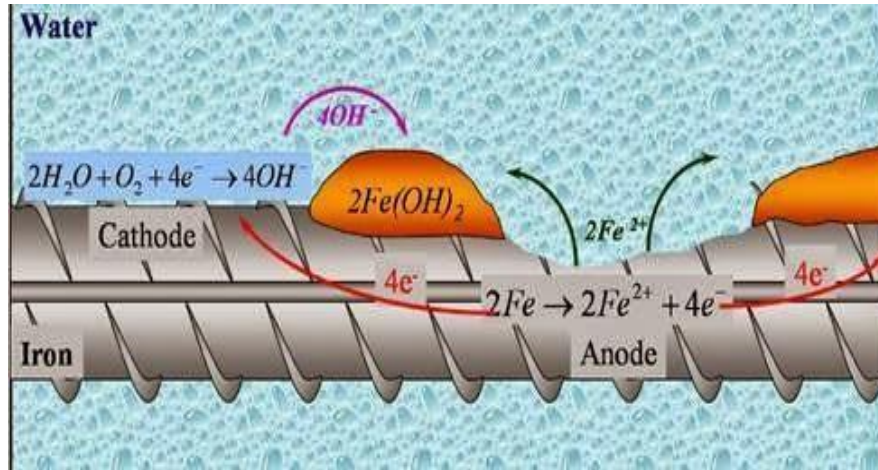
**Figure1. 4:Illustration of corrosion in iron rod**

## 1.1.3 Types of Corrosion

There are two categories of corrosion such as wet corrosion and high temperature corrosion. We have many common types of corrosion **[4].**

### General Corrosion

This type of corrosion is due to the interaction of some chemicals such as acids for example hydrochloric acid and sulphuric acid that damage the passive layer of steel at some specific concentration.

### Pitting Corrosion

Chemical species can attack the passive layer; one of the common is chloride ion that is present in the daily use materials such as bleaching powder and table salt. Pitting corrosion can be evaded by preventing our stainless steel from long term interaction with these detrimental chemicals. We can also select such grade of steel that is more attack resistant (Figure 1.5).
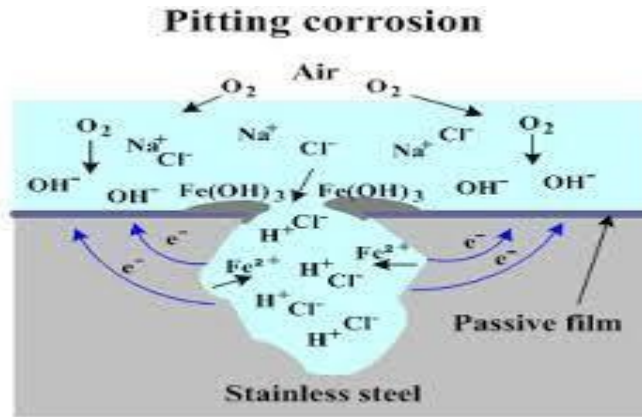
**Figure1. 5: Pitting corrosion demonstration**

## Stress Corrosion Cracking

This type of corrosion rarely happens and requires chloride ions and corrosive species to occur (Figure 1.6).
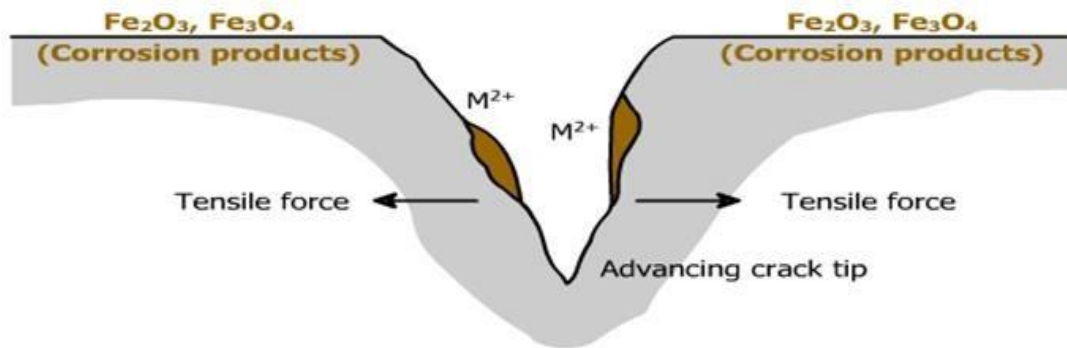


**Figure1. 6: Schematic of stress corrosion cracking**

## Crevice corrosion

The source of oxygen is mandatory to confirm that passive layer can establish on the surface of metal or not (Figure 1.7). This type of corrosion is prevented by closing crevices by a sealant also we can select steel with grade of more corrosion resistance.
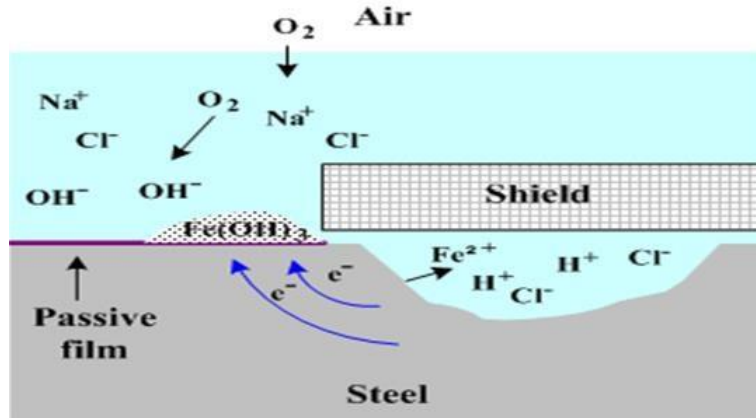
**Figure1. 7: Representation of Crevice corrosion**

## Intergranular Corrosion

Steel with more carbon can have this type of corrosion. This high level of carbon conglomerates with the Cr and form the chromium carbide (Figure 1.8). This formation of chromium carbide occurs at a specific temperature.
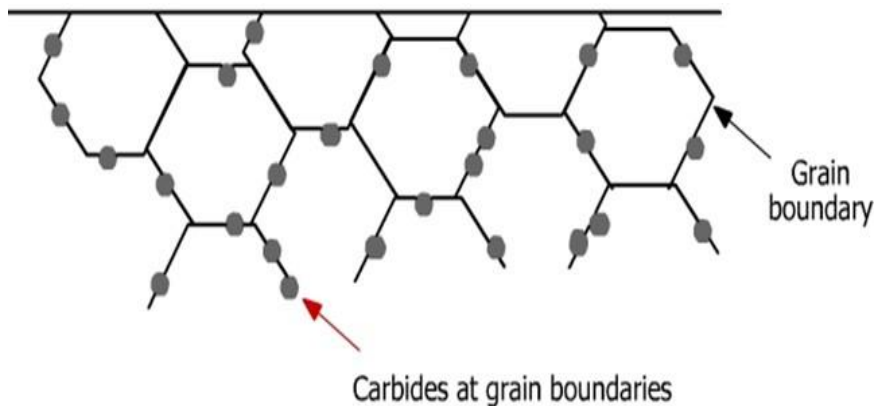


**Figure1.8: corrosion at grain boundaries due to regions of Cr depletion**

## 1.2.    Characterization Techniques

### 1.2.1. X-Ray powder diffraction (XRPD)

The phenomenon of X-ray diffraction was discovered by Max Von Laue in 1912[5]. X-ray powder diffraction is a powerful non-destructive analytical technique mostly used for the phase identification of a crystalline material also for sample purity measurement

and can provide information on unit cell dimension. X-ray powder diffraction today is a common technique to study atomic spacing and crystal structure. It offers information on crystal texture, strain, grain size, crystallanity and crystal flaws. The investigated material is strongly homogenized, ground and descriptive bulk composition is determined. The constructive interference of monochromatic x-rays and a crystalline sample take place in x-ray diffraction phenomenon. A cathode ray tube is used to generate x-rays and then sieved to produce monochromatic radiations. These rays are then collimated to concentrate and then focused on the sample. The interaction of incident rays with the sample produces phenomenon of constructive interference. This happens when circumstances fulfill Bragg's law (Figure 1.9).

$$n\lambda = 2d\sin\theta$$

Here n is an integer, $\lambda$ is the wavelength of x-rays, d is the separation between atomic planes and $\theta$ is the diffraction angle.
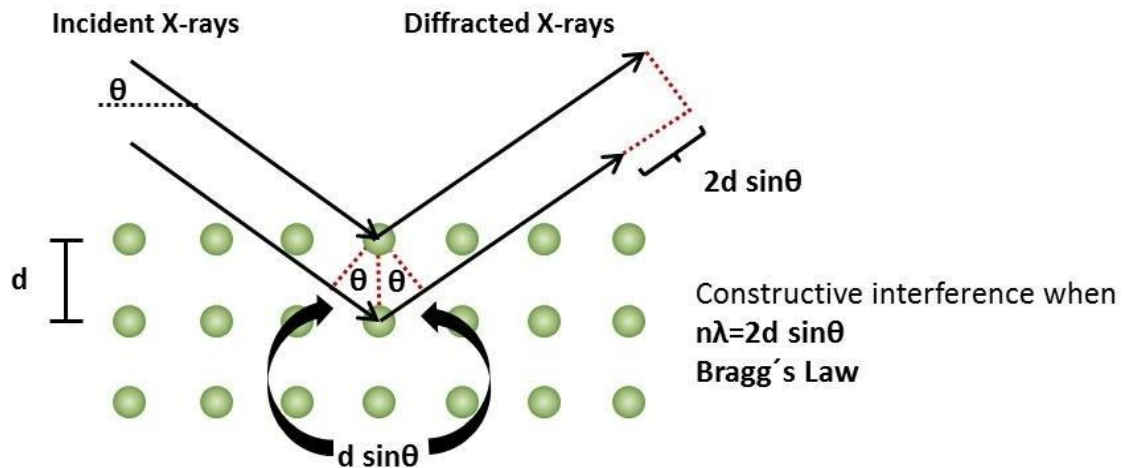


**Figure1.9: Illustration of Bragg's Law**

Bragg's law shows the relation of wavelength of electromagnetic radiations to the lattice spacing in a crystalline specimen and diffraction angle. The diffracted x-rays are thenidentified, handled and calculated. Diffraction peaks conversion to d-spacing

permits the identification of composite because each composite has a set of characteristic d-spacing.

## Construction and working of XRPD

X-ray diffractometer consists of three simple parts, x-ray tube, sample holder and a detector [6]. Filament is heated to produce electrons in the cathode ray tube. Electrons are then accelerated by applied voltage followed by their bombardment on the target material (Cu, Fe, Mo, Cr).When electrons have sufficient energy to remove inner shell electrons of the target material, characteristic X-rays are generated with broad spectra of wavelength. The monochromater is used to filter the polychromatic X-rays which are then collimated and focused onto the sample. The intensity of reflected X-rays is recorded as the sample and detector is rotated. The sample rotates in the route of the collimated X-ray beam at an angle θ, while the detector is at a distance to collect the diffracted x-rays and rotates at an angle of 2θ. An instrument named as Goniometer is used to maintain the angle and to rotate the sample. When the diffracted beam reaches the detector, software processes it as a count rate. In JCPDS, the achieved results are matched with thereference database and the crystallographic information can be achieved. Figure 1.10 shows the schematic diagram of XRPD.
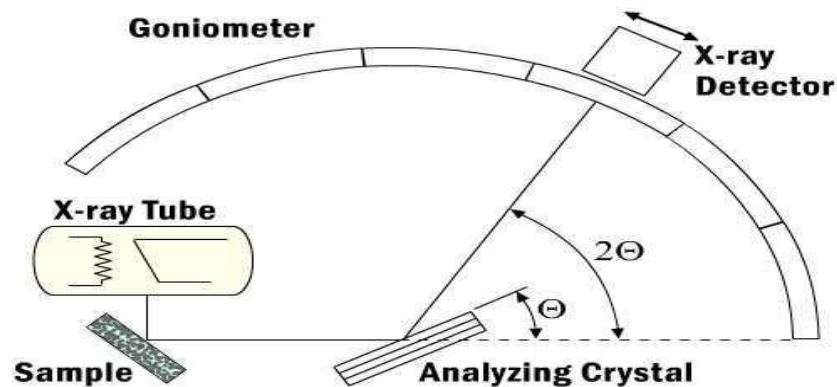


**Figure1.10: Schematic representation of X-Ray Powder Diffraction**

**Uses and Applications of X-Ray Powder Diffraction**

XRPD is an analytical technique that can be used for the characterization of crystalline phases and typically for the non-destructive determination of unknown materials. XRPD provides information on structure imperfections, lattice parameters, crystal alignment, crystalline size, atomic arrangement and various other properties of crystalline material. Due to its versatility and precision in providing maximum structural information about sample, XRPD is used in nearly every single field of life**[7].**

## 1.2.2  Optical Imaging Microscopy

OIM (Optical imaging microscopy) is a technique for the investigation of the surface of studied sample. Optical microscope can magnify an image of small subjects using a combination of light and a system of lenses. The more it is clearer the more specifics we perceive. Optical microscope depends on the light in the visible spectrum to image the topography of the sample down to the micron range. Mechanical properties of the metals and alloys are greatly influenced by their microstructures.

## Construction and working of optical microscope

Optical microscope uses focused light and arrangement of lenses to magnify the image of observed specimen. Optical microscope consists of ocular lens, objective lens, slide holder, stage, condenser lens, light, coarse adjustment and fine adjustment knob. Stage is the place that holds the specimen that can be moved in upward and downward directions to adjust the focus. To focus the light source through the sample and into the objective lens a condenser lens is used. Light from the mirror is reflected through the object to be observed that forms the first magnification. Through the eye piece lens, the image formed by objective lens is again magnified that act as simple magnifying glass. (Figure 1.11)
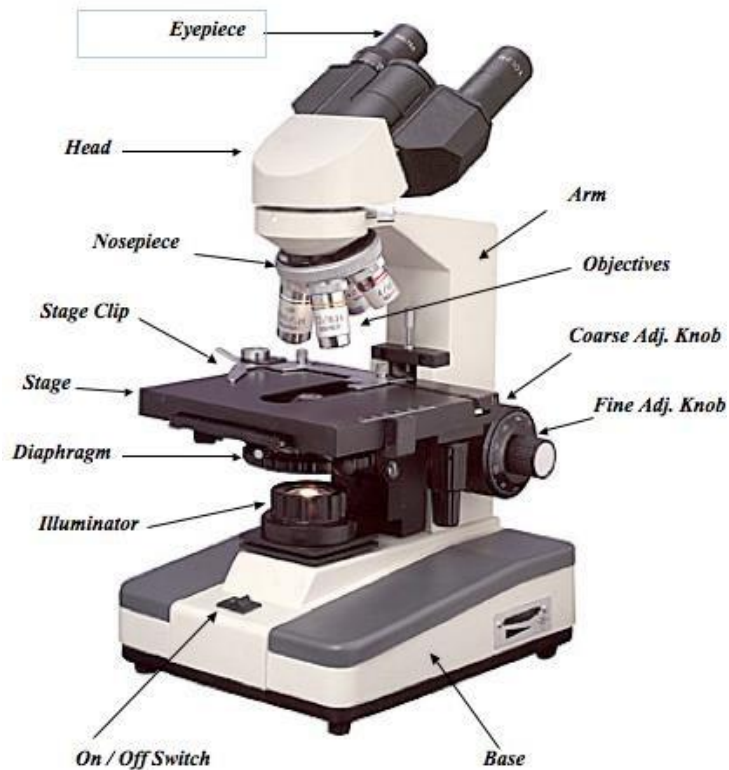
**Figure1.11: Labeled diagram of optical microscope**

Uses and applications of optical microscope

Optical microscopeis used for accuracy measurement. Optical microscopy is used in almost every field of life such as medical diagnosis, biotechnology, research, nanophysics, microelectronics andchemistry. Optical microscope can be used to identify the rock type, determine the crystallization sequence and deformation in crystal structure **[8].**

## 1.2.3 Scanning electron microscopy

In 1937 Manfred von Ardenne invented scanning electron microscope. SEM produces image of a sample by scanning the surface with a focused beam of high energy electron. This results in the interaction of electrons with the atoms in the sample that produces variety of signals that divulge the information about the sample composition, topography and crystalline structure. SEM reveals the levels of information and complexity that is unreachable by light microscopy. For the investigation of a material, SEM can achieve

aresolution down to 1nm. For the investigation through SEM, the tested specimen must be conducting otherwise non conducting material is coated by a thin layer of gold, aluminum orgraphite**[9].**

## Construction and working

Scanning electron microscope consists of a microscopic column that includes the electron gun at the top of the column, down which the electron beam travels and a sample chamber at the base. Thermionic electron gun consists of three parts the filament, the anode and wehnelt cap. By the applied voltage, thermoelectrons produced by the filament are accelerated among the filament and the anode. This produces an electron beam that travels down the microscopic column. The electron column thus focuses and lightens the sample by means of electron beam that is produced by electron gun. Secondary and backscattered electrons are generated and identified as the beam is scanned over the sample. An image is formed by intensifying and moderating the brightness of the identified electron signals. Condenser lens of the magnetic lens system can control the intensity of electron beam that arrives the sample. The objective lens is capable of bringing the electron beam into focus on sample. To reduce or exclude scattered electrons, objective lens aperture is used. To achieve high resolution secondary electron images, an ideal aperture diameter should be designated. A pair of scanning coils is used to deflect the electron beam in X and Y axes. For enhanced resolution and a particular area analysis holder can be skewed, revolved and moved in Z directions. Secondary electron detector is positioned at the back of thespecimen. An electronic signal is produced when these secondary electrons reach the detector. This signal is amplified and converted into a digital signal perceived on the display unit for more processing **[10].** Figure 1.12 shows the different components of SEM.
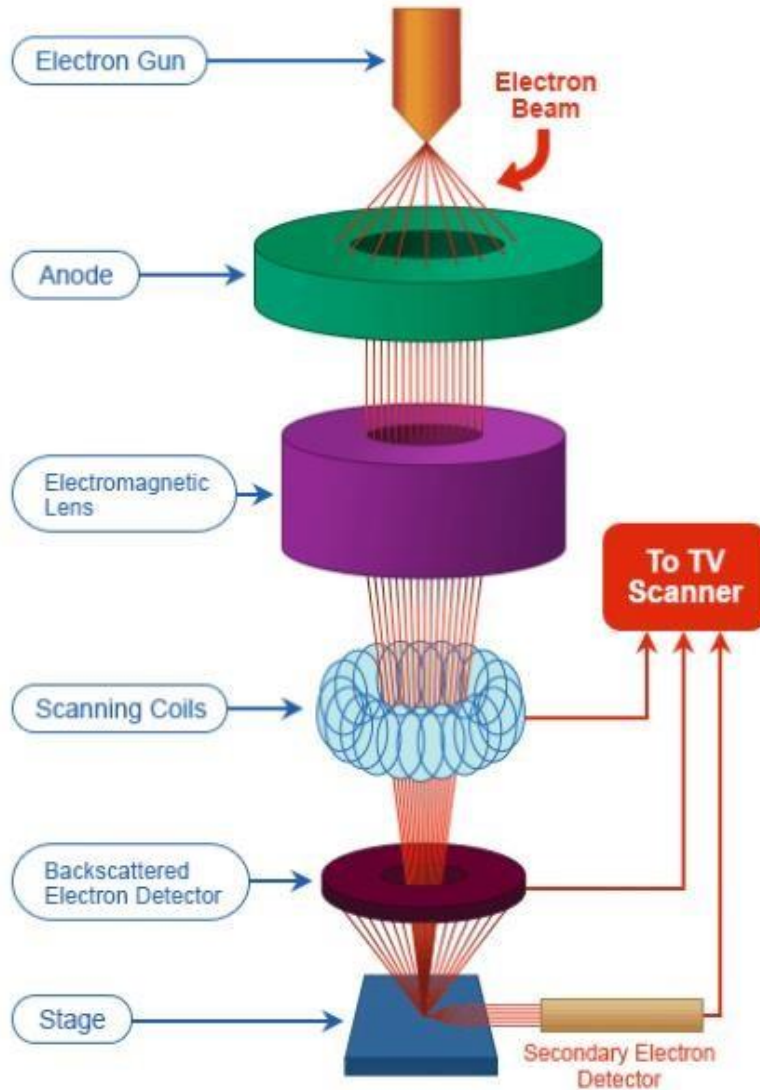
**Figure1.12: Schematic diagram of SEM**

Electron beam interaction with the specimen atoms consequences in the discharge of numerous signals which comprises characteristic X-rays, Auger electrons (AE), back scattered electrons (BSE) and secondary electrons (SE) (Figure1.13). Analysis of all these signals provides diverse information about the specimen. Back scattered electrons and secondary electrons are used for imaging. For the investigation ofmorphology and detailed surface investigation SE plays animportant role, while for phase determination BSE are important. These BSE are more sensitive for heavy components than SE. For surface investigation Auger electrons are used while for elemental and  compositional

analysis of the specimen characteristic X-rays are used in energy dispersive spectroscopy (EDS) **[11].**
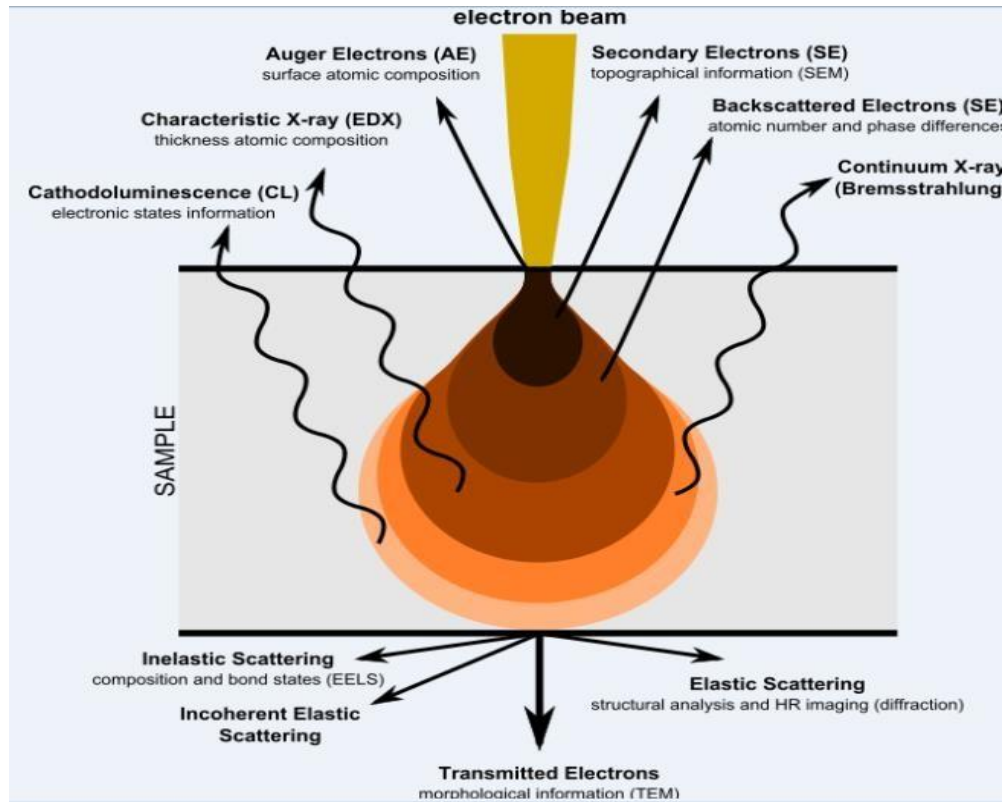


**Figure1. 13: Emission of various radiations by interaction of electron beam with samples.**

## Uses and applications

SEM is an extraordinarily useful technique. SEM can be used in almost all scientific fields such as engineering, forensic science, biological science, archeology and medical science. In the field of industry and research, there is a rising emphasis on quality control at microscopic level. SEMs are used in material science for quality control, research and failure analysis. SEM can be used to image the morphology of any specimen such as coating, metals, film and bulk material.

## 1.2.4 Hardness test

In 1921 Vickers hardness test was developed by Robert L. Smith and George E. Sandland [12].Vickers micro-hardness represents the hardness testing method that uses lighter loads and smaller indentations. Micro Hardness Testing generally deals with static indentations made by loads of 1kgf or less. This test employs a diamond indenter with an apical angle of 136º. The surface of tested specimen must be highly polished for hardness testing. Higher metallographic finishing is needed when smaller force is applied Figure (1.14).
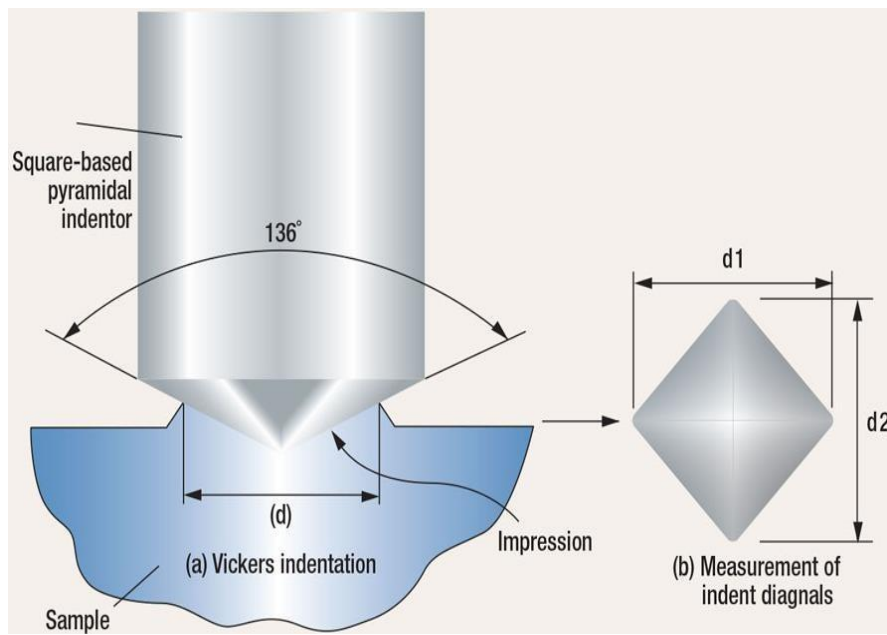


**Figure1.14: Illustration of vicker Hardness**

Construction and working

This tester comprises of an indenter probe which is moved into a surface under a particular load. This indentation has a fixed dwell time. Conventional mechanical testing includes the measurement of size or depth of this indentation to determine hardness. Vicker indenter is pressed into the surface of the tested specimen to a fixed force. That force is usually seized for 10sec. When the indentation is done, the resulting indent is observed optically to measure the lengths of the diagonal for the determination of magnitude of the imprint. (Figure 1.15)
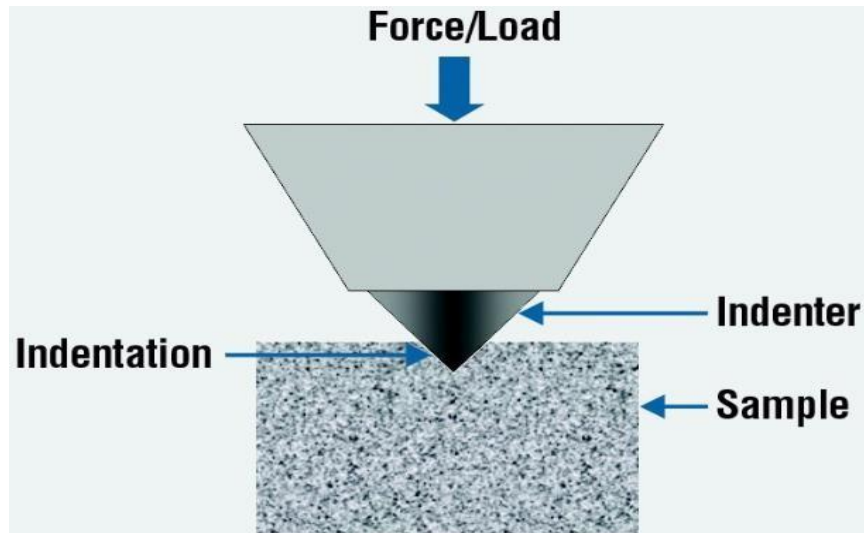
**Figure1.15: Demonstration of Vicker Indenter**

## Uses and applications

Vickers microhardness testing of materials permits to determine hardness of small samples or small part of large sample. Microhardness testing is used to determine the characteristics of foils, sheets, paints and fine wire **[13].**

## 1.2.5 Corrosion testing

Corrosion is an electrochemical process of oxidation and reduction reactions. As corrosion happens, electrons are released by the metal (oxidation) and gained by elements (reduction) in the corroding solution. Because there is a stream of electrons (current) in the corrosion reaction, it can be measured and regulated electronically. Therefore measured electrochemical experimental methods can be used to describe the corrosion properties of metals and metal components in combination with various electrolyte solutions. The corrosion characteristics are distinctive to each metal/solution system. Most metallic corrosion occurs via electrochemical reactions at the borderline between the metal and an electrolyte solution. For example, a thin film of moisture on a metal surface forms the electrolyte for atmospheric corrosion. Among opposing electrochemical reactions, equilibrium of two reactions define the corrosion rate. One is oxidation (anodic reaction) in which metal is oxidized while other is reduction (cathodic

reaction). When both of these reactions are in equilibrium condition there is no net electronic flow.

When two metals are electrically connected, the two reactions take place that are explained in the following graph. The perpendicular axis is electrical potential and the parallel axis is the logarithm of total current. The theoretical current for the anodic and cathodic reactions is represented as straight lines. Sum of cathodic and anodic reactions is represented by the curved line. When potential of the metal fluctuates with the potentiostat, this current is measured. Curve has a sharp point that represents the point where the current inverses the polarity as the reaction changes from anodic to cathodic and vice versa. Due to the occurrence of passivity, the current frequently changes by six orders of magnitude through a corrosion experimentation (Figure 1.16).
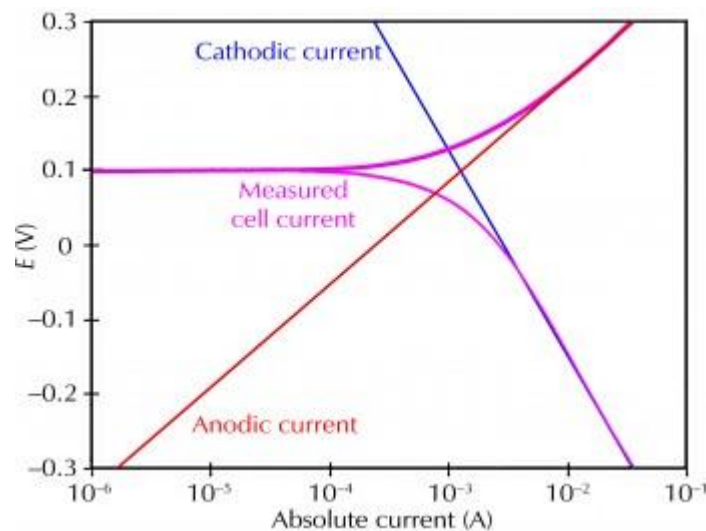


**Figure1.16: Corrosion process showing anodic and cathodic components of current**

An electronic apparatus named as potentiostat is proficient in regulating the voltage difference between a reference electrode and a working electrode. Both electrodes are surrounded in an electrochemical cell. Implementation of this control is done by introducing the current into the cell through counter electrode **[14]**(Figure 1.17).

**Figure1.17: Demonstration of Gamry potentiostat/Galvanostat/ZRA**

## Construction andworking

Potentiostat consists of an electrochemical cell and three electrodes; working electrode, reference electrode and counter electrode. Working electrode is generally an electrode where current is measured and potential is regulated. The specimen of interest acts as a working electrode in corrosion testing experiment. Measurement of working electrode potential is done by the reference electrode. Reference electrode must have a determined electrochemical potential until no current streams through it. Silver/silver chloride (Ag/AgCl) is the most common reference electrode (Figure 1.18).



**Figure1.18: Illustration of Ag/AgCl reference electrode**

The counter electrode generally Pt (platinum)or graphite works as a conductor which is proficient in finalizing the cell circuit. The current that streams into the solution through working electrode leaves the solution through auxiliary or counter electrode. Electrodes

are dipped in an electrically conductive solution (Electrolyte) usually a solution that bears a resemblance to the actual application environment of the sample being examined. Electrochemical cell consists of these three electrodes, solution and the flask containing the solution. In corrosion testing experiment the first step is the measurement of $E_{oc}$ .When there is no electrical connection, the equilibrium potential assumed by the tested metal sample is called as open circuit potential. The corrosion current $I_{corr}$ is the valueof either anodic or cathodic current. Potentiostat measures the corrosion potential($E_{CORR}$) as an energy difference between reference electrode and working electrode [15].The use of this technique enables to determine the corrosion rate, pitting susceptibility and passivity. Using Potentiostat E versus log [I] plots are obtained that represent the information of the tested specimen. Classic Tafel analysis is executed by extrapolating the linear portions of a logarithmic current in contrast to the potential plot back to their joining at the intersection value of anodic or cathodic current is called Icorr[16]. Figure 1.19 shows the Classic Tafel analysis.
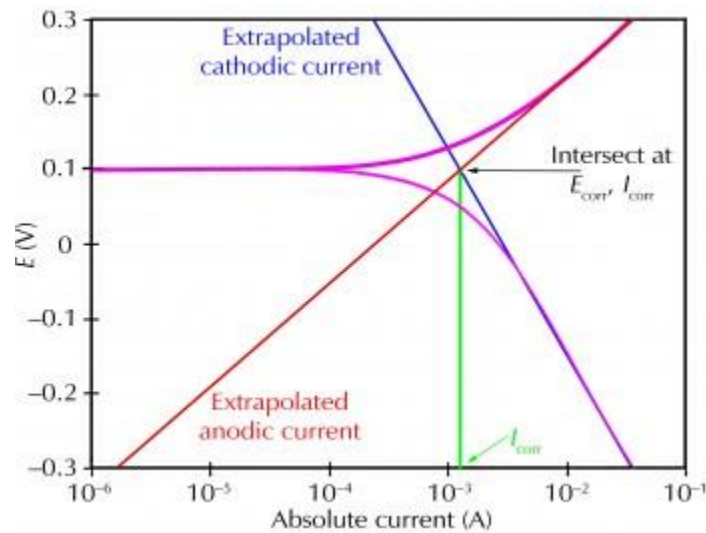


**Figure1.19: Classic Tafel analysis**

Uses and applications

To examine the corrosion potential an understanding of electrochemical procedure is necessary. Potentiostat is extensively used to acquire polarization curves and corrosion current. Underground pipelines and marine assemblies are often secured against

corrosion. This is done by cathodic protection that includes the structure to polarize under potentiostat circumstances inspite of associating to sacrificial anode **[17].**

# Chapter 2

# Literature Review

Synthesis of nitrogen alloyed steel has become the center of focus for researchers because of their engineering, medical and constructional applications. In term of strength and resistance to corrosion, nitrogen proved to be an essential alloying element to steel **[18] [19].** Nitrogen was observed as a strong element for stabilizing austenitic phase followed by solid solution strengthening **[20] [21].**

## 2.1 Synthesis of nitrogen added steel

Various laser beam scan rates were used to melt the surface of steel in the atmosphere of argon and nitrogen at different gas flow rates. Carbon dioxide ($co_2$) laser beam was used to melt the circular form specimens on one surface with 5kw output power. At various speeds, specimens were moved under the laser beam. At the rate of 500mm/min, the specimens were treated in nitrogen atmosphere. There was observed a great improvement in the resistance of pitting corrosion for the samples prepared in nitrogen atmosphere as compared to the base metal **[22].**

Air induction remelting method was used to prepare high nitrogen nickel free austenitic stainless steels, treated by the conventional electro slag remelting technique deprived of nitrogen gas pressure consumption over the melted specimen. Figure 2.1 represents the schematic of conventional electro slag remelting furnace(ESR).
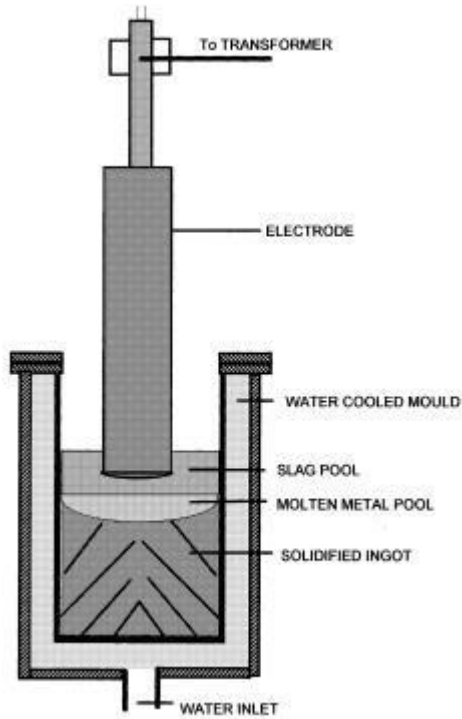
**Figure 2.1: Schematic of conventional ESR (Electro slag remelting) furnace**

By means of air induction furnace, remelting of a number of nickel free steels was done by nitrided ferroalloys. Without any $N_2$ gas pressure on the melt, the steel specimens were then exposed to conventional electro slag remelting. Chemical analysis of the specimens was done earlier and later of electro slag remelting.
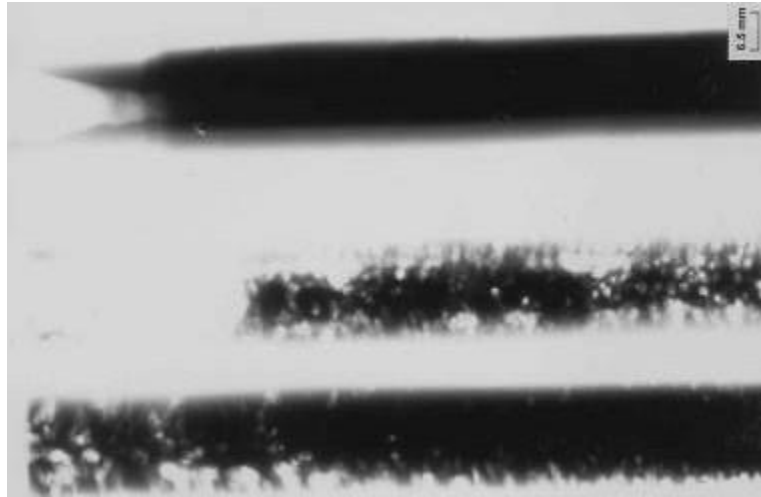
**Figure 2.2: Illustration of porosity in steel before ESR processings**

Figure 2.2 shows the porosity cast nitrogen steel rods after conventional induction melting with nitrided ferroalloys addition showing porosity in some of the rods before ESR processings. Much more porosity was observed in the air induction melted steel specimens while electro slag remelted steel samples were free from pores **[23].**

IBAD (Ion beam assisted deposition) was used to incorporate nitrogen into stainless steel samples. In this case, a glass substrate before deposition was ultrasonically washed by acetone for about 20min followed by drying in air. Ion beam assisted deposition was used to deposit stainless steel coats on glass substrate by using Kaufman ion beam gun and an electron gun. Thermal evaporation was done by electron gun and argon-nitrogen gas mixture was bombarded on the substrate by Kaufman ion beam gun. Pressure in vacuum chamber was decreased after the sample was loaded in the unit. Figure 2.3 represent the schematic diagram of ion beam assisted deposition system.
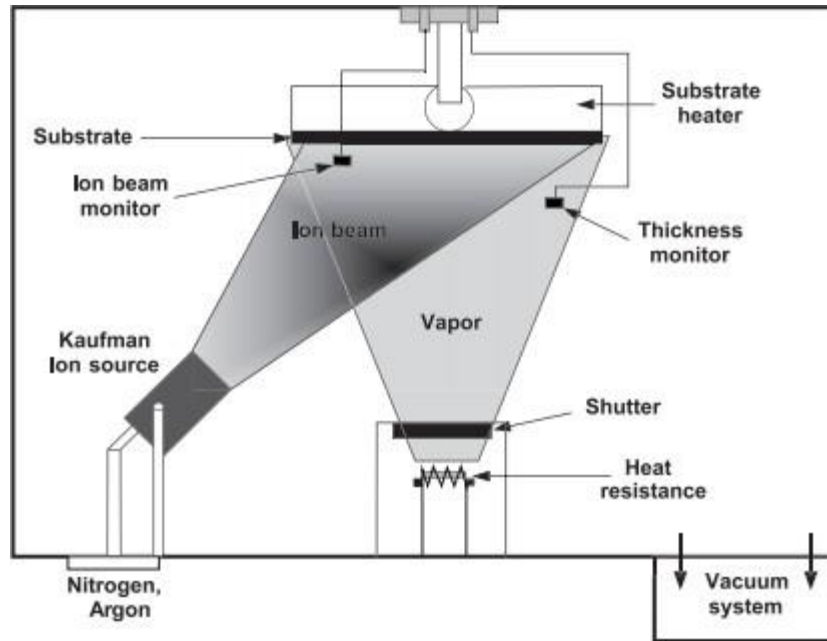
**Figure 2.3: Schematic diagram of ion beam assisted deposition system**

For the elimination of remaining contaminations, the substrate was pre-sputtered with the help of Kaufman ion beam gun at an argon flow rate of 40sccm (standard cubic centimeter per min) for about 20 minutes. Then thermal evaporation of stainless steel layers on glass substrate was done by changing the quantity of reactive gases such as argon and nitrogen [24].

Below 450ºC temperature the glow discharge of plasma was used to alloy the superficial of austenitic stainless steels with both nitrogen and carbon at a time. Samples in the form of discs were cut from hot rolled steel slabs. To obtain fine finishing, samples were ground manually using down to 1000 grade silicon carbide emery papers. Both nitride and carbide precipitation in the alloyed region was avoided by keeping the treating temperature suitably low. Otherwise it will result in the deterioration of the corrosion resistance of alloyed area. In the DC plasma nitriding component, the hybrid process was performed between 380 and 430ºC for the duration of about 15 -40hours. In this case, 95% nitrogen and 5% $CH_4$ was used as gas mixture. $CH_4$ in this gas mixture was used as a carburizing species and nitrogen as nitriding specie. This hybrid performance at low temperature resulted in a twofold layer structure, which consists of a nitrogen enriched layer on top of carbon layer [25].

A high vacuum furnace was used for the formation of high nitrogen stainless steel (HNS). The procedure involved the dissolution of raw material followed by modeling. Then hot rolling and cold rolling of experimental specimens were done. The samples were solution heat treated at 1050ºC for half an hour. Finally water quenching at room temperature was done [26].

High nitrogen austenitic steels (HNAS) are the best replacement of conventional iron chromium steels containing expensive nickel. HNAS have nitrogen that can stabilize austenitic phase. Vacuum induction furnace and electro slag remelting furnace were used to prepare high nitrogen austenitic steel materials using nitrogen atmosphere. Experimentally prepared cold rolled plates were solution treated at 1100ºC for 90min. These plates were water quenched and then their grinding was done to remove the impurities and oxides from the both joint and upper facades [27].

9Cr18 is the high chromium martensitic stainless steel that can attain extraordinary wear and corrosion resistance and excellent hardness by different quenching tempering methods. The experimental steels were prepared in the vacuum induction furnace. Steel ingots were homogenized for 1hr at 900 ºC, temperature is then increased to 1150ºC by 100ºC per second and homogenized again for 1hr. Specimens were then forged between 850-1150ºC into slabs that were gradually cooled down to room temperature [28].

In a high vacuum system, films were deposited with the help of reactive magnetron sputtering technique. In this case 304Stainless steel was used as a target material. The distance between target and the substrate was about 8cm. In the presence of mixture of argon- nitrogen atmosphere, deposition was performed with the ratio of nitrogen in the sputter gas changed by varying the argon and nitrogen flow rate. The magnetron sputter gun of 50milimeter diameter driven by the RF power center was used [29]. Pressurized induction melting was used to prepare the samples of Fe-18Cr-10Mn0.4N (0.4nitrogen) and Fe-18Cr-10Mn0.6N (0.6nitrogen). The sample bars were then hot rolled in the form of 3milimeter width plates. For about one an hour specimens were stabilized at 1100ºC followed by quenching at room temperature. The purpose of quenching was to achieve the comparable grain size that is an important factor for fatigue behavior [30].

## 2.2. Properties of nitrogen added steel

There are several properties enhanced by the nitrogen added steels as compared to the conventional alloys that make their use more suitable. Steel being a progressively significant manufacturing material with satisfactory mechanical properties has great importance in every field of life. These days, critical focus of material research is to improve the properties of steel. Nitrogen was proved to be an active element to enhance the properties of steel. Following properties of nitrogen added steels are improved:

- High corrosion resistance
- High yield and ductility
- Greater tensile strength and toughness
- Improved wear resistance
- Enhanced mechanical properties
- High hardness
- Biocompatibility
- Improved magnetic properties

### 2.2.1 Corrosion Resistance

The addition of nitrogen in FeCrNiMo steels resulted in excellent pitting and crevice corrosion resistance in the presence of harsh environment like acidic solution. This nitrogen addition improved the efficiency of chromium and molybdenum on corrosion resistance [31].

PACVD (Plasma-assisted chemical vapor deposition) was used to coat the sample with titanium nitride. After plasma nitride process, corrosion resistance of these coated specimens were examined and compared with unprocessed material. Corrosion resistance was noticeably improved by applying the titanium nitride film compared to the uncovered stainless steel sample. Bare stainless steel samples undergo corrosion more rapidly than the samples coated with titanium nitride by PACVD [32].

In the presence of pure Argon (Ar) and nitrogen gases, anodic potentiodynamic polarization curves of duplex SS weldments were observed. This observation was done

in 3.5 percent by weight of brine solution. Effect of nitrogen incorporation on the corrosion resistance property of specimens was shown by these polarization curves. In case of duplex stainless steels, corrosion strength of weldment specimens was based on the microstructures that involve both the morphology and austenite content. Corrosion resistance of weldment samples was improved due to nitrogen gas sheltering [33].

## 2.2.2 Hardness

Nitrogen content is directly proportional to milling time. With the 10 to 20 h increase in milling time, nitrogen concentration was also increased from 2.56percent to 3.20percent. Nitrogen concentration reached to 3.69percent with the milling time increase to 30hours. Milling time also influenced the micro hardness. 10 to 20 hours increase in the milling time resulted in the average Vickers micro hardness increase from 399HV to 489 HV. With the maximum nitrogen concentration and further rise in milling time from 25 -30 hours resulted in the micro hardness from 523HV to 549HV. This micro hardness was greater than that the commercial stainless steel which was about 325HV. In the process of mechanical alloying, enormous amount of manganese, chromium and nitrogen dispersed into iron matrix, which hindered the disruption movement and resulted in the improvement in micro hardness [34]. Due to various nitrogen concentrations in the different steel samples, the hardening properties observed were different. High nitrogen containing steel sample X40CrMoV5-1 resulted in extraordinary hardness property [35].

Nitrogen alloyed martensitic stainless steel melted specimens ranges from 341 to 471HV hardness. The reason of this low hardness is chromium and low amount of nitrogen. High hardness was associated with the high nitrogen steel sample. This variation in hardness of nitrogen alloyed martensitic stainless steel was due to changes in the concentrations of carbon and nitrogen [36].

## 2.2.3 Creep Resistance

Nitrogen addition in the austenitic stainless steel resulted in improved creep resistance. Nitrogen addition enhanced the rupture strength without the reduction of rupture ductility. Strengthening effect of nitrogen was greater than the carbon. Nitrogen solid

solution reinforcement was more effective than carbon at higher temperature. For increasing creep rupture strength and rupture ductility, nitrogen was proved to be more effective than carbon [37].

## 2.2.4 Biocompatibility

Titanium nitride (TiN) coatings on the steels not only exhibited enhanced mechanical properties but also proved to be biocompatible for the use of surgical tools. Titanium nitride coating on medical tools resulted in excellent property of biocompatibility from the cytotoxicity test. Thus the samples coated with titanium nitride proved to be free from any detrimental effects even in the inflated situations with remote cells [38].

## 2.2.5 Mechanical Properties

After quenching at 1323K followed by tempering at 863K for about 3.5hours, the mechanical properties of steel specimens were observed. Nitrogen H13 die steel samples were with maximum average impact toughness of about $15.8Jcm^2$ and hardness of 49.3HRC. Hardness of experimental AISI H13 die steel was enhanced by three to five times however sustaining the impact toughness. This nitrogen addition was also capable of making the steel samples more wear resistant and increasing life span [39].

## 2.2.6 Wear Resistance

Wear resistance of nitrogen alloyed austenitic stainless steel was measured and compared with the same specimens coated with amorphous carbon coatings. This coating of carbon layers was done by PECVD (plasma enrich chemical vapor deposition method). Wear stability of both coated and uncoated specimens of dissimilar grain size were observed by BOD (ball on disk) experiments. Nitrogen doping in carbon coating resulted in the extensive wear stability [40].

## 2.3 Applications of nitrogen added steel

High nitrogen steels have great importance as engineering material. Numerous characteristics make the use of nitrogen added steel more promising than the conventional alloys. Dissolved nitrogen in steel improves several properties of that steel.

A number of applications of nitrogen added steels in various fields of life are written below:

- Power generating industry
- Railways
- Ship buildings
- Chemical equipment
- Petroleum industry
- Dental instruments
- Nuclear industry
- Pressure vessels
- Superconducting magnetic housing
- Gears, valves and bearings
- Surgical tools

A profitable application of nitrogen added steel was observed in making rings of electrical generators. Nitrides in the replacement material precipitated slowly than the carbides present in the conventional material.

Specific properties were mandatory for these rings such as satisfactory ductility, great strain hardening potential, high yield strength greater than 1000MPa, little magnetic penetrability, resistance to stress and pitting corrosion. Cold forming was used to achieve the high strength for the rings. The process of cold forming was able to hasten carbide nitride precipitation. Thus it was compulsory to use such material with low vulnerability to undergo precipitation **[41] [42].**

## 2.4 Research objectives

Although 30CrMnSiA and 316SS are often chosen because of their resistance to corrosion to an extent but they are not immune to it .Therefore there must be a technique that can enhance their resistance to corrosion even in the marine environment. A lot of research work has been done on steel to improve its properties by alloying it with different elements such asNi, Mo, B, Ti, and Si.

But there is still a need to develop an easy, cost effective and simple method to produce steel of enhanced properties. The aim of this research work is to make steel with improved properties such as

To make marine application steel with,

1. High hardness
2. High corrosion resistant

# Chapter 3

# Experimentation

The materials used in this work were 30CrMnSiA steel and 316stainless steel with the chemical composition as shown below.

**Table 3: Chemical composition of Steels; a) CrMnSiA30 and b) 316SS**

| Steel | C | Si | Cu | Mn | Ni | P | Cr | S | Fe | Mo | N |
|-------|-----------|-----------|--------|----------|-------|--------|-----------|--------|-----|----|------|
| a | 0.28~0.34 | 0.90~1.20 | ≤0.025 | 0.80~1.1 | ≤0.03 | ≤0.025 | 0.80~1.10 | ≤0.025 | - | - | - |
| b | 0.08 | 0.75 | - | 2.00 | 10 | 0.045 | 16 | 0.030 | bal | 2 | 0.10 |

## 3.1. Synthesis

Samples were cut with the help of EDM (electro discharge machining) wire Cut from rods of 12mm into 2mm pieces. Steel specimens after weighing by electronic balance of readability 0.0001g were placed in furnace. These steel pieces were melted in ARC melting furnace at various nitrogen pressures by arc of 3A current (Figure 3.1). Steel ingots were melted by high temperature electric arc in the presence of vacuum, 0.1bar and 0.3bar nitrogen pressure. In order to ensure the homogenization each sample was measured three times by turning its sides.



**Figure 3.1: Illustration of Arc melting furnace**

Melted steel ingots after cool down to room temperature were anneal at 840ºC for 20min. Prior to annealing samples were wrapped in stainless steel foil to prevent their interaction with oxygen. Then samples were quenched in brine solution quickly after annealing in order to trap the alloying metal within the grain boundaries which leads to hardening and strengthening of samples.

## 3.2. Characterization

Phase identification and crystal arrangement of prepared specimens were observed by X-Ray Powder Diffraction, XRD (D8 ADVANCE) with Cu-k$_{\alpha 1}$ ($\lambda$=1.5418Å) as the radiation source operating at 40kV and 30mA, within 10º$\leq$2$\theta$$\geq$80º range. The database incorporated in the software was used for the identification of powder patterns.

Prepared steel ingots were again cut by the EDM wire cut from 8-10mm diameter pieces followed by the hot mounting through automatic mounting press (metkon Hydropress) at 240ºC while embedded into Bakelite resin. To produce mirror like finishing surface, grinding was done by Metkon forcipol2v grinder. Flat surfaces of samples were manually grinded using silicon carbide (Sic) emery papers ranging from 120-2000 grade followed by polishing in the presence of alumina solution (Al$_2$O$_3$), washed and then dried. Figure 3.2 shows the image of grinder polisher.



**Figure 3.2: Image of grinder and polisher**

30CrMnSiA steel samples were chemically etched by nital for 15s, a solution of 10ml HNO$_3$ and 100ml ethanol followed by washing, drying and cleaning with acetone. On the other hand, 316SS specimens were etched by an etchant known as carpenter for 15s. Carpenter is a solution of cupric chloride (CuCl$_2$) 2.4g, hydrochloric acid (HCl) 122ml,

ferric chloride (FeCl$_3$) 8.5g, alcohol (C$_2$H$_5$OH) 122ml and nitric acid (HNO$_3$) (6ml). Stainless Steel samples were also washed with acetone and dried carefully. The purpose of etching was to expose the shape, size of grain boundaries, inclusions, cracks, metallic phases and quality of material. All the samples were viewed as prominently as possible by Optical Microscope (OM) MM500T (Figure 3.3). This optical microscope with a series of lenses was used to generate a magnified image of the sample that was positioned in the focal plane of the lens. OM was used to obtain detailed images of tested specimens, check any kind of cracks or flaws, contamination observation, holes or pits confirmation and for the determination of grain boundaries of the sample surface.



**Figure 3.3: Illustration of optical microscope MM-500T**

Surface topography and compositional analysis was done by Scanning Electron Microscope (VEGA3 TESCAN) equipped with an EDX system operating at 20kV. The sample stubs were then placed in the vacuum chamber for imaging one by one.

## 3.3. Physical Properties

### 3.3.1 Vickers Hardness.

Samples after optical imaging microscopy were polished with alumina solution carefully in order to remove the etched surface followed by the measurement of Vickers hardness. Micro-Hardness Tester 401/402 MVD was used to check the hardness of prepared samples through a series of loads ranging from 50-1000g was used each sustained for 10s. To achieve a steady indentation shape and decent measurement surface of tested specimen was made perfectly smooth. Figure 3.4 shows the image of testing Vickers micro- hardness.
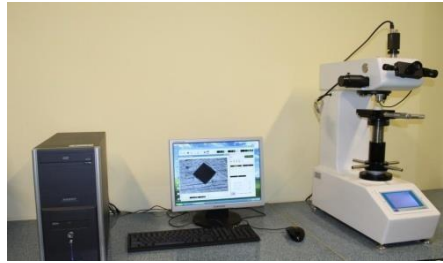
**Figure 3.4: Representation of microhardness test 401/402 MVD**

## 3.4 Corrosion Testing.

For the corrosion testing of studied samples, electrodes were prepared by cold mounting method. Steel pieces of calculated surface area and density were used followed by their soldering with copper wire. (Figure 3.5)



**Figure 3.5: Image of cold mounted electrode**

Cold mounting of these samples was then performed using a mixture of epoxy resin and hardener of equal ratio. Sample soldered with copper wire was then dipped in the mixture of epoxy and resin present in a mold. (Figure 3.6)
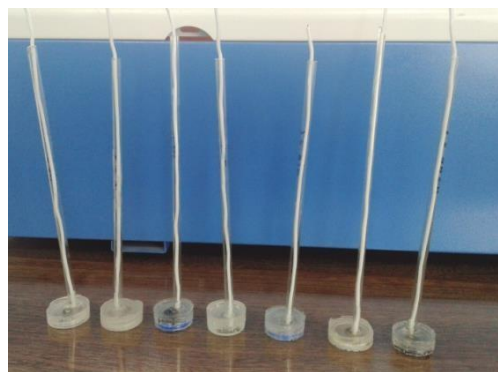


**Figure 3.6: Illustration of 30CrMnSiA Steel and 316SS for corrosion testing**

After hardening of epoxy-resin mixture, the mold was removed. Grinding of cold mounted sample was accomplished by 1500 and 2000 grade emery paper followed by a fine polishing with alumina (0.05micron). This mirror like surface was mandatory for better results of corrosion testing. An electrolyte of 3.5wt% NaCl solution was used to check the electrochemical measurement of prepared samples. This electrolyte was prepared by the dissolution of pure NaCl at room temperature in the deionized water. Other electrolytes such as $Na_2Co3$ (1wt%), $H_2So4$ (0.1M) and $NaHC03$ (1wt %) were also used to check the corrosion resistance of prepared steel samples. Three electrodes such as prepared sample; working electrode, counter electrode of graphite and reference electrode of Ag/AgCl, were used for corrosion testing of samples using Gamry instrument potentiostat / Galvanostat/ZRA. Tefel plots and polarization resistance of all steel samples were calculated at a scan rate of 0.467mV/sec. By multiplying length and width, area of every sample was measured before testing. Mass was measured by an analytical electronic balance with accuracy of 0.0001g.After testing each sample was washed by means of running water and alcohol followed by their drying. (Figure 3.7) shows the demonstration of Gamry Potentiostat).



**Figure 3.7: Demonstration of Gamry potentiostat**

# Chapter 4

# Results and Discussion

## 4.1.X-ray Powder diffraction

X-ray powder diffraction has been done to examine the phase of prepared steel samples. Figure 4.1shows the XRPD pattern of 30CrMnSiA steel and 316SS respectively. No phase change was observed for both the steels synthesized in different condition such as steel samples melted in the presence of Ar, 0.1bar and 0.3 bar nitrogen. As a result of melting process, carbon was replaced by nitrogen and results in the no change of crystal structure so all samples have the same peaks in X-ray diffraction pattern.
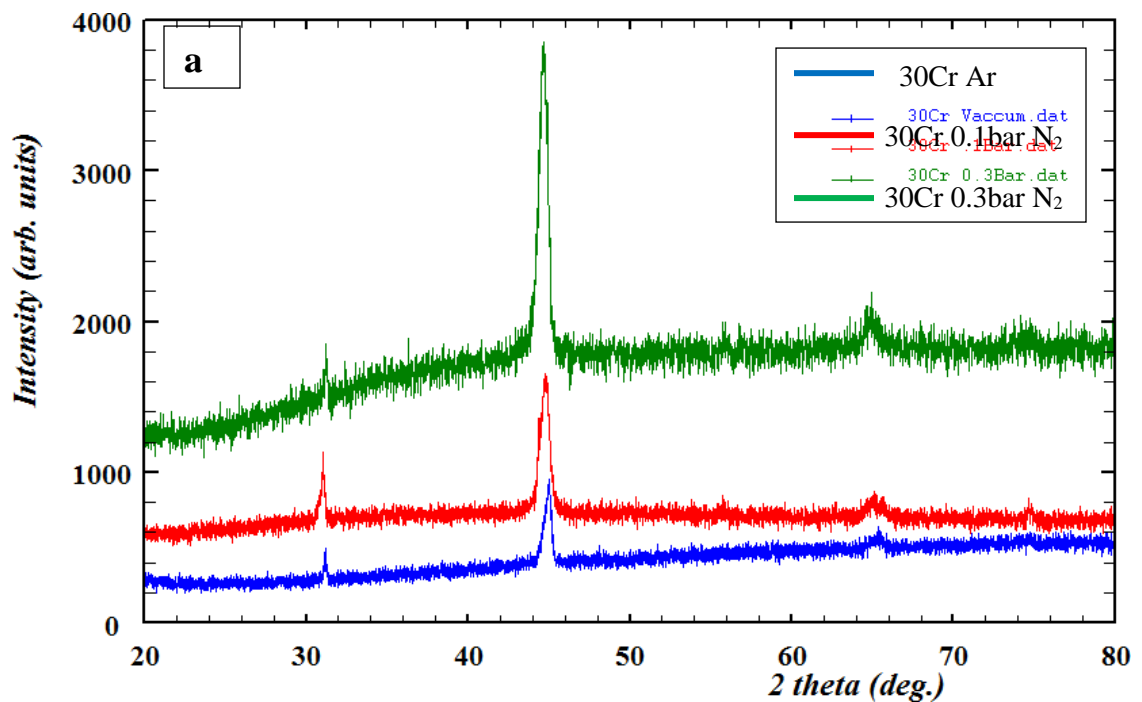


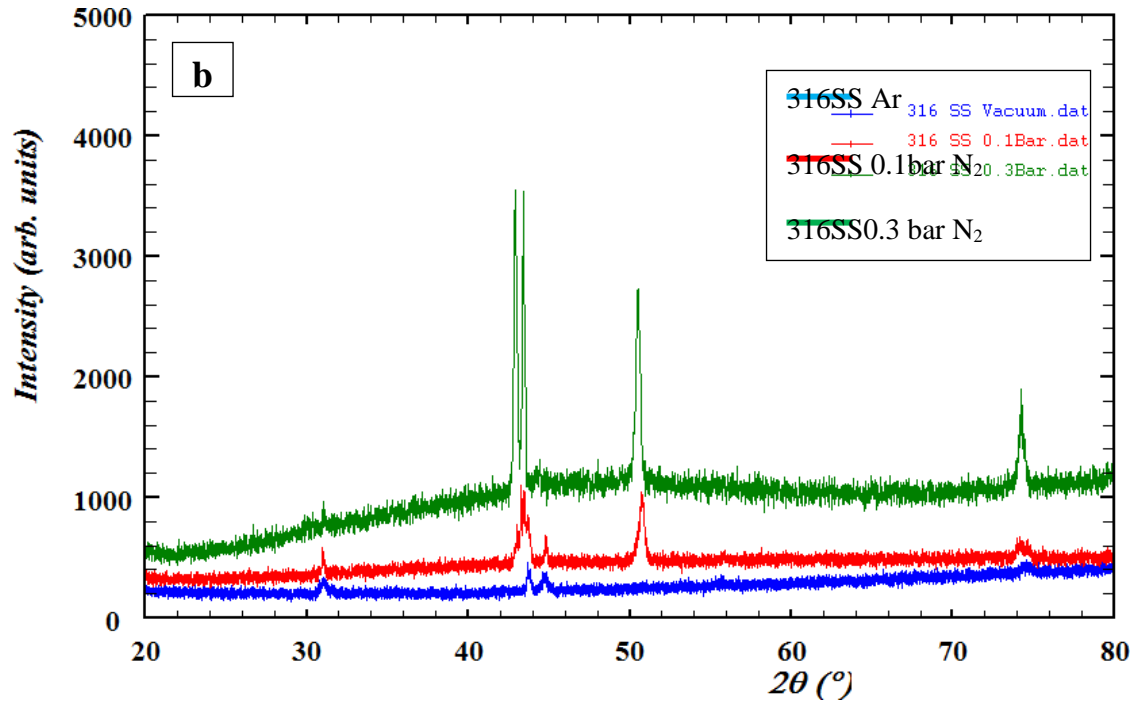**Figure 4.1(a): XRPD pattern of 30CrMnSiA steel**

**Fig 4.1(b): XRPD pattern of 316 SS**

## 4.2 Scanning Electron microscopy (SEM)

Fig 4.2 (a-d) scanning electron micrographs depict the microstructures of raw steel and nitrogen added steel materials It is revealed that nitrogen content had a significant effect on the microstructures of both steel samples of 30CrMnSiA and 316Stainless Steel. SEM (Scanning electron microscopy) detects no nitrogen in the untreated and argon (Ar) melted steel samples. The raw steel samples showed microstructures which had irregular shape and uneven size. The nitrogen added steel samples exhibited obvious alterations in microstructure dimension and shape as compared to the untreated and argon melted steel samples. When the nitrogen content was increased from 0.1 to 0.3 bars, the samples were further alloyed.

Fig 4.2 and fig 4.3 (a) show the microstructures of raw steel samples of both steels 30CrMnSiA and 316Stainless Steel respectively processed by the same melting process. Fig 4.2 and 4.3 (b) gave the morphology of 30CrMnSiA and 316Stainless steel samples melted in argon atmosphere at 3500℃ in Arc melting furnace. While fig (c),(d) gave  the

images of steel samples of nitrogen added at various pressure (0.1 and 0.3 bar). The difference in the morphology of all steel samples is due to the nitrogen addition.
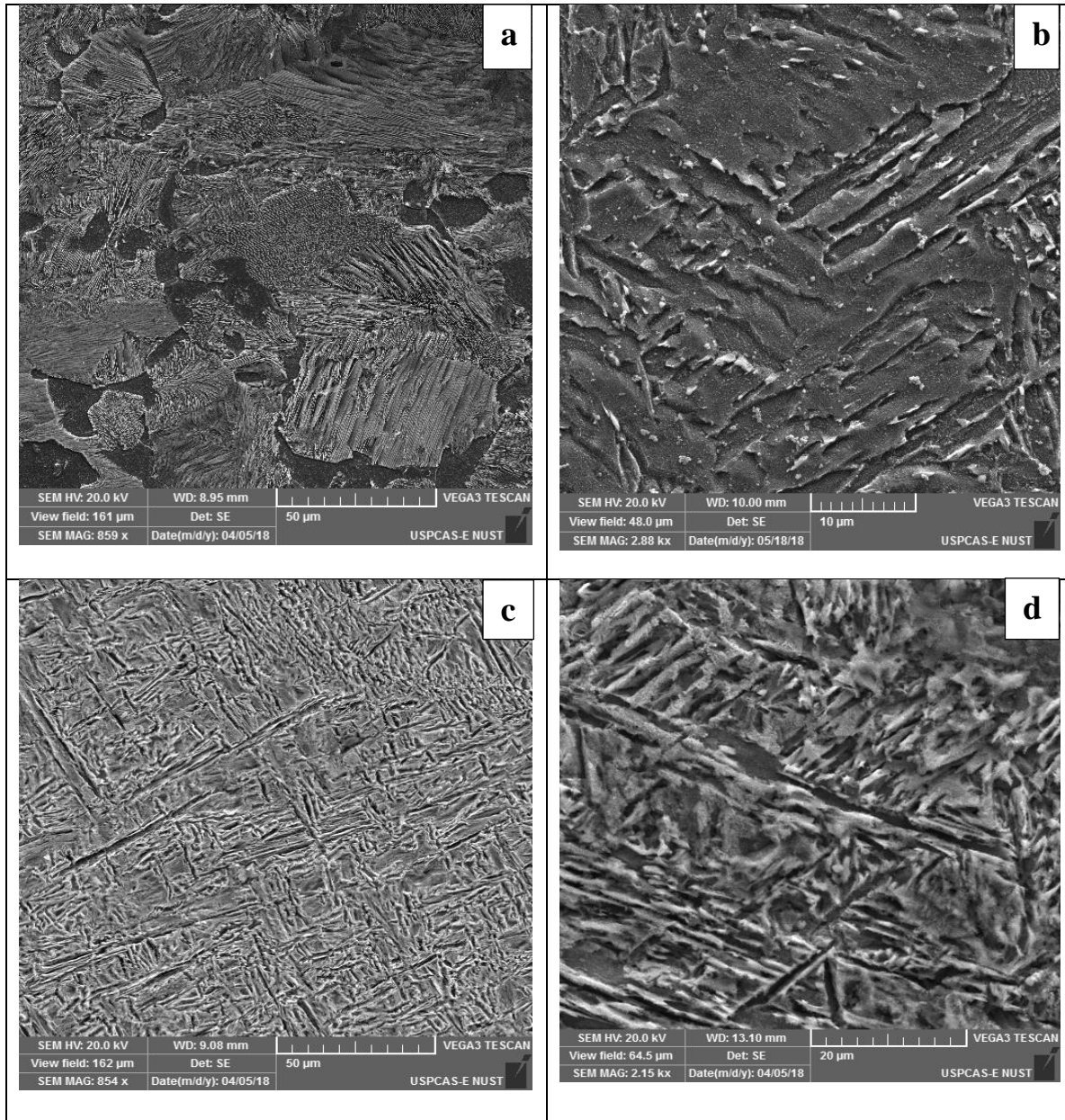


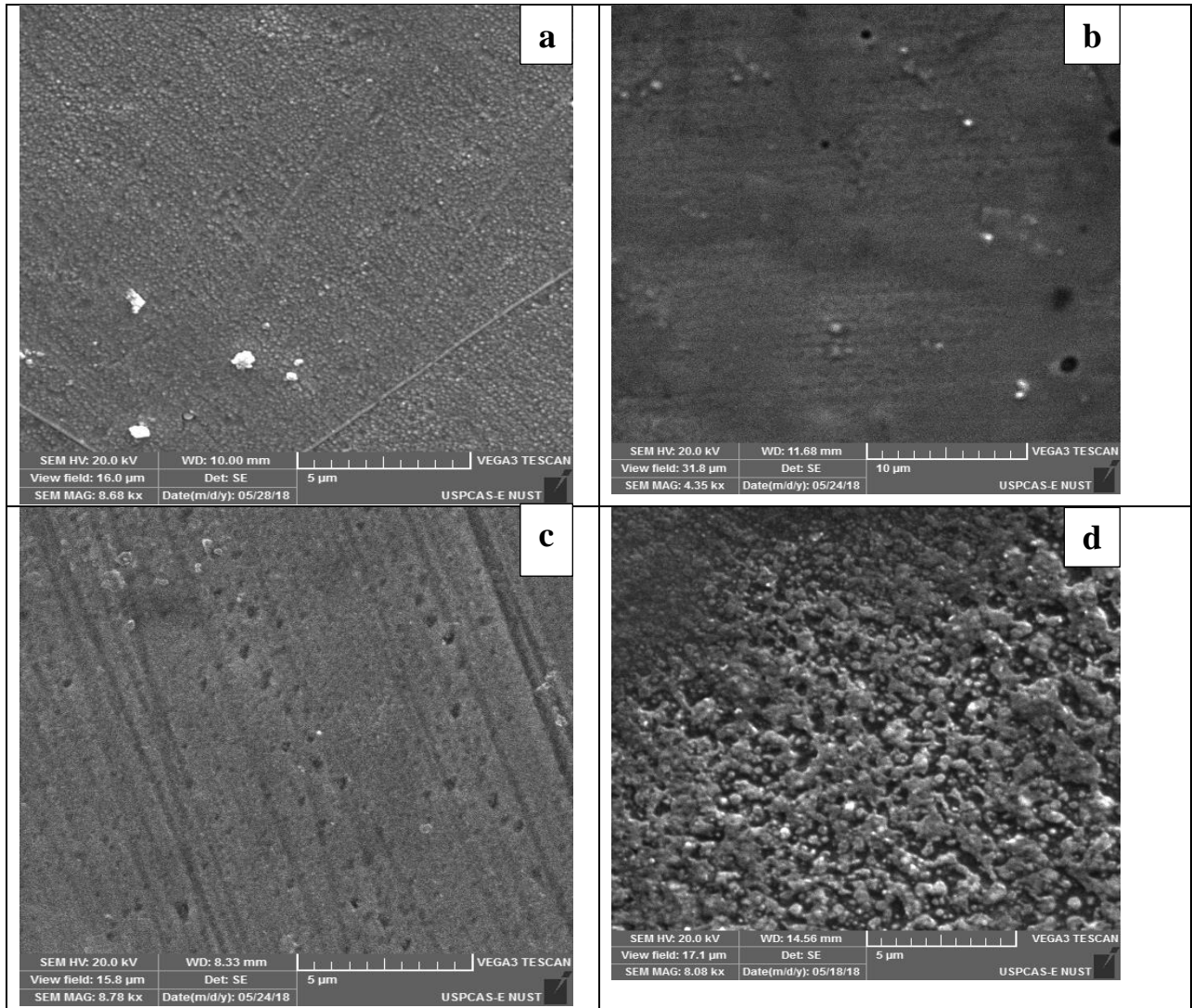**Figure 4.2: SEM images of 30CrMnSiA Steel (a) untreated (b) Ar melted (c) 0.1 bar N$_2$ (d) 0.3 bar N$_2$**

**Figure 4.3: SEM images of 316 SS(a) untreated (b) Ar melted (c) 0.1 bar $N_2$ (d) 0.3 bar $N_2$**

EDX (Energy dispersive x-ray spectroscopy) equipped with SEM gives the elemental analysis of experimental specimens. Fig 4.4 illustrates the EDX spectra of nitrogen added steel approving the presence of nitrogen content.
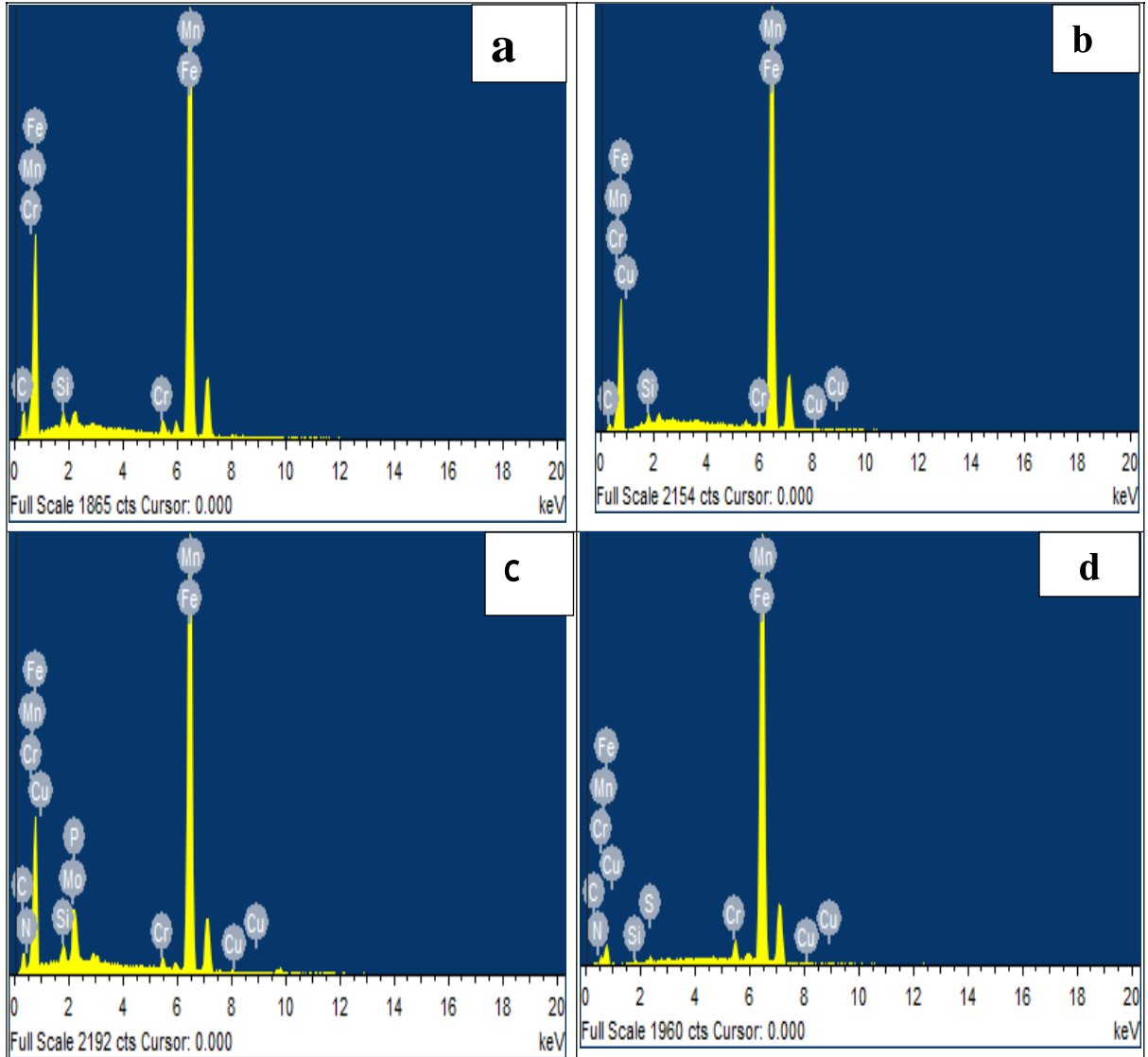
**30CrMnSiA Steel**



**Figure 4.4:EDX Spectra of 30CrMnSiA Steel (a) untreated (b) Ar melted (c) 0.1 bar $N_2$ (d) 0.3 bar $N_2$**

**Table 4: EDX analysis of 30CrMnSiA steel samples**

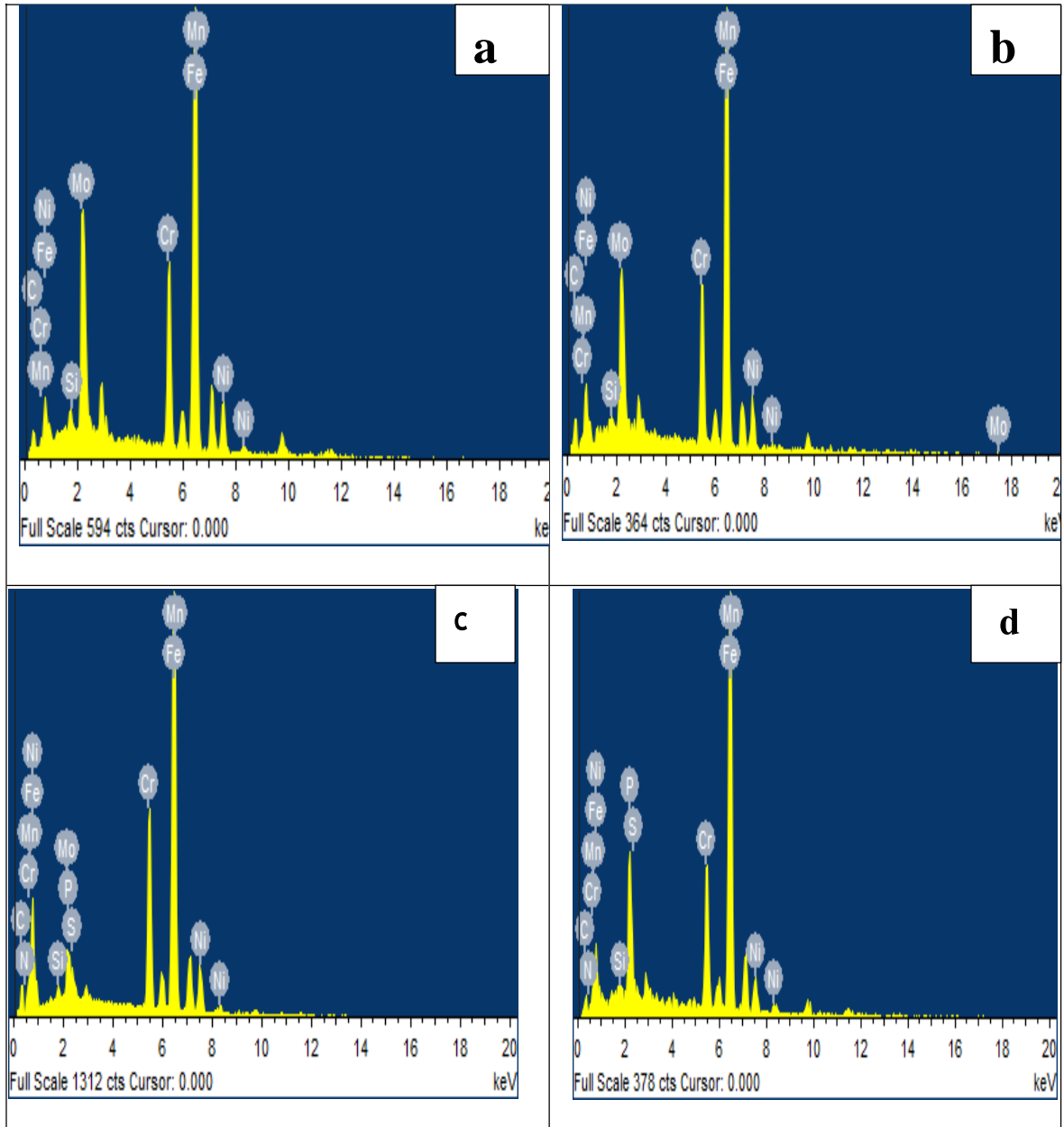| Reaction conditins for30Cr MnSiA steel | Element wt% | | | | | | | | | | |
|---|---|---|---|---|---|---|---|---|---|---|---|
| | Fe | Ni | Cr | C | Mn | Cu | Si | P | S | Mo | N |
| 30Cr untreated | 72.25 | - | 1.41 | 21.13 | 1.46 | - | 0.75 | - | - | | - |
| | 78.85 | - | 1.36 | 17.75 | 0.99 | - | 1.05 | - | - | - | - |
| | 77.75 | - | 1.52 | 18.91 | 0.96 | - | 0.86 | - | - | - | - |
| 30Cr Ar melted | 89.49 | - | 0.55 | 8.14 | 0.68 | 0.38 | 0.76 | - | - | | - |
| | 77.01 | 0.50 | 1.02 | 19.60 | 0.70 | - | 0.88 | - | 0.29 | - | - |
| | 78.94 | - | 0.65 | 18.60 | 0.91 | - | 0.83 | - | 0.08 | - | - |
| 30Cr 0.1 bar $N_2$ | 76.04 | - | 1.05 | 19.68 | 0.77 | 0.20 | 0.89 | 0.15 | - | 0.53 | 0.68 |
| | 79.32 | - | 0.85 | 17.36 | 0.65 | 0.36 | 0.76 | 0.09 | - | 0.43 | 0.18 |
| | 79.03 | 0.04 | 1.10 | 17.16 | 0.59 | 0.72 | 1.06 | - | - | 0.10 | 0.20 |
| 30Cr 0.3 bar $N_2$ | 71.04 | 0.25 | 1.28 | 16.53 | 0.94 | 0.96 | 0.73 | 0.10 | 0.16 | - | 8.01 |
| | 69.02 | 0.03 | 1.08 | 22.58 | 0.52 | 0.56 | 0.88 | 0.21 | 0.18 | - | 4.96 |
| | 75.81 | 0.42 | 1.44 | 16.26 | 0.65 | 0.34 | 0.72 | - | - | - | 4.37 |

**316 SS EDX**



**Figure 4.5: EDX spectra of 316SS (a) untreated (b) Ar melted (c) 0.1 bar $N_2$ (d) 0.3 bar $N_2$**

**Table 5: EDX analysis of 316SS samples**

| Steel grade | Element wt% | | | | | | | | | |
|---|---|---|---|---|---|---|---|---|---|---|
| | Fe | Ni | Cr | Mn | C | Mo | Si | P | S | N |
| 316 untreated | 52.91 | 8.60 | 13.89 | 1.72 | 20.57 | 2.15 | 0.16 | - | - | - |
| | 54.39 | 6.67 | 14.93 | 1.28 | 19.44 | 2.97 | 0.31 | - | - | - |
| | 47.37 | 7.10 | 13.14 | 1.12 | 26.40 | 3.93 | - | 0.94 | - | - |
| 316 Ar melted | 49.05 | 7.93 | 11.76 | 0.82 | 28.96 | 1.11 | 0.37 | - | - | - |
| | 48.70 | 5.77 | 14.70 | 1.92 | 24.03 | 4.65 | 0.22 | - | - | - |
| | 54.79 | 8.77 | 13.07 | 1.27 | 19.00 | 2.80 | 0.31 | - | - | - |
| 316 0.1 bar $N_2$ | 50.33 | 7.83 | 14.92 | 1.49 | 21.48 | 2.08 | 0.47 | 0.07 | 0.38 | 0.96 |
| | 53.52 | 7.43 | 13.50 | 0.88 | 21.10 | 2.98 | 0.54 | 0.04 | - | - |
| | 55.37 | 7.66 | 13.58 | 1.01 | 17.20 | 1.87 | 0.33 | - | 0.10 | 2.88 |
| 316 0.3 bar $N_2$ | 60.39 | 7.61 | 13.73 | 1.28 | 12.45 | - | 0.38 | 0.12 | 1.04 | 3.00 |
| | 64.72 | 5.44 | 18.48 | 1.57 | 5.34 | 2.79 | 0.17 | - | - | 1.50 |
| | 55.04 | 6.47 | 13.81 | 1.43 | 19.21 | 2.29 | 0.05 | - | - | 1.70 |

## 4.3. Optical microscopy (OM)

Optical micrographs represent the topography of the steel specimens. The influence of nitrogen addition on microstructures of both steel samples (30CrMnSiA and 316SS) was investigated using computer aided image analysis. Figure 4.6 (a) and 4.7 (a) illustrate the irregular grain structure of untreated steel sample of 30CrMnSiA and 316SS at the same 20X magnification.
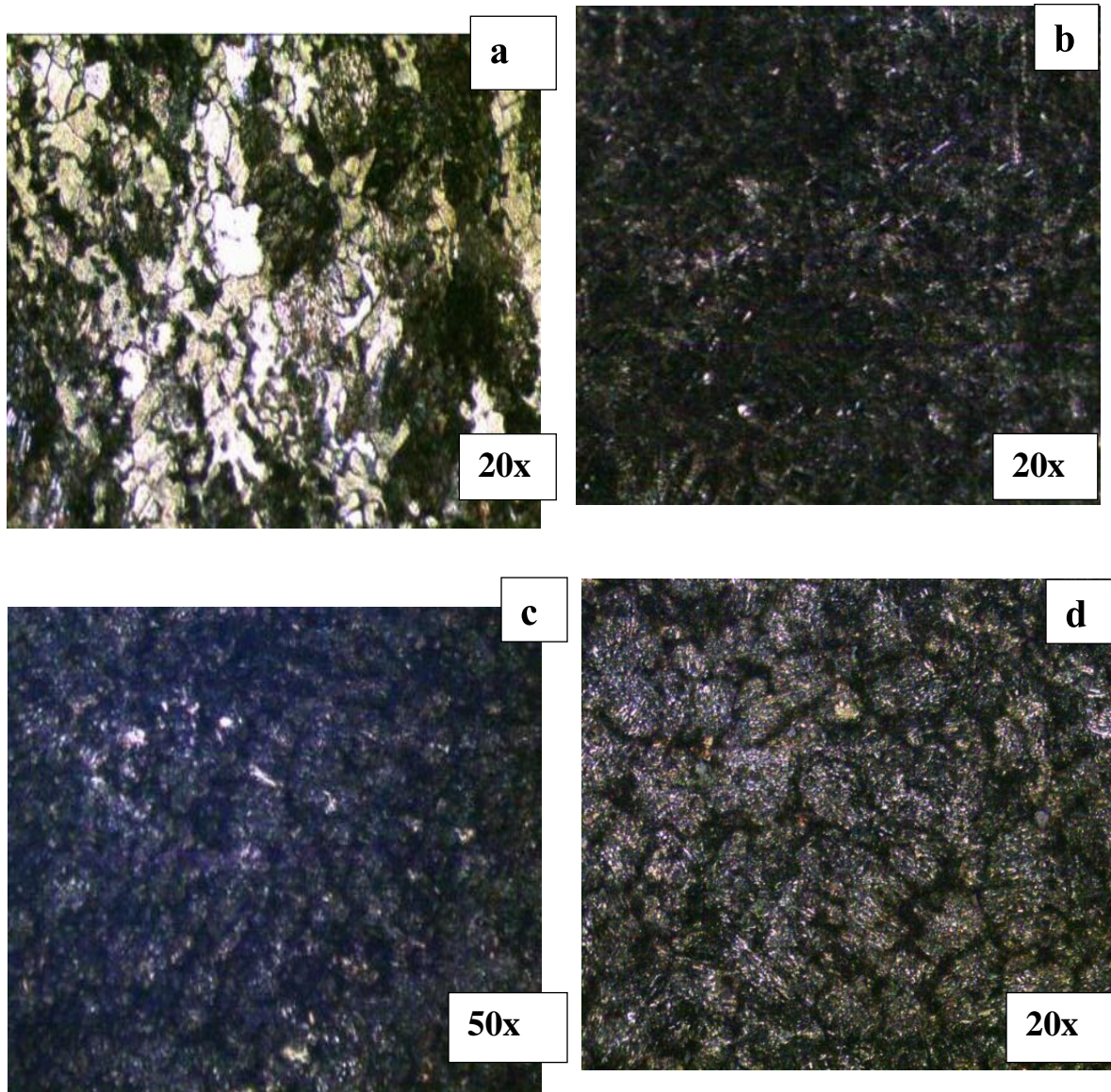
**Figure 4.6: Optical micrographs of 30CrMnSiA steel (a) untreated (b) Ar melted (c) 0.1 bar N₂ (d) 0.3 bar N₂**

Fig 4.6(d) shows the eutectic and globular boundaries that are enriched with nitrogen **[43].**While (b) of fig 4.6 and 4.7 represent the micrograph of steel sample melted in argon atmosphere in the Arc melting furnace. Fig (c),(d) of both Fig 4.6 and 4.7 represent when sample was melted at 3500ºC in the presence of nitrogen atmosphere at various pressure 0.1 and 0.3barsN₂ respectively. Clearly visible micrographs can be seen in these figures with a huge difference of optical images from untreated to higher

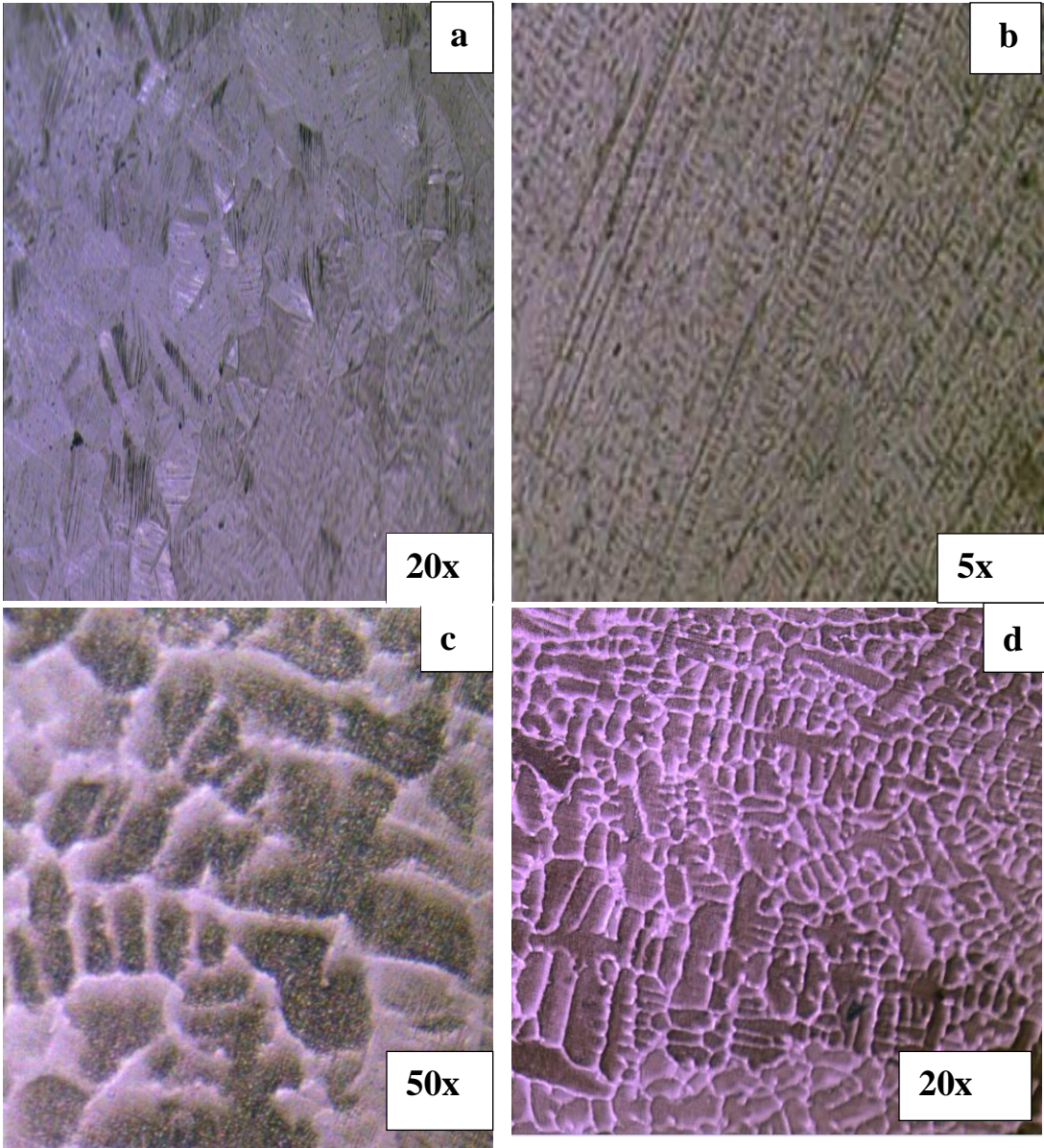nitrogen content (0.3 bar nitrogen).Figure 4.7 (d) illustrates the fine intergranular and aligned boundaries.



**Figure 4.7: Optical micrographs of 316SS (a) untreated (b) Ar mleted (c) 0.1 bar N$_2$ (d) 0.3 bars N$_2$**
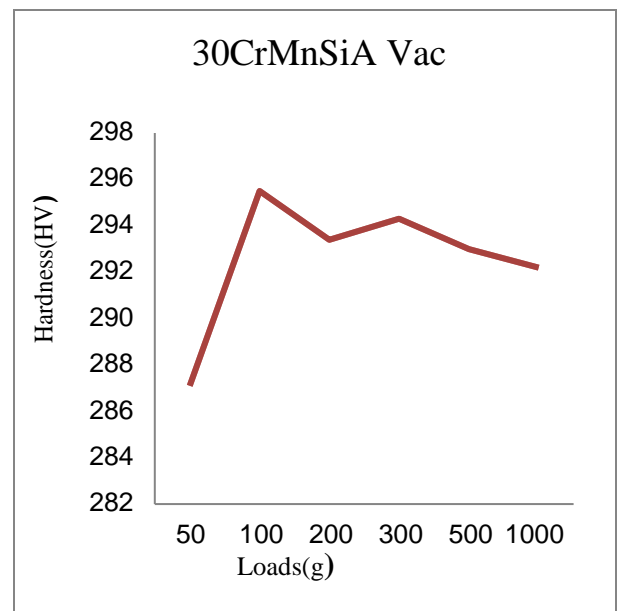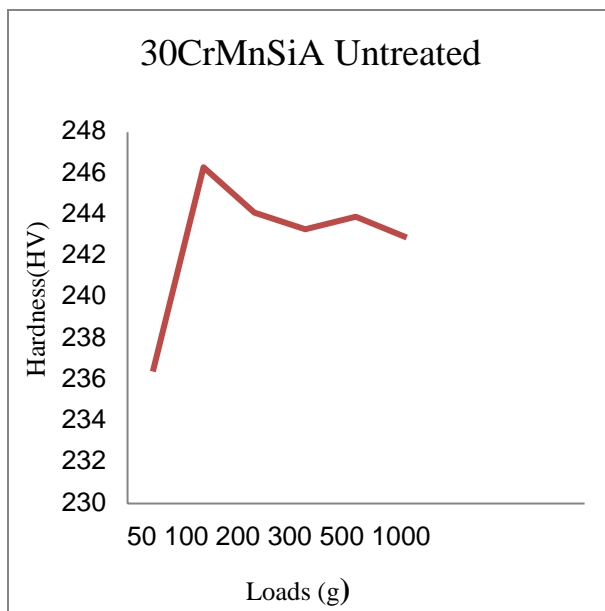
## 4.4. Physical Properties

## 4.4.1 Vickers Microhardness Test

Berns et al reported, nitrogen is a very effective solid solution hardener which provides high strength without substantial decrease in rupture strength but also improves the corrosion resistance of the steel.As a result of variation in the nitrogen content there are alterations in the hardening properties of experimental specimens. This is confirmed for the 30CrMnSiA steel and 316 Stainless Steel. Being synthesized in the same working conditions, the 30CrMnSiA steel and 316SS with 0.3bar $N_2$ content have prominently higher hardness as compared to the corresponding steel samples with lower nitrogen content (0.1 bar nitrogen). With the increase of nitrogen content from 0.1bar to 0.3 bars, the Vickers microhardness values increase from 359.82HV to 514.86 HV and from 268.52HV to 345.76HV for 30CrMnSiA and 316SS respectively. For both steel samples the higher nitrogen content is associated to the higher hardness. The crucial features of this nitrogen hardening were verified by Sandstrom and Bergquist. For untreated and Ar melted steel samples observed hardness is extremely low because of absence of any nitrogen content. After melting at 3500ºC in Arc melting furnace followed by quenching at 840ºC, the hardness of 30CrMnSiA Steel and 316SS (0.3bar nitrogen) have hardness values 514.86 and 345.76 HV respectively. These microhardness values were higher as compared to the untreated samples of 30CrMnSiA Steel and 316SS ranges from 244.1HV to 158.18HV respectively. Melting process carried out in nitrogen atmosphere thus effectively improves the microhardness values for both steels **[44] [45] [46].**

Table 8 represents the Vickers microhardness of 30CrMnSiA steel samples melted in argon atmosphere and various nitrogen pressures 0.1 and 0.3 bars respectively in Arc melting furnace.

**Table 6: Vickers microhardness of 30CrMnSiA steel samples**

| AISI 30CrMnSiA | Average Vickers Hardness (Hv) |
|---|---|
| Untreated | 244.10 |
| Ar melted | 293.68 |
| Melted at 0.1bar $N_2$ | 359.82 |
| Melted at 0.3 bar $N_2$ | 514.86 |



30CrMnSiA Untreated



30CrMnSiA Vac

## 30CrMnSiA 0.1Bar
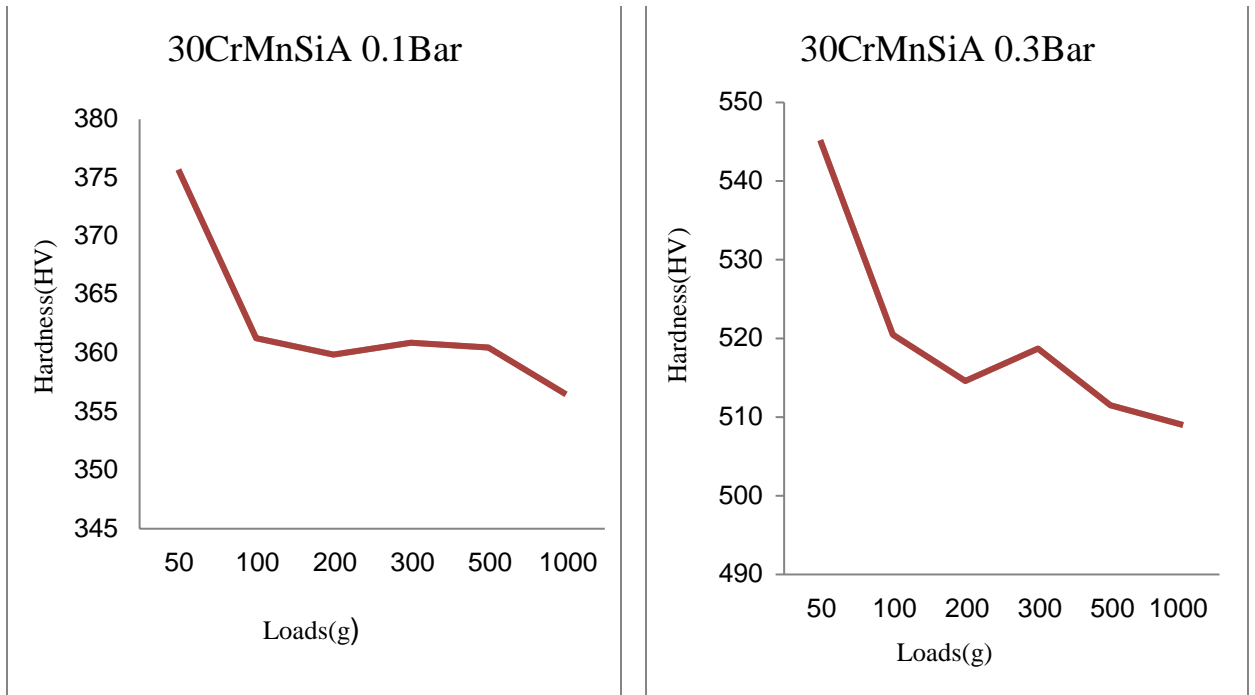
Hardness(HV) vs Loads(g)

## 30CrMnSiA 0.3Bar

Hardness(HV) vs Loads(g)

**Figure 4.8: Hardness of 30CMnSiA steel (a) untreated (b) Ar melted (c) 0.1 bar N$_2$ (d) 0.3 bar N$_2$**



## 30CrMnSiA Steel

Hardness (HV) vs Loads(g)

30CrMnSiA Untreated — 30CrMnSiA Vacuum — 30CrMnSiA 0.1bar — 30CrMnSiA 0.3bar

**Figure 4.9: Summarized hardness of 30CrMnSiA Steel samples**

**Table 7: Hardness of 316SS samples**

| AISI 316SS | Average Vickers Hardness (Hv) |
|---|---|
| Untreated | 158.18 |
| Ar melted | 207.52 |
| Melted at 0.1bar $N_2$ | 268.52 |
| Melted at 0.3 bar $N_2$ | 345.76 |

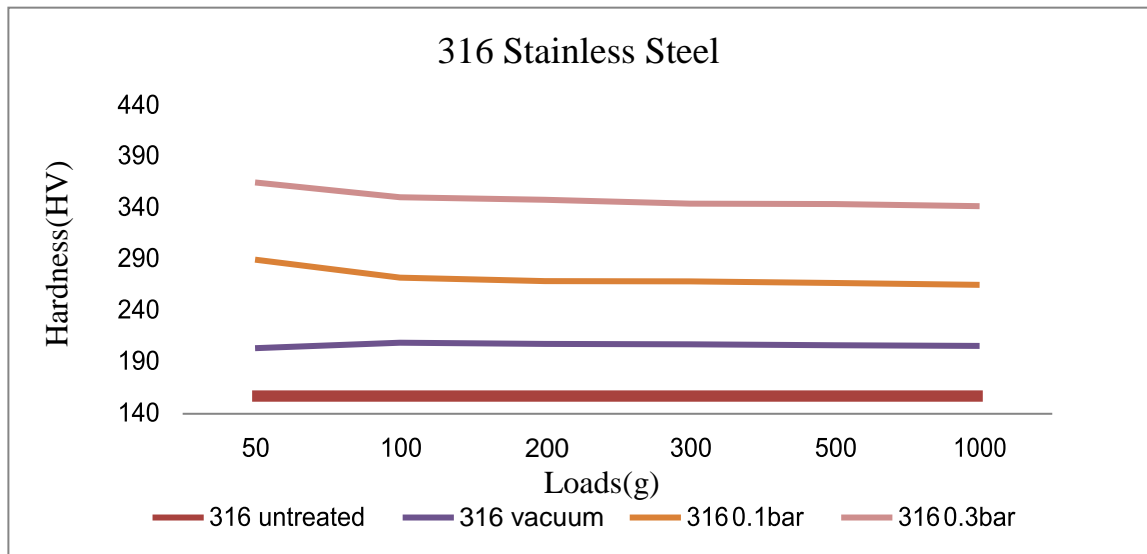**Figure 4.10: Hardness of 316SS (a) untreated (b) Ar melted (c) 0.1 bar $N_2$ (d) 0.3 bar $N_2$**



**Figure4.11 : Summarized Hardness of 316SS samples**

## 4.5 Corrosion testing

For the comparison of corrosion resistance of 30CrMnSiA steel and 316SS synthesized in argon and nitrogen atmosphere in Arc melting furnace with untreated material, polarization resistance and Tafel scan tests were measured in 3.5wt% of NaCl solution. Tafel scans describes that the corrosion rates were notably decreased from untreated to nitrogen added samples. Corrosion rate of 30CrMnSiA for Ar melted (13.15mpy), 0.1 bar nitrogen (11.21mpy) and 0.3bar nitrogen steel sample (6.70mpy) explains that as nitrogen content is increased, the corrosion rate is decreased. For 316SS corrosion rates were from 0.05519mpy and 0.02677mpy for Ar melted and 0.3 bar nitrogen steel sample respectively. Greater corrosion resistance properties were observed in nitrogen comprising steel as compared to non –nitrogen steel samples of similar composition. Addition of nitrogen influences thenature of semiconducting passive film, also increases crevice and pitting corrosion resistance **[47] [48][49].**The effect of nitrogen addition on corrosion rate of both steel grades was more pronounced for 0.3bar nitrogen condition. From the table (8-11), it can be observed that corrosion resistance increases correspondingly to the nitrogen content. Influence of nitrogen addition in stainless steels has been profusely investigated, and it is observed that by the favorable involvement ofnitrogen, the corrosion resistance can be enhanced noticeably**[50] [51][52].**Thus from the results it is concluded that the nitrogen addition improves the corrosion resistance in both steel grades.

## Tafel Scan

Tafel technique is used to obtain an accurate estimate of the corrosion rate.The graphical output of the experiment is a plot of log(current) versus potential.

Analysis of the curve can yield the following types of information:

- Corrosion potential.

Corrosion current and corrosion rate

## Polarization resistance

Polarization resistance is a non-destructive technique that is used to achieve a rapid estimate of corrosion rate of a metal in a solution. Current readings are taken during a very small, slow curve of the potential. Current-vs- voltage curve is approximately linear. A linear fit of the data to a standard model yields an approximation of the Polarization Resistance $R_p$. which is then used to calculate corrosion rate. .

Polarization resistance (Rp) is the ratio of applied potential and resulting current**.**

$$R_P = \left(\frac{\Delta E}{\Delta i}\right)_{\Delta E \to 0}$$

High Rp of a metal indicates high corrosion resistance and low Rp suggests low corrosion resistance. This "resistance" is inversely related to the uniform corrosion rate of a metal. The polarization resistance technique is shorter scan so acquires data more quickly than the Tafel technique

## 4.5.1. NaCl electrolyte

With the increase in nitrogen content, the corrosion resistance behavior of prepared steel is much enhanced.According to ammonium theory, ammonium ions formation leads to the increase in pH value that support repassivation**[53].**

According to ammonium theory nitrogen reacts as:

$[N]+ 4H^+ +3e^- \to NH^+_4$
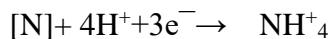
The general idea of surface enrichment theory is build-up of nitrogen in the passive layer. Negatively charged $N^-$ are supposed to enrich at the metal oxide interface. The passivating film of metal that is considered to be immune from corrosion is affected. These negative ions lower the potential gradient and also reject the chloride ions present in the solution. This consequently leads to low corrosion rate and supports repassivation.

.

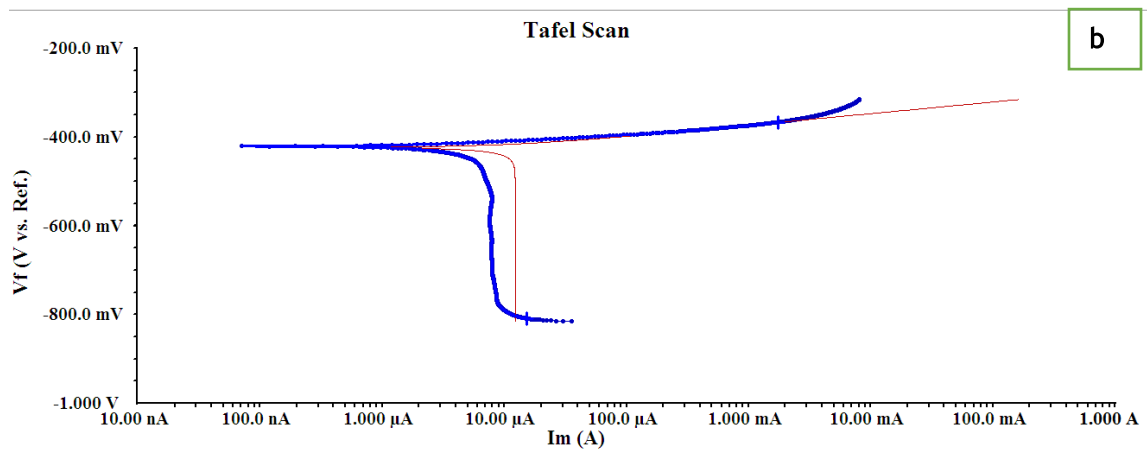**Table 8: Ecorr, Icorr and Corrosion rate of 30CrMnSiA steel in Nacl electrolyte**

| Sample 30CrMnSiA | $E_{corr}$(mV) | $I_{corr}$(μA) | Corrosion rate (mpy) | Corrosion rate (μm*) |
|---|---|---|---|---|
| Ar melted | -414.7 | 18.12 | 13.15 | 333.75 |
| 0.1 bar $N_2$ | -423.7 | 12.26 | 11.21 | 284.73 |
| 0.3 bar $N_2$ | -420.2 | 7.332 | 6.70 | 170.18 |

*Micro meter per year

## 30CrMnSiA Ar melted
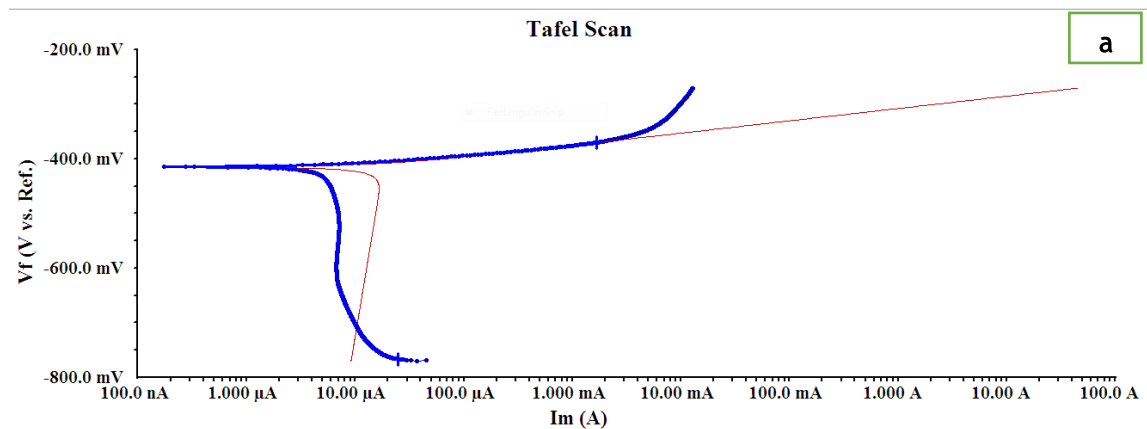


## 30CrMnSiA melted at 0.1bar nitrogen

# 30CrMnSiA 0.3 bar nitrogen
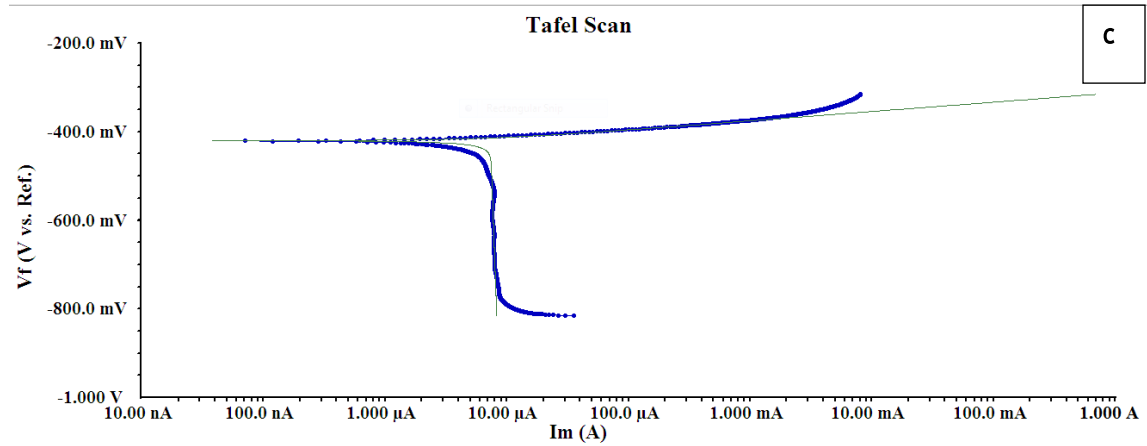


**Figure 4.12: Tafel scans of30CrMnSiA at scan rate of 0.467mv/sec (a) Ar melted (b) 0.1 bar N₂ (c) 0.3 bar N₂inNacl electrolyte**

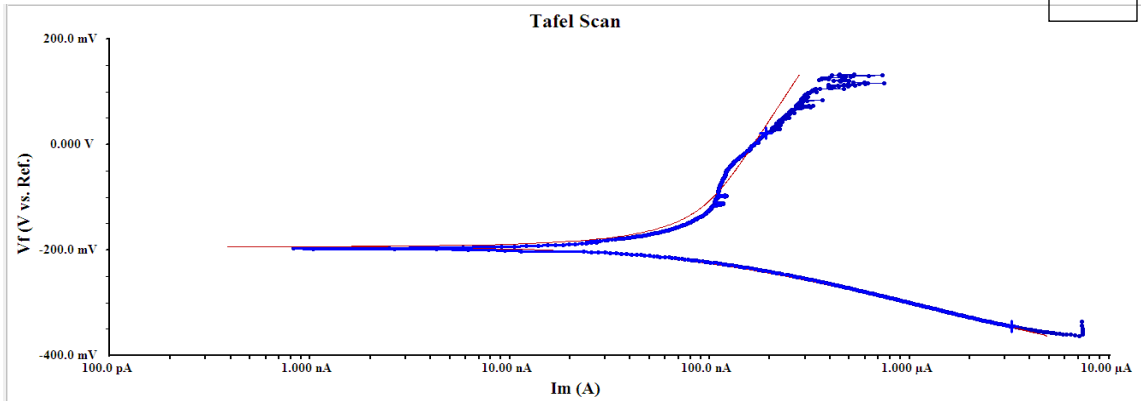**Table 9: Ecorr, Icorr and Corrosion rate of 316SS in Nacl electrolyte**

| Sample 316 SS | $E_{corr}$(mV) | $I_{corr}$(nA) | Corrosion rate (Mpy) | Corrosion rate (µmpy*) |
|---|---|---|---|---|
| Ar melted | -153.3 | 79.72 | 0.055 | 1.401 |
| 0.1 bar N₂ | -193.8 | 75.07 | 0.049 | 1.244 |
| 0.3 bar N₂ | -157.1 | 42.18 | 0.026 | 0.679 |

*micro meter per year
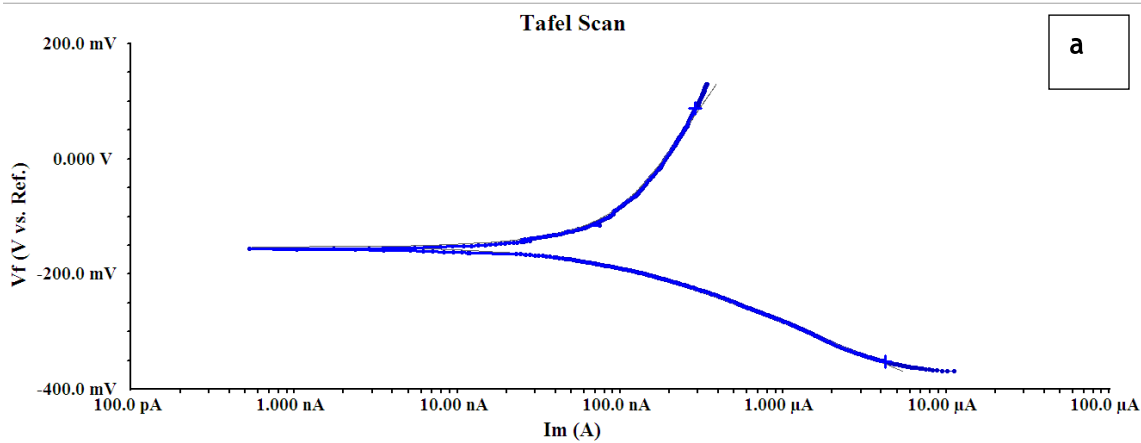
## 316 Ar melted



## 316 0.1 bar nitrogen
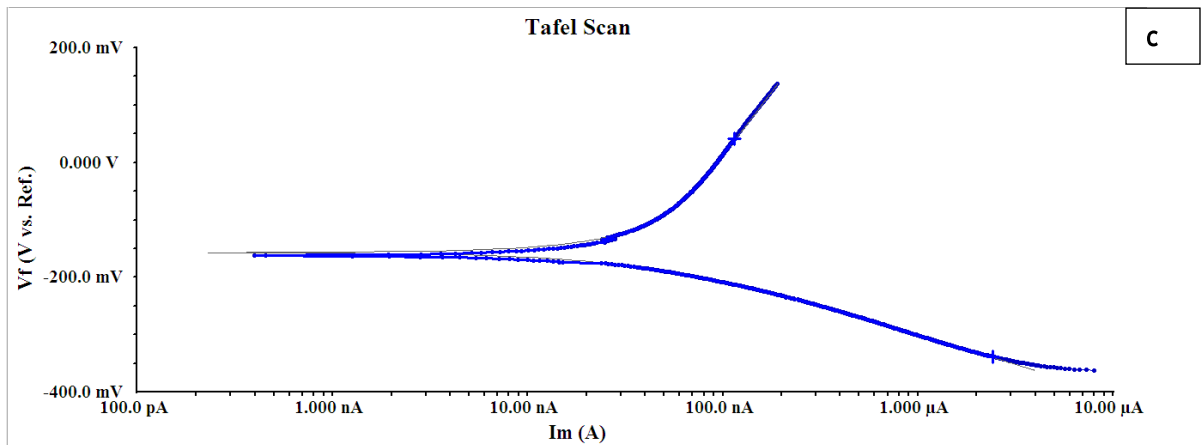
## 316 0.3 bar nitrogen



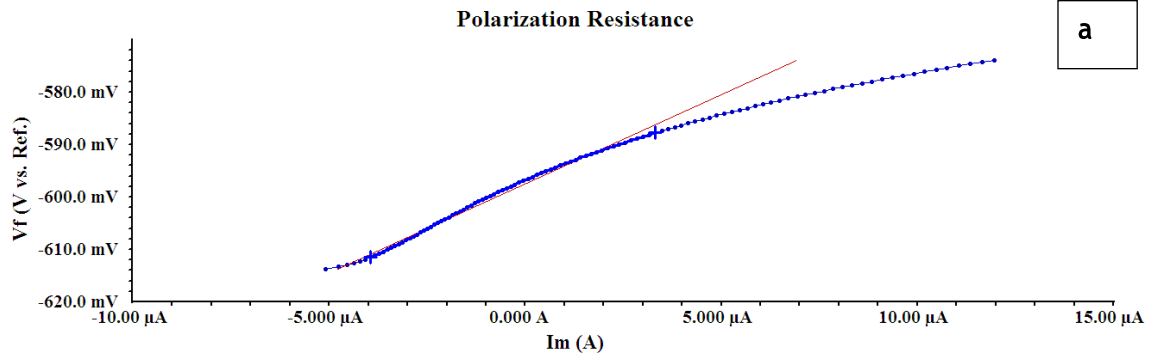**Figure 4.13: Tafel scans of 316SS (a) Ar melted (b) 0.1 bar N$_2$ (c) 0.3 bar N$_2$in Nacl electrolyte**

Polarization resistance

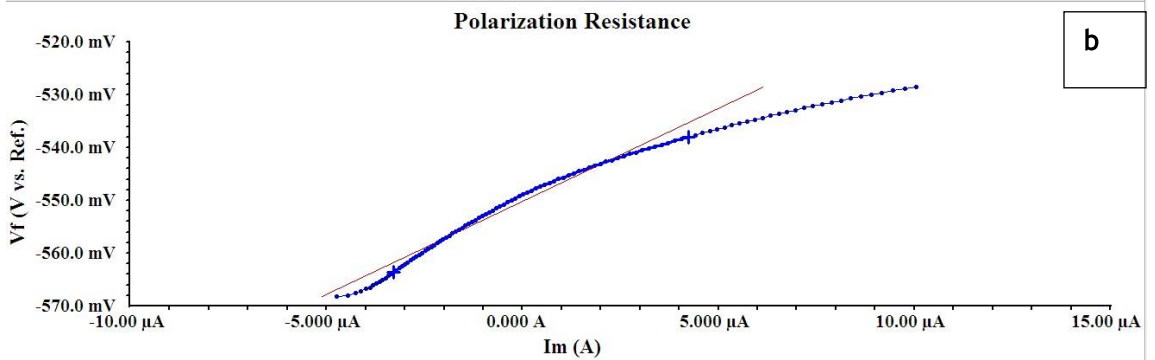**Table 10: Rp, Ecorr, Icorr and Corrosion rates of 30CrMnSiA steel samples in Nacl electrolyte**

| Sample 30CrMnSiA | E$_{corr}$(mV) | I$_{corr}$(μA) | Corrosion rate(Mpy) | Polarization resistance(Rp) (kohm) | Corrosion rate (μmpy*) |
|---|---|---|---|---|---|
| Ar melted | -596.9 | 7.66 | 10.00 | 3.400 | 254.000 |
| 0.1 bar N$_2$ | -548.9 | 7.379 | 6.744 | 3.531 | 171.297 |
| 0.3 bar N$_2$ | -639.8 | 5.273 | 4.819 | 4.941 | 122.402 |

**\*micro meter per year**

## 30 CrMnSiA Ar melted
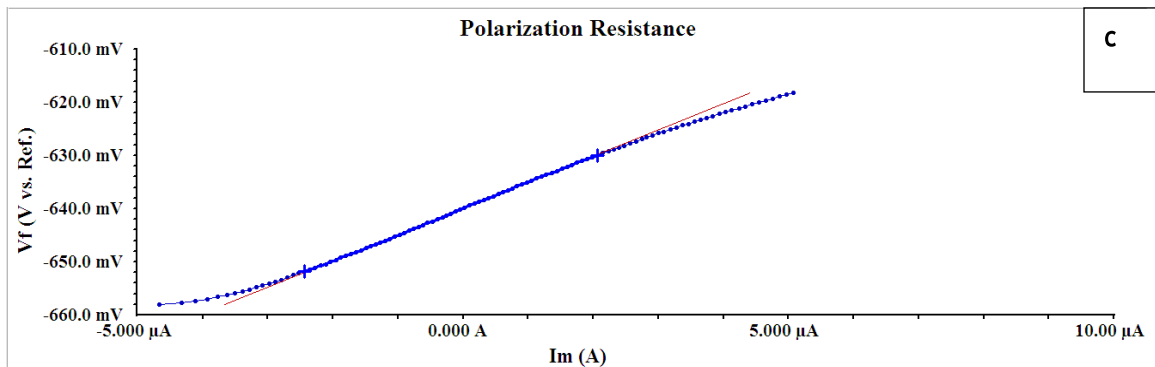


## 30CrMnSiA 0.1 bar



## 30CrMnSiA 0.3 bar



**Figure 4.14: Polarization resistance graphs of 30CrMnSiA steel (a) Ar melted (b) 0.1 bar N$_2$ (c) 0.3 bar N$_2$in Nacl electrolyte**

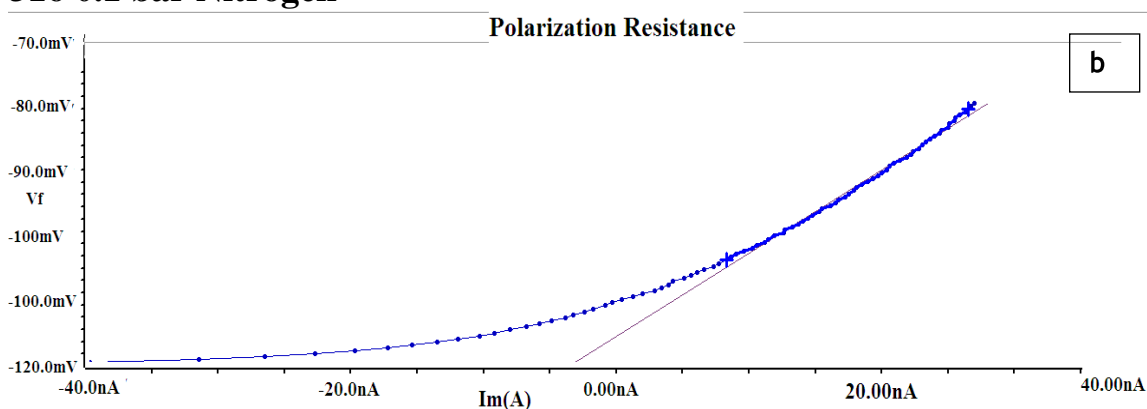**Table 11: Ecorr, Icorr and Corrosion rates of 316SS samples in Nacl electrolyte**

| Sample id | $E_{corr}$(mV) | $I_{corr}$(μA) | Corrosion rate (Mpy) | Polarization resistance(Rp) (kohm) | Corrosion rate (μmpy*) |
|---|---|---|---|---|---|
| 316SS Ar melted | -67.11 | 30.47 | 0.017 | 901.8 | 0.431 |
| 316SS 0.1 bar $N_2$ | -110.4 | 20.80 | 0.012 | 1253 | 0.304 |
| 316SS 0.3 bar $N_2$ | -69.29 | 16.36 | 0.010 | 1592 | 0.254 |

**\*micro meter per year**
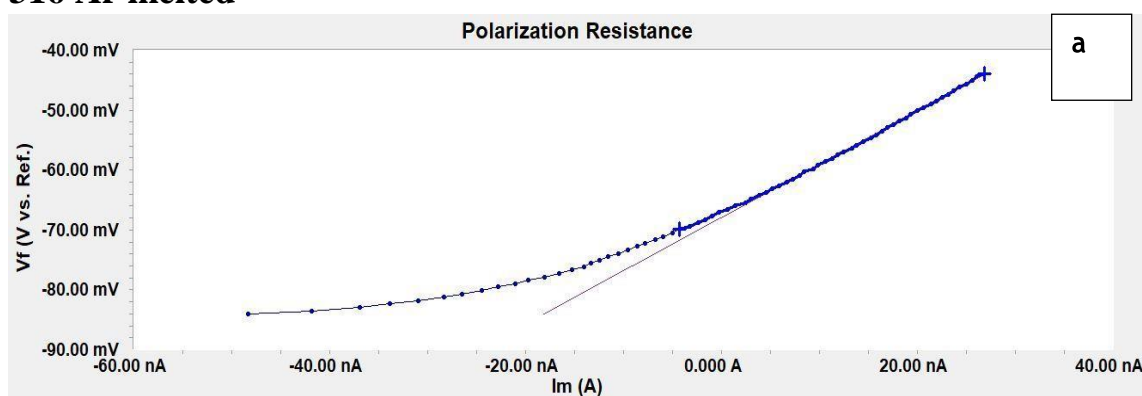
## 316 Ar melted



## 316 0.1 bar Nitrogen
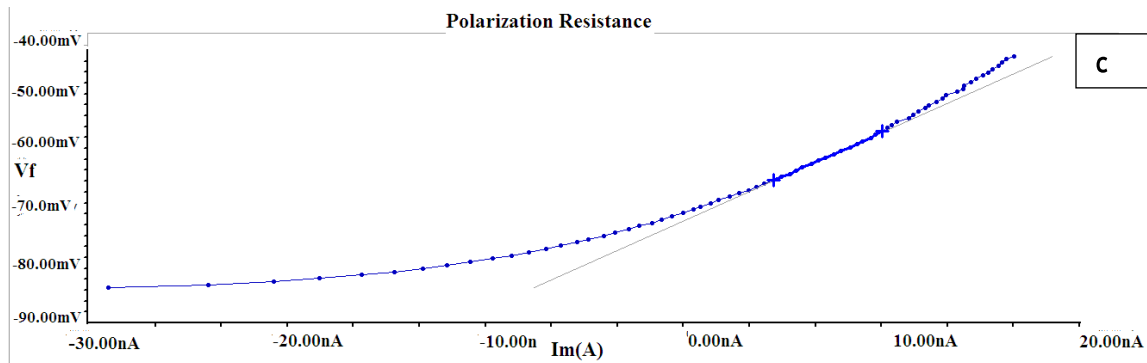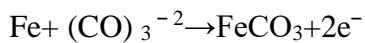
**316 0.3 bar nitrogen**



**Figure 4.15: Polarization resistance of 316SS (a) Ar melted (b) 0.1 bar $N_2$ (c) 0.3 bar $N_2$in Nacl electrolyte**

## 4.5.2 $Na_2CO_3$ Electrolyte

In carbonate solutions such as sodium carbonate, Thomas, et al linked the increase in anodic peak with carbonate concentration that leads to the formation of $FeCO_3$.

$Fe+ (CO)_3{}^{-2} \rightarrow FeCO_3 + 2e^-$

Lee, et al reported the color change of passive film occurs due to carbonates reaction with metal resulting in the formation of green rust. They reported that carbonate complex $Fe^{2+}$ions make the $FeCO_3.H_2O$ films increasingly more porous. Therefore makes corrosion rates higher.

Nitrogen in the designed steel results in the formation of formation of $NO_3{}^-$. Consequently formation of $NH_4{}^+$resulted and their high amount is observed immediately above the redox boundary **[54].** $NH_4+$ ions block the boundary and stop the exchange of ions thus reduce the corrosion rate.

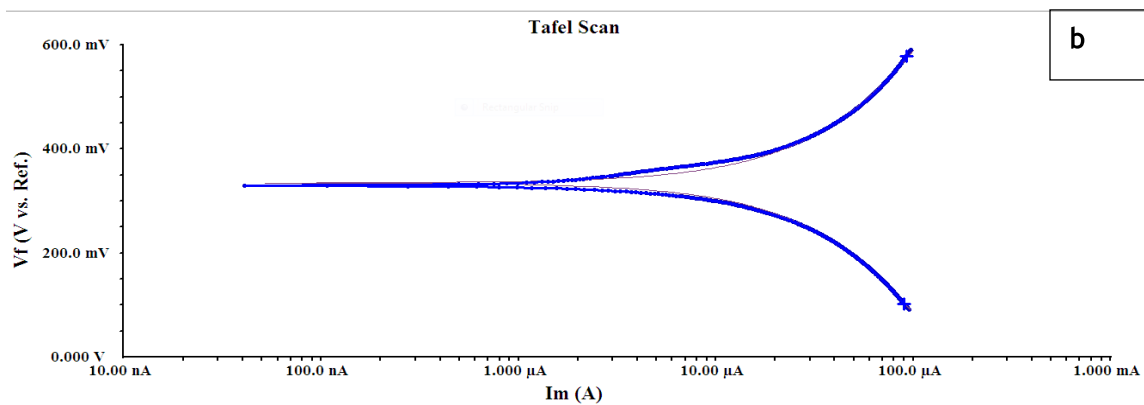**Table 12: Ecorr, Icorr and Corrosion rates of 30 CrMnSiA steelsamples in Na₂CO₃ electrolyte**

| Sample 30CrMnSiA | $E_{corr}$(mV) | $I_{corr}$(µA) | Corrosion rate (mpy) | Corrosion rate (µmpy) |
|---|---|---|---|---|
| Ar melted | 360.2 | 55.47 | 40.23 | 1021.84 |
| 0.1 bar $N_2$ | 334.6 | 41.98 | 35.52 | 902.20 |
| 0.3 bar $N_2$ | 340.8 | 27.66 | 25.28 | 642.11 |

**\*µmpy micrometer per year**

## 30 CrMnSiA Ar melted
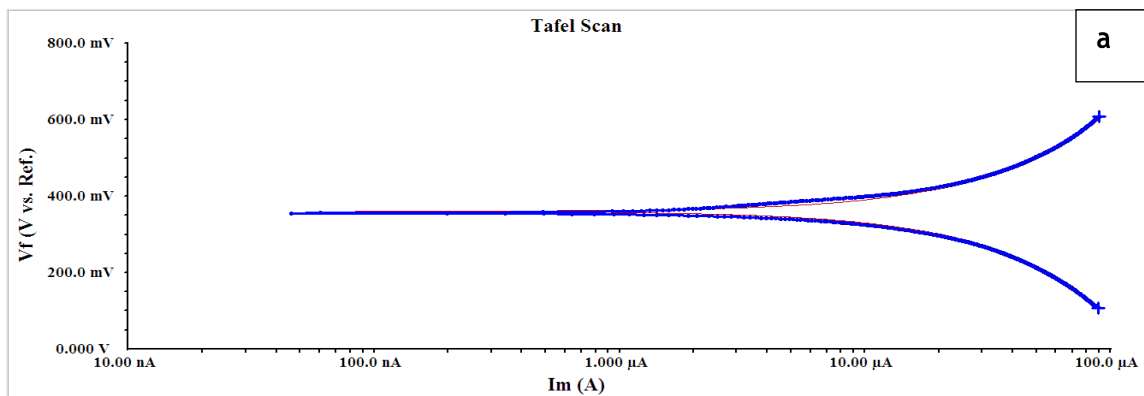


## 30 CrMnSiA 0.1Bar N₂
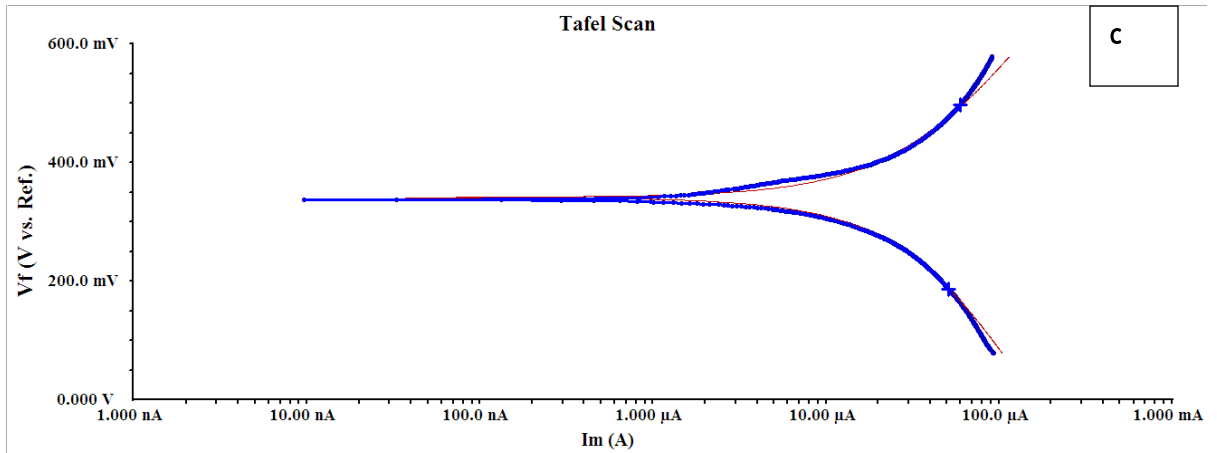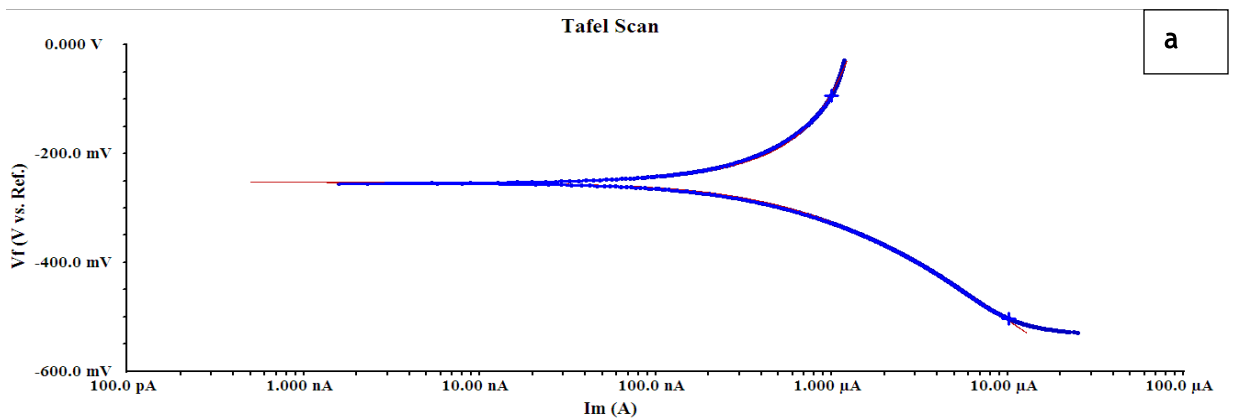
## 30 CrMnSiA 0.3Bar N$_2$



**Figure 4.16: Tafel Scans of 30 CrMnSiA (a) Ar melted (b) 0.1 bar N$_2$ (c) 0.3 bar N$_2$in Na$_2$CO$_3$ electrolyte**
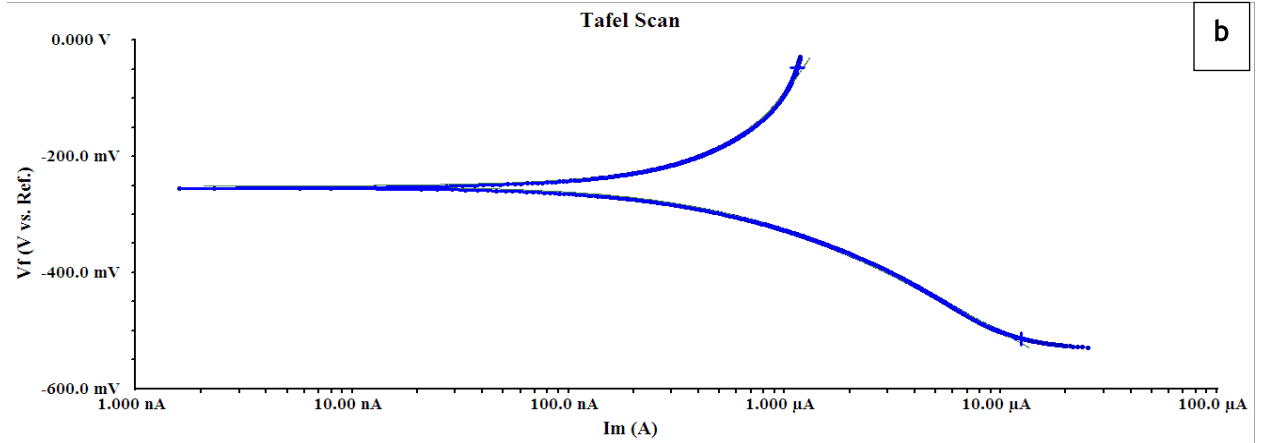
**Table 13: Ecorr, Icorr and Corrosion rates of 316SS samples in Na$_2$co$_3$ electrolyte**

| Sample 316SS | E$_{corr}$(mV) | I$_{corr}$(nA) | Corrosion rate (mpy) | Corrosion rate (µmpy) |
|---|---|---|---|---|
| Ar melted | -253.1 | 819.1 | 0.5671 | 14.40 |
| 0.1 bar N$_2$ | -251.3 | 657.7 | 0.4553 | 11.56 |
| 0.3 bar N$_2$ | -207.9 | 276.9 | 0.1757 | 4.46 |

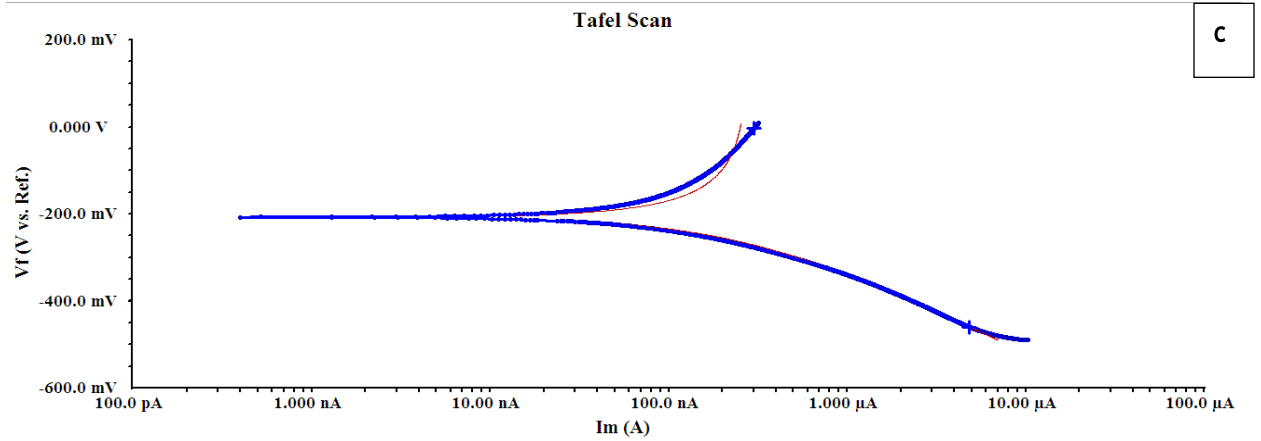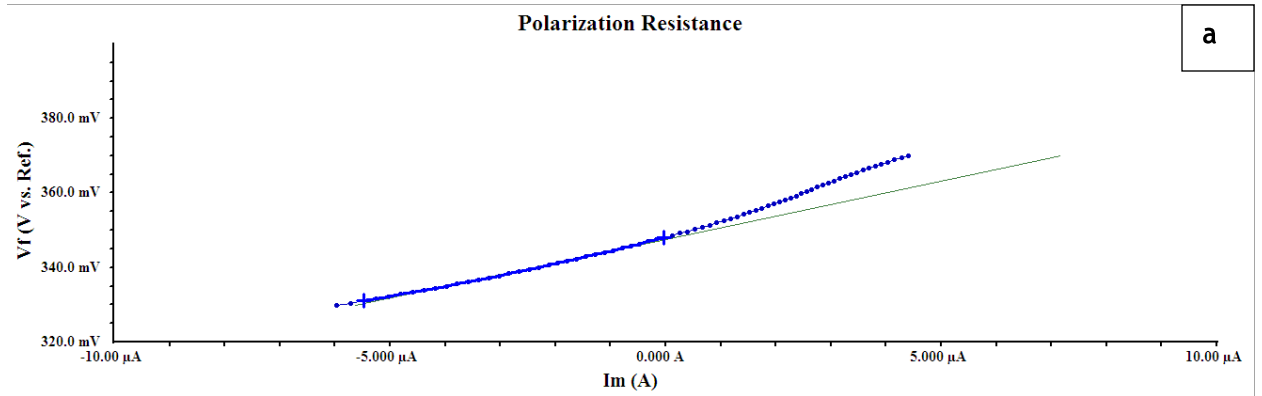## 316 Ar melted

**316SS 0.1bar N₂**



**316SS 0.3 bar N₂**



**Figure 4.17: Tafel Scans of 316SS (a) Ar melted (b) 0.1 bar N₂ (c) 0.3 bar N₂in Na₂CO₃ electrolyte**

Polarization resistance

**Table 14: Ecorr, Icorr and Corrosion rates of 30CrMnSiA Steel samples in Na₂CO₃ electrolyte**

| Sample<br><br>30CrMnSiA Steel | $E_{corr}$(mV) | $I_{corr}$(µA) | Polarization resistance(Rp) kohm | Corrosion rate (mpy) | Corrosion rate (µmpy) |
|---|---|---|---|---|---|
| Ar melted | 348.0 | 8.318 | 3.132 | 6.033 | 153.23 |
| 0.1 bar N₂ | 333.4 | 6.503 | 4.006 | 5.503 | 139.77 |
| 0.3 bar N₂ | 326.7 | 5.542 | 4.701 | 5.064 | 128.62 |

# 30CrMnSiA Steel Ar melted



# 30CrMnSiASteel 0.1bar $N_2$
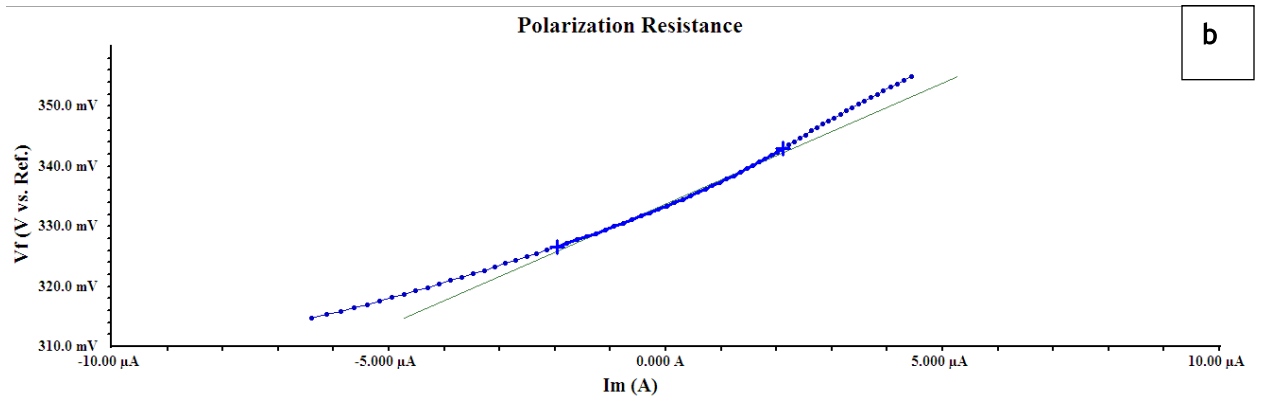


# 30CrMnSiASteel 0.3 bar $N_2$



**Figure 4.18:Polarization resistance of30CrMnSiASteel (a) Ar melted (b) 0.1 bar $N_2$ (c) 0.3 bar $N_2$in $Na_2CO_3$ electrolyte**
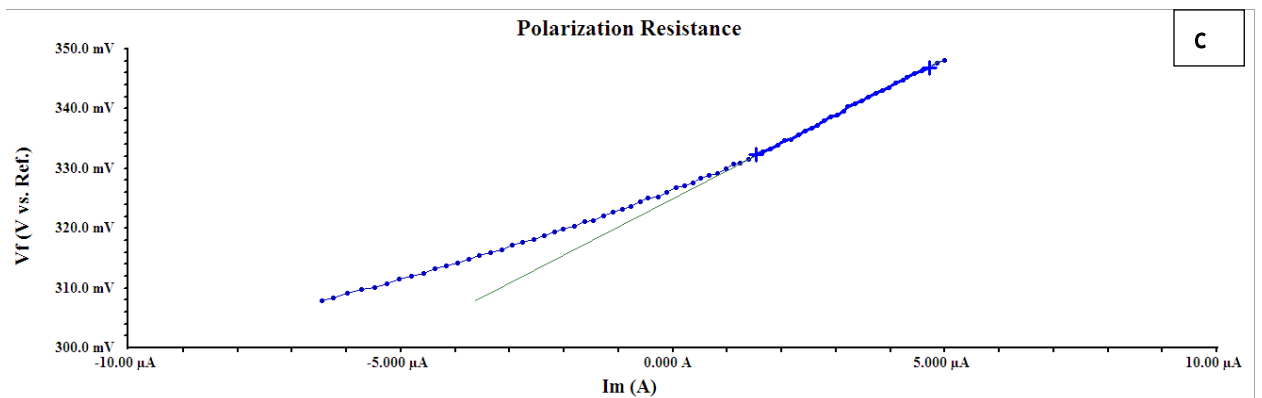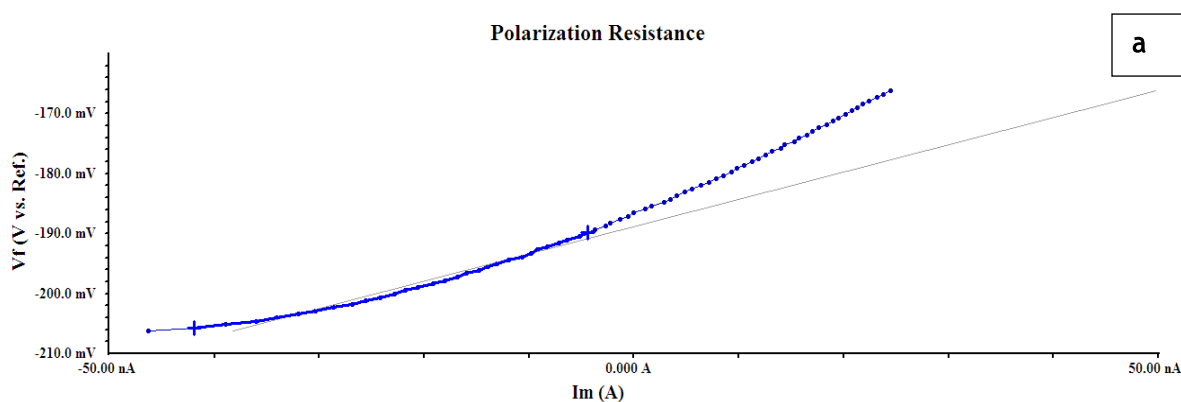
**Table 15: Ecorr, Icorr and Corrosion rates of 316SS samples in Na$_2$CO$_3$ electrolyte**

| Sample 316SS | E$_{corr}$(mV) | I$_{corr}$(nA) | Polarization resistance(Rp) kohm | Corrosion rate (mpy) | Corrosion rate (μmpy) |
|---|---|---|---|---|---|
| Ar melted | -186.5 | 57.12 | 456.1 | 0.03625 | 0.9207 |
| 0.1 bar N$_2$ | -193.5 | 49.50 | 526.3 | 0.03427 | 0.8704 |
| 0.3 bar N$_2$ | -172.8 | 30.48 | 854.7 | 0.01934 | 0.4912 |

## 316SSAr melted



## 316SS 0.1bar N$_2$

**316SS 0.3 bar N₂**



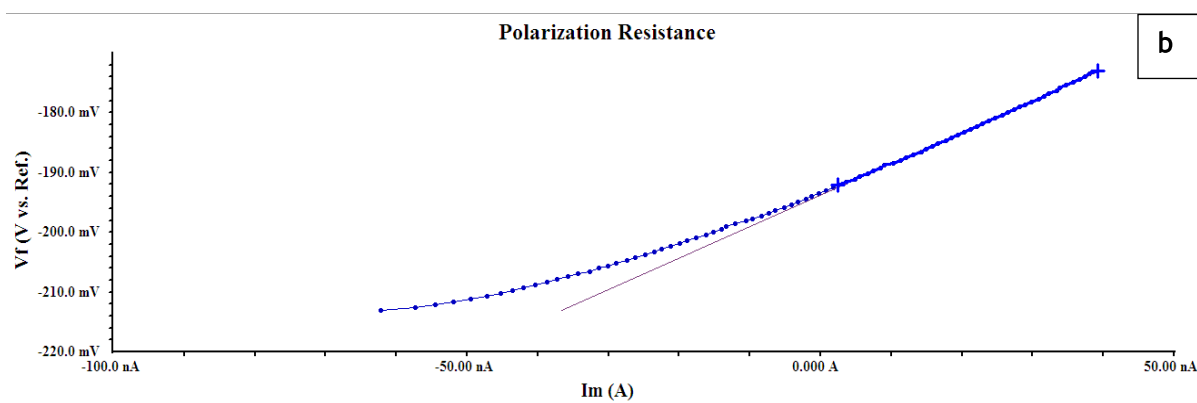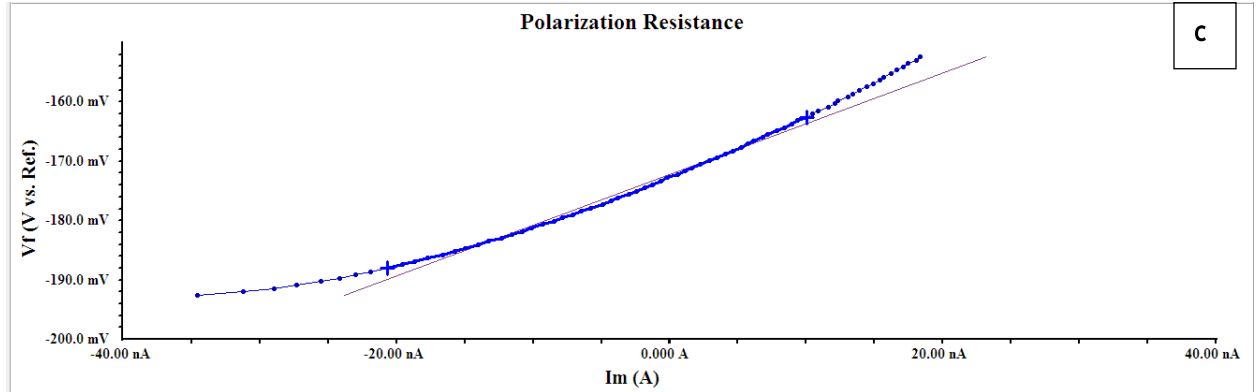**Figure 4.19:Polarization resistance of316SS (a) Ar melted (b) 0.1 bar N₂ (c) 0.3 bar N₂in Na₂CO₃ electrolyte**

## 4.5.3 $H_2SO_4$ electrolyte

When steel comes in contact with dilute sulfuric acid, an immediate attack on the metal takes place with the formation of hydrogen gas and ferrous ions.

- Anodic reaction

  $Fe \rightarrow Fe^{2+} + 2e^-$

- Cathodic reaction

  $2H^+ + 2e^- \rightarrow H_2$

According to Dean and Grab, the rate of corrosion of steels in dilute acids depends strongly on steel chemical compositions, especially the carbon content.When steel contacts sulfuric acid, it reduces to form $H_2$ and the iron oxidizes with the formation of ferrous sulfate ($FeSO_4$).

$H_2SO_4 + Fe \rightarrow FeSO_4 + H_2$
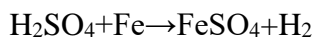
According to Dean and Grab, The $FeSO_4$ adheres to the steel surface and forms a protective layer. This layer prevents the metal against further attack by sulfuric acid. Therefore, the durability of steel depends on the preservation of the $FeSO_4$ layer. But the FeSO4 layer is soft and poorly adherent, which means that it can be easily damaged. In the case of steel in sulfuric acid, the most important factors that cause an increase in the

corrosion rate are the FeSO$_4$ solubility in the acid, the temperature and the relative movement between the metal and the acid. Shyan Liang Chou and co- workers explained that nitrogen is able to enhance the passivity of steel. High nitrogen steels have more stable passive film as compared to low nitrogen steels in the presence of H$_2$SO$_4$ solution. According to Shyan, addition of nitrogen to steel promotes the passivation of steel in dearetaed sulphuric acid[55].Huang et al reported the formation of NH$_3$in the nitrogen added steel. The high film resistance is attributed to the formation and adsorption of ammonia, which forms a barrier between alloy and the electrolyte. This retarded local corrosion reaction, thus leads to high polarization resistance and low corrosion rate [56].

**Table 16: Ecorr, Icorr and Corrosion rates of 30CrMnSiA Steelsamples in H$_2$SO$_4$ electrolyte**

| Sample 30CrMnSiA Steel | E$_{corr}$(mV) | I$_{corr}$(μA) | Corrosion rate (mpy) | Corrosion rate (μmpy) |
|---|---|---|---|---|
| Ar melted | -564.0 | 703.0 | 509.7 | 12946.3 |
| 0.1 bar N$_2$ | -532.0 | 470.0 | 398.0 | 10109.2 |
| 0.3 bar N$_2$ | -520.0 | 303.0 | 277.0 | 7035.8 |

**\*μmpy micrometer per year**

## 30CrMnSiA Steel Armelted
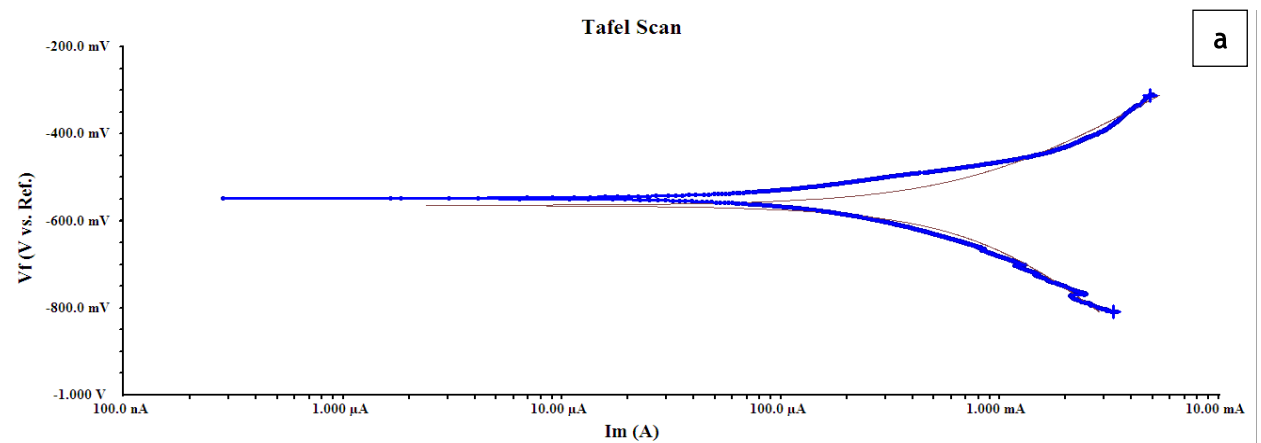
## 30CrMnSiA Steel 0.1 bar N₂
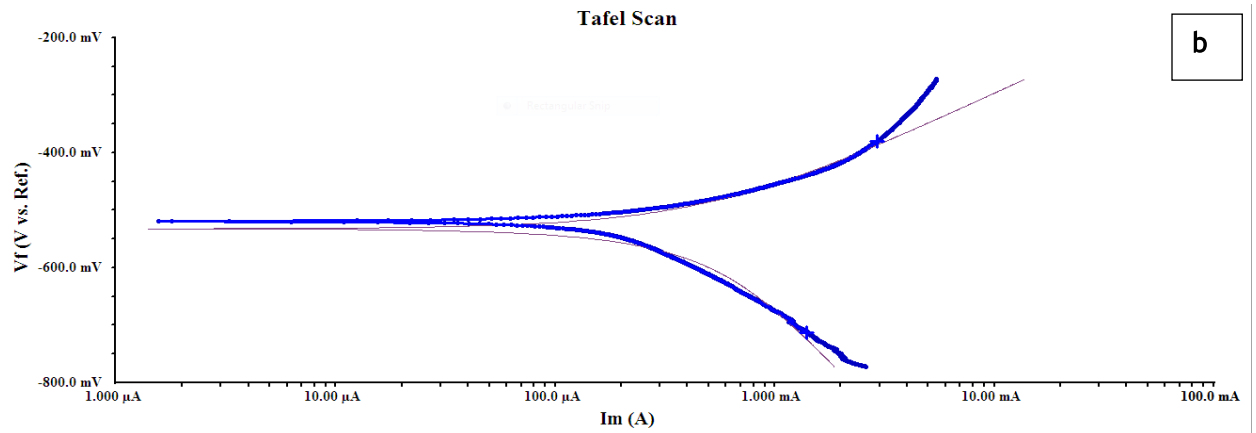


## 30CrMnSiA Steel 0.3 bar N₂
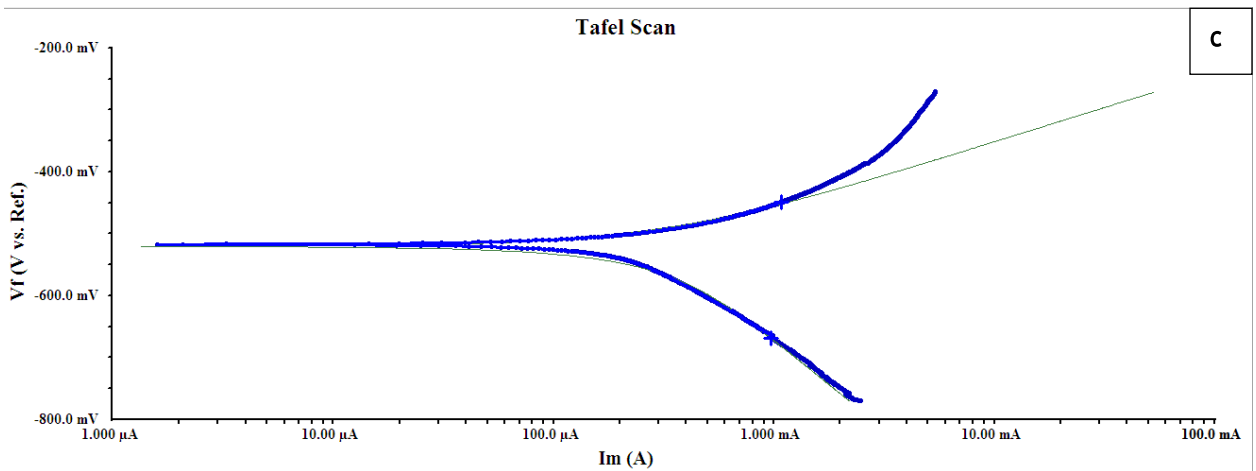


**Figure 4.20: Tafel Scans of 30 CrMnSiA (a) Ar melted (b) 0.1 bar N₂ (c) 0.3 bar in H₂SO₄ electrolyte**

**Table 17: Ecorr, Icorr and Corrosion rates of 316SSsamples in H₂SO₄ electrolyte**

| Sample 316SS | $E_{corr}$(mV) | $I_{corr}$(nA) | Corrosion rate (mpy) | Corrosion rate (μmpy) |
|---|---|---|---|---|
| Ar melted | -109.1 | 2046 | 1.335 | 33.909 |
| 0.1 bar N₂ | -76.80 | 762.8 | 0.528 | 13.411 |
| 0.3 bar N₂ | -75.06 | 345.1 | 0.219 | 5.562 |

*μmpy micrometer per yea

# 316 SS Ar melted
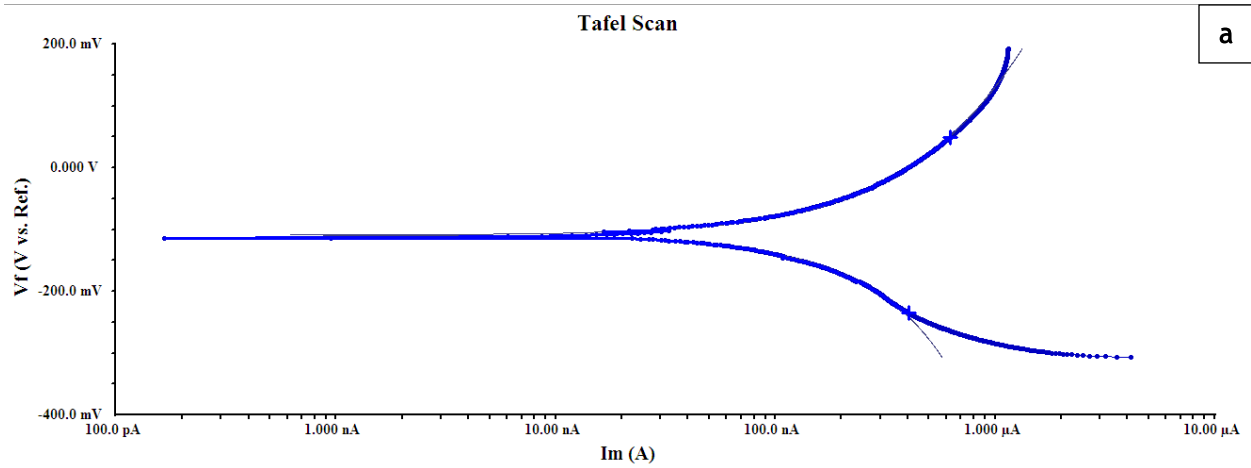


# 316 SS 0.1 bar N₂
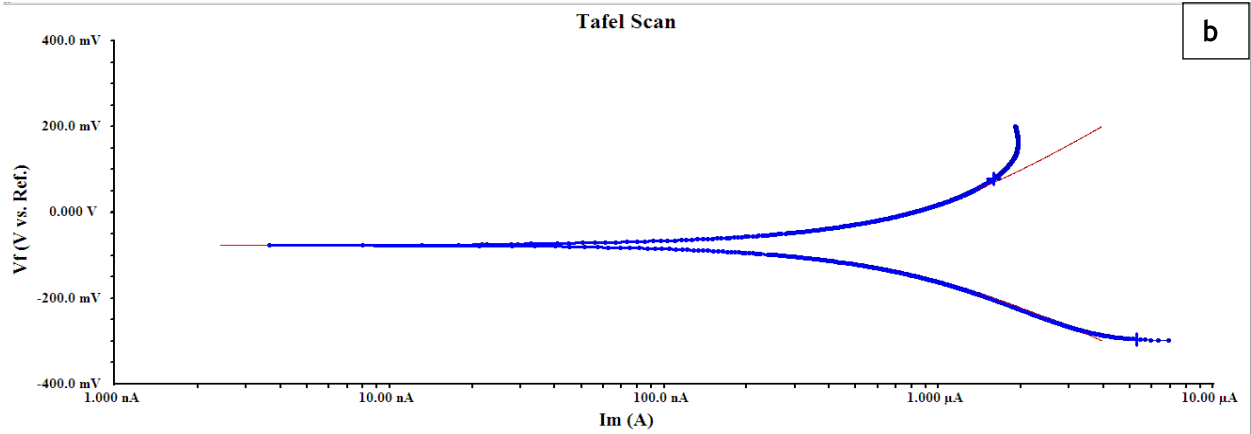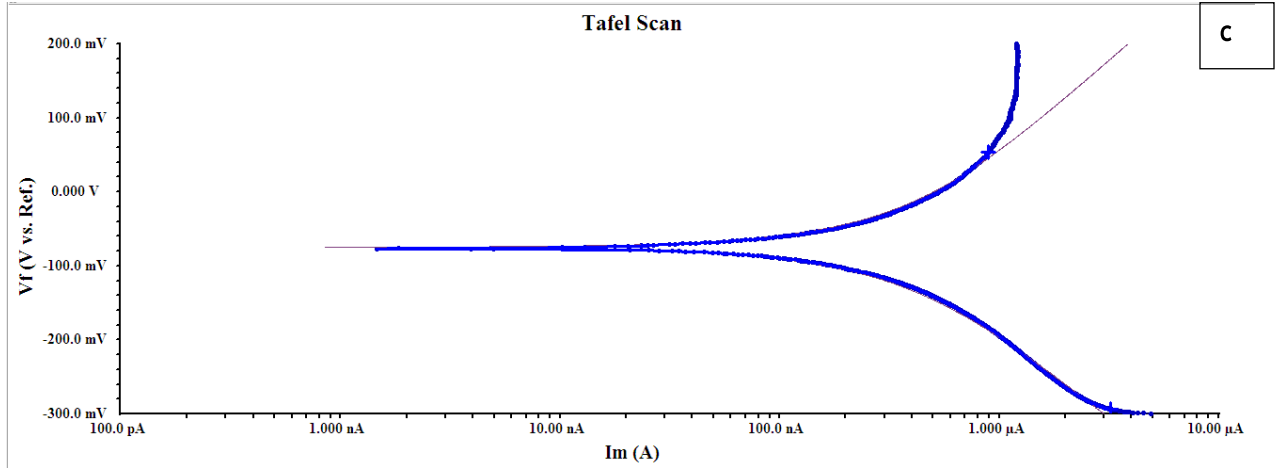
**316 SS 0.3 bar N$_2$**



**Figure 4.21: Tafel Scans of 316SS (a) Ar melted (b) 0.1 bar N$_2$ (c) 0.3 bar in H$_2$SO$_4$ electrolyte**

Polarization resistance

**Table 18: Ecorr, Icorr and Corrosion rates of 30CrMnSiA Steelsamples in H$_2$SO$_4$ electrolyte**

| Sample<br><br>30CrMnSiA Steel | E$_{corr}$(mV) | I$_{corr}$(μA) | Polarization resistance(Rp) (ohm) | Corrosion rate (mpy) | Corrosion rate (μmpy) |
|---|---|---|---|---|---|
| Ar melted | -566.8 | 226.0 | 115.3 | 169.3 | 4300.22 |
| 0.1 bar N$_2$ | -521.5 | 183.5 | 141.9 | 155.3 | 3944.62 |
| 0.3 bar N$_2$ | -521.5 | 159.1 | 163.8 | 134.6 | 3418.84 |

## 30CrMnSiA Ar melted
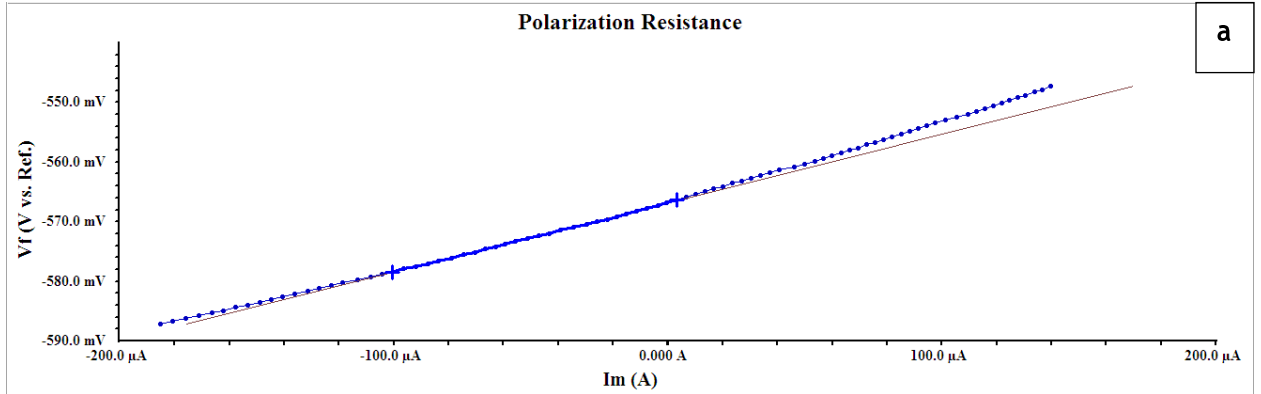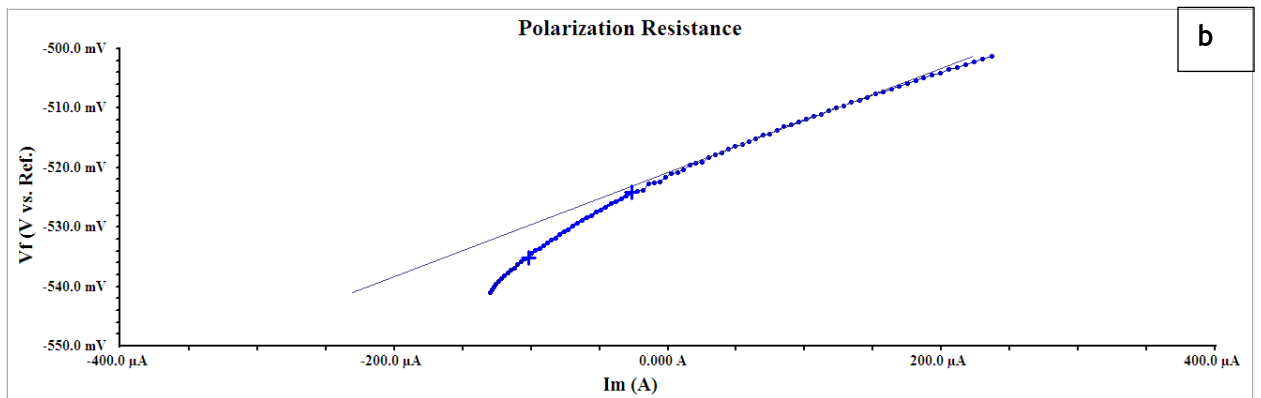


## 30CrMnSiA 0.1 bar N₂
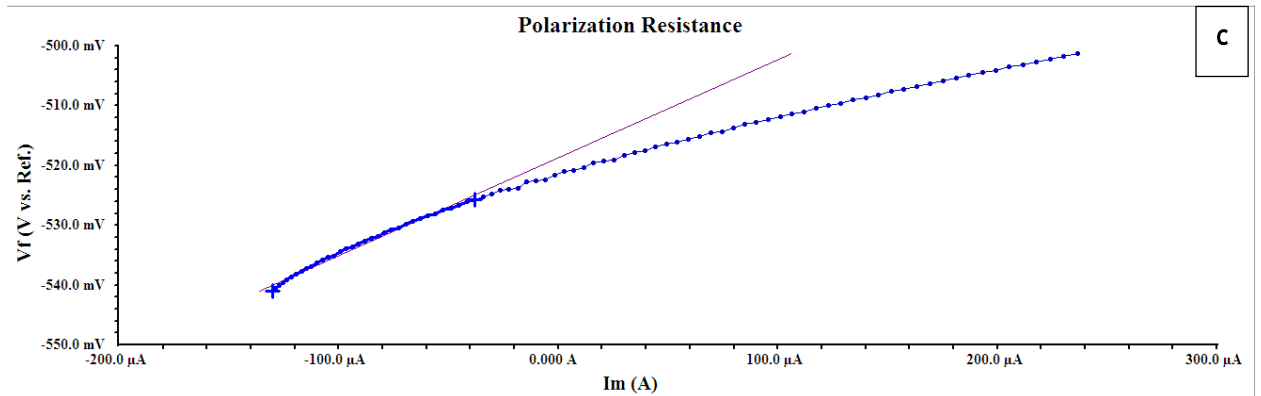


## 30CrMnSiA 0.3 bar N₂



**Figure 4.22:Polarization resistance of30CrMnSiASteel (a) Ar melted (b) 0.1 bar $N_2$ (c) 0.3 bar $N_2$in $H_2SO_4$ electrolyte**

**Table 19: Ecorr, Icorr and Corrosion rates of 316SSSteelsamples in $H_2SO_4$ electrolyte**

| Sample id  316SS | $E_{corr}$(mV) | $I_{corr}$(nA) | Polarization resistance(Rp) kohm | Corrosion rate (mpy) | Corrosion rate (µmpy) |
|---|---|---|---|---|---|
| Ar melted | -63.70 | 497.8 | 52.33 | 0.325 | 8.25 |
| 0.1 bar $N_2$ | -91.79 | 403.6 | 64.55 | 0.263 | 6.68 |
| 0.3 bar $N_2$ | -69.43 | 334.5 | 77.89 | 0.212 | 5.38 |

## 316SS Ar melted
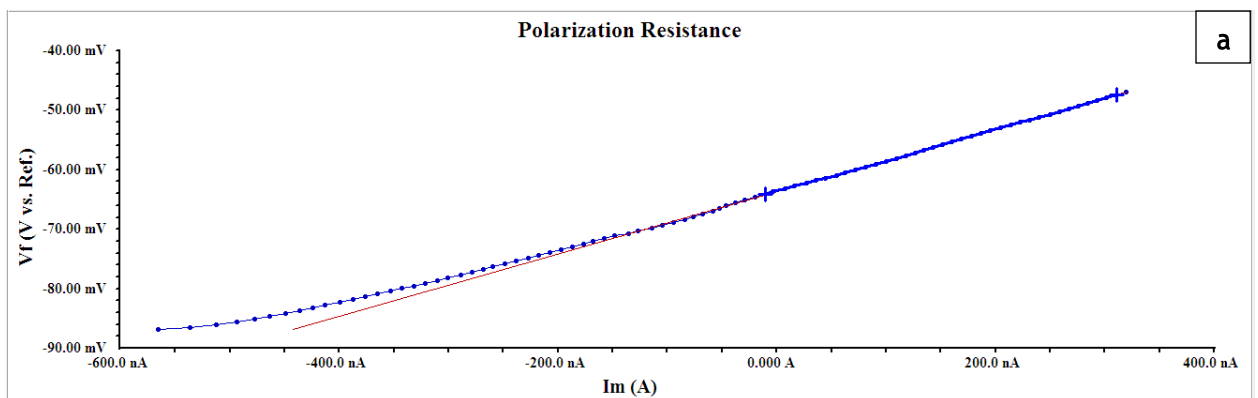


## 316SS 0.1 bar $N_2$
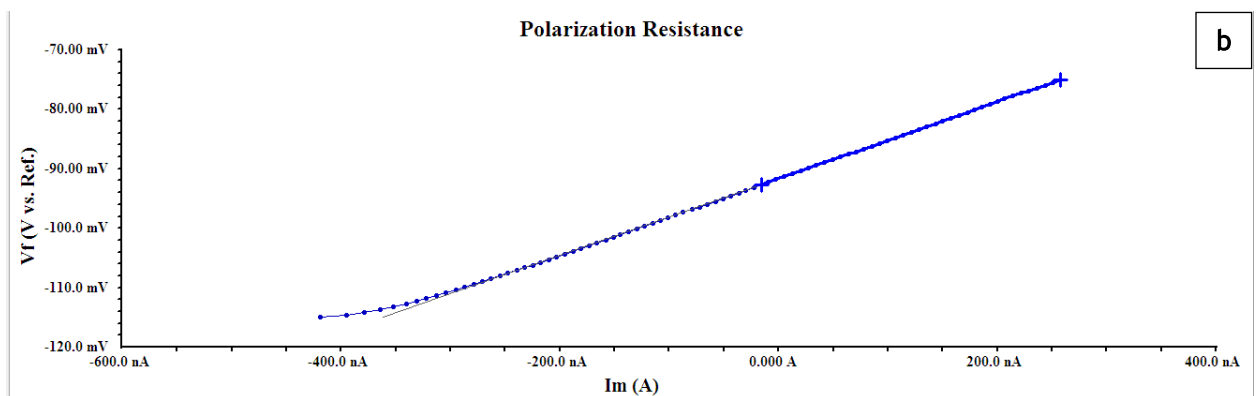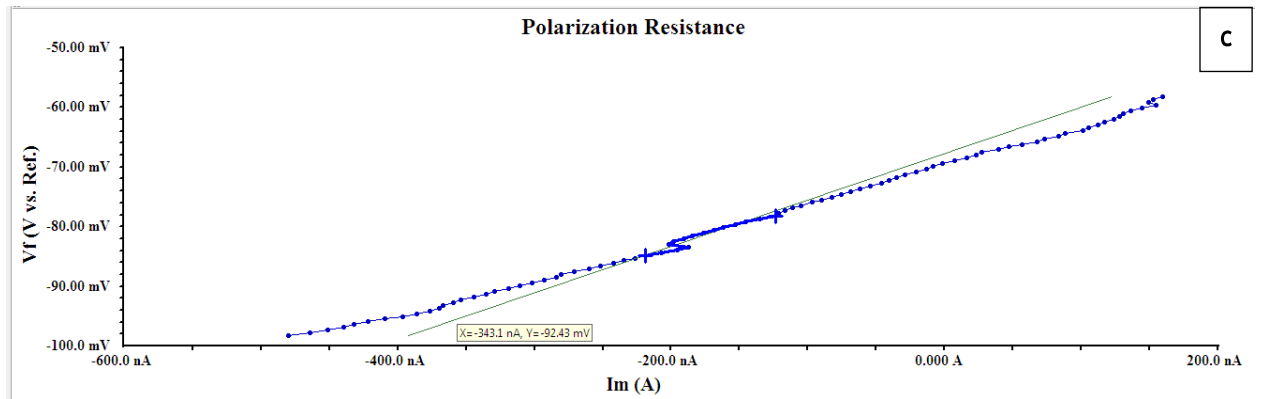
**316SS 0.3 bar N₂**



**Figure 4.23:Polarization resistance of316SS (a) Ar melted (b) 0.1 bar N₂ (c) 0.3 bar N₂in H₂SO₄electrolyte**

## 4.5.4 NaHCO3 electrolyte

Bicarbonates are involved in the anodic step when the surface dissolves and forms a hydroxide-based monolayer. This passivates to form reactive carbonate and oxide-based passive film.

$Fe+H_2O \rightarrow Fe.H_2O$
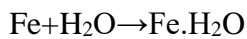
Bicarbonate is reported to be uninvolved with this oxidation step.

$Fe.H_2O \rightarrow FeOH^- + H^+$

$Fe.OH^- \rightarrow FeOH + e^-$
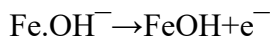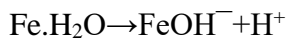
Bicarbonate impedes the formation of FeOH monolayer as it reacts with FeOH to produce complex $FeHCO_3^+$ ions:

$FeOH + HCO_3 \rightarrow FeHCO_3^+ + OH^- + e^-$

Sodium bicarbonates protects and promotes passivation to some extent but it is postulated to disrupt the first oxidation step during which Fe(OH) ₂ forms, as bicarbonate attacks the monolayer, making the dissolving surface bare again. It is proposed that the

73

nitrite ions react with the ferrous ions in the alkaline environment. This forms a passivating layer on steel surface that protect it from corrosion and increases the polarization resistance[57].

**Table 20: Ecorr, Icorr and Corrosion rates of30CrMnSiASteelsamples in NaHCO₃ electrolyte**

| Sample<br><br>30CrMnSiA Steel | E$_{corr}$(mV) | I$_{corr}$(µA) | Corrosion rate (mpy) | Corrosion rate (µmpy) |
|---|---|---|---|---|
| Ar melted | -778.7 | 24.03 | 20.33 | 516.382 |
| 0.1 bar N₂ | -764.7 | 20.44 | 17.30 | 439.41 |
| 0.3 bar N₂ | -768.0 | 15.08 | 12.76 | 324.104 |

**\*µmpy micrometer per year**

## 30CrMnSiA Steel Ar melted
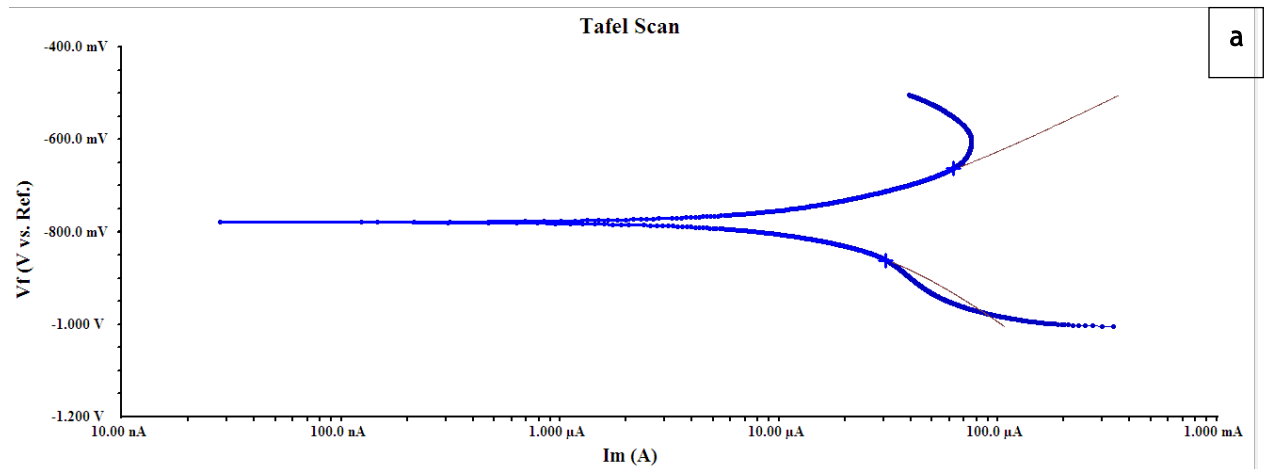
## 30CrMnSiA Steel 0.1 bar N$_2$
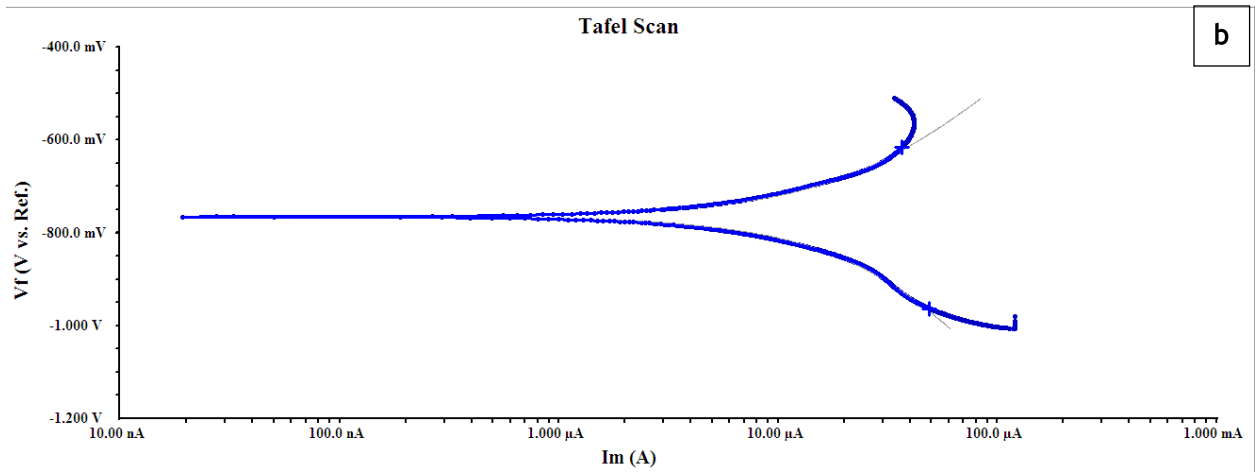


## 30CrMnSiA Steel 0.3 bar N$_2$
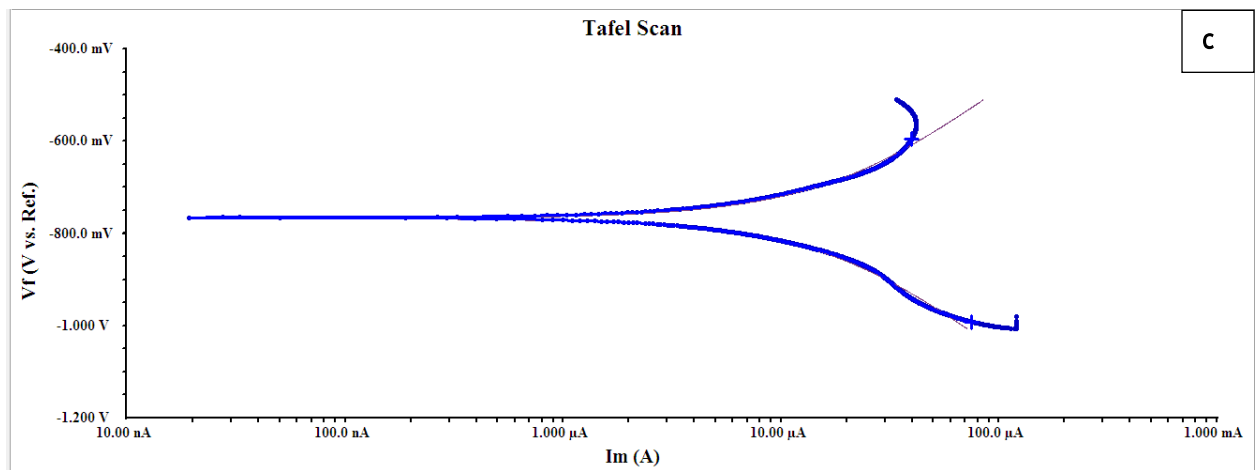


**Figure 4.24: Tafel Scans of 30 CrMnSiA (a) Ar melted (b) 0.1 bar N$_2$ (c) 0.3 bar in NaHCO$_3$ electrolyte**

**Table 21: Ecorr, Icorr and Corrosion rates of316SS Steelsamples in NaHCO₃ electrolyte**

| Sample

316SS | $E_{corr}$(mV) | $I_{corr}$(nA) | Corrosion rate (mpy) | Corrosion rate (μmpy) |
|---|---|---|---|---|
| Ar melted | -227.2 | 298.8 | 0.195 | 4.953 |
| 0.1 bar N₂ | -239.1 | 124.7 | 0.086 | 2.184 |
| 0.3 bar N₂ | -258.7 | 97.27 | 0.061 | 1.549 |

**\*μmpy micrometer per year**

## 316 SS Ar melted
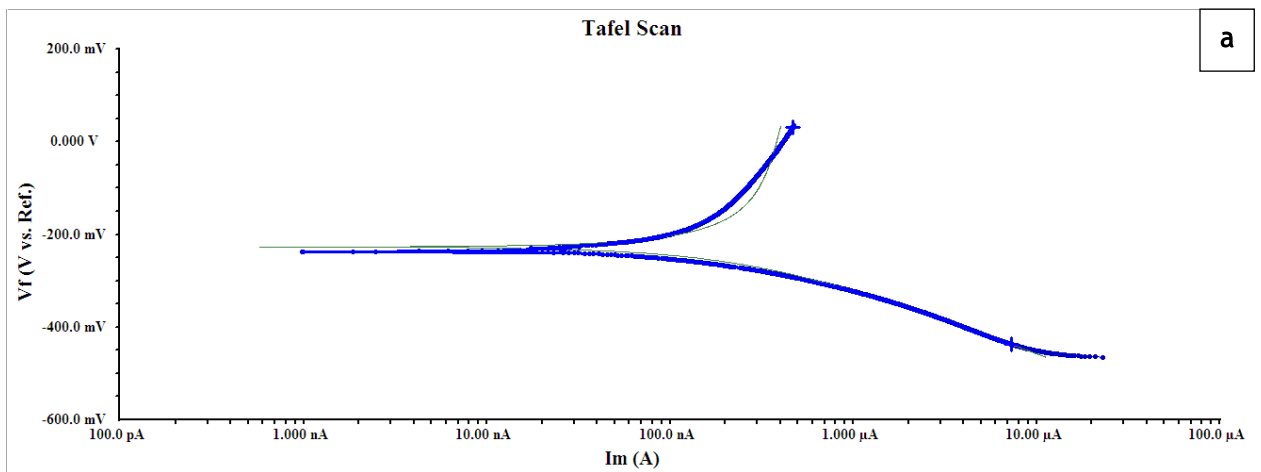


## 316 SS 0.1bar N₂
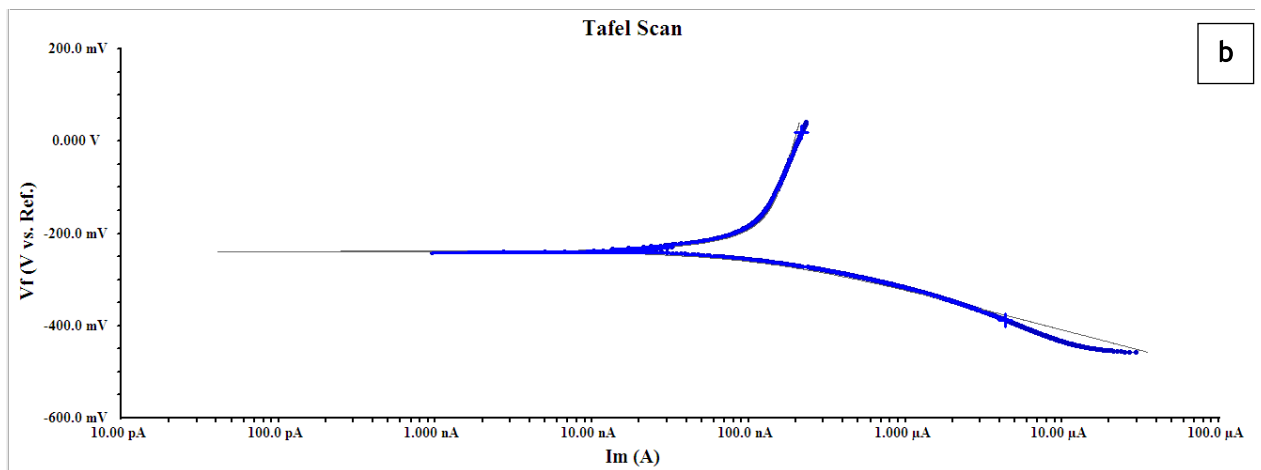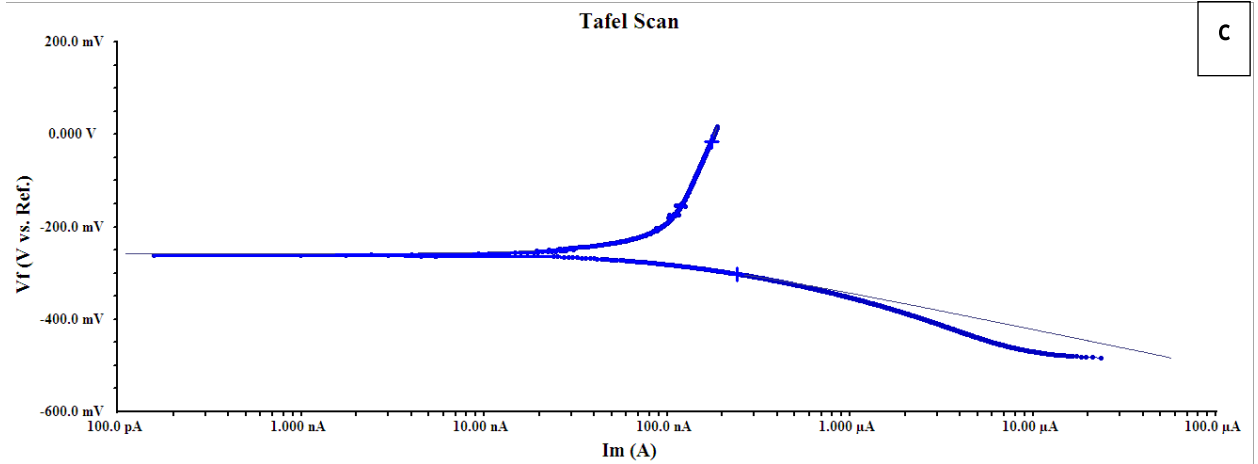
## 316 SS 0.3 bar N₂



**Figure 4.25: Tafel Scans of 316SS (a) Ar melted (b) 0.1 bar N₂ (c) 0.3 bar in NaHCO₃ electrolyte**

Polarization resistance

**Table 22: Ecorr, Icorr and Corrosion rates of30CrMnSiA Steelsamples in NaHCO₃ electrolyte**

| Sample 30CrMnSiA Steel | $E_{corr}$(mV) | $I_{corr}$(μA) | Polarization resistance(Rp) kohm | Corrosion rate (mpy) | Corrosion rate (μmpy) |
|---|---|---|---|---|---|
| Ar melted | -753.9 | 15.69 | 1.660 | 11.38 | 289.05 |
| 0.1 bar N₂ | -750.0 | 8.642 | 3.015 | 7.312 | 185.72 |
| 0.3 bar N₂ | -422.2 | 6.019 | 4.328 | 5.501 | 139.72 |

## 30CrMnSiA Ar melted



77
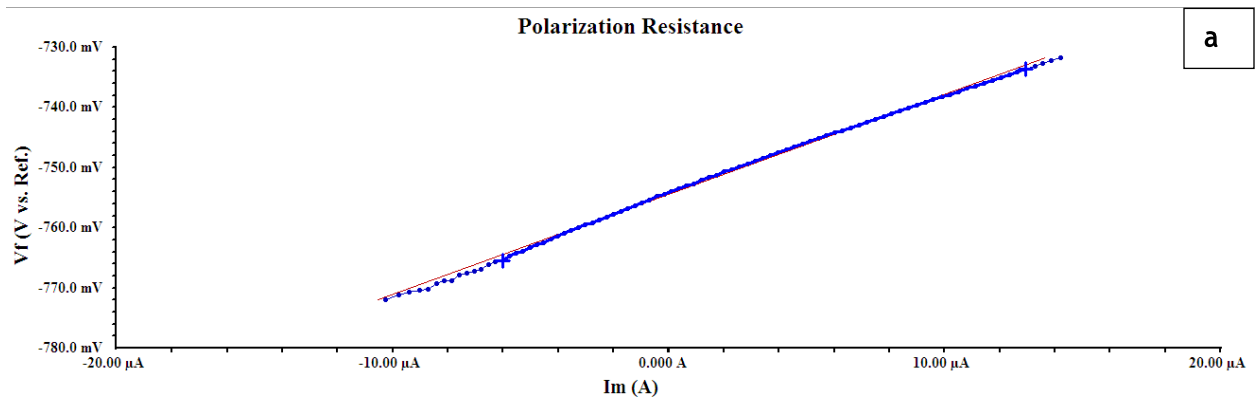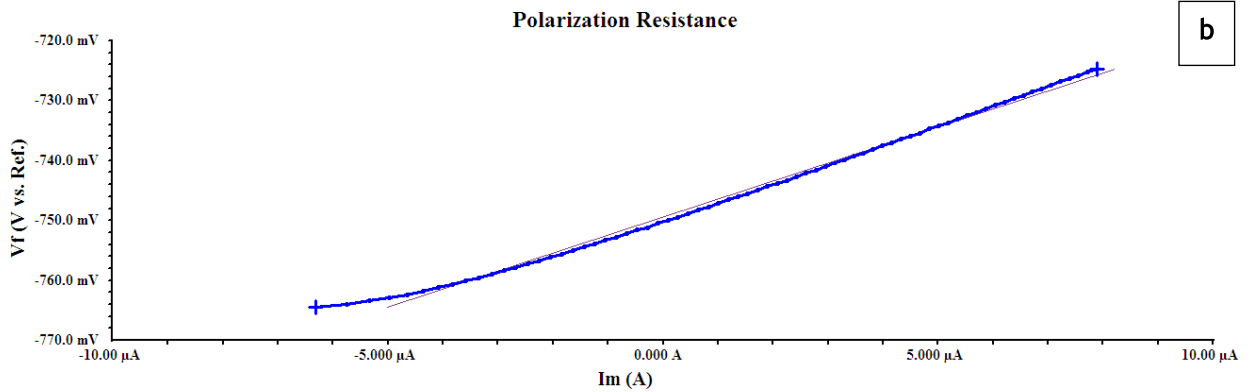
## 30CrMnSiA 0.1bar $N_2$
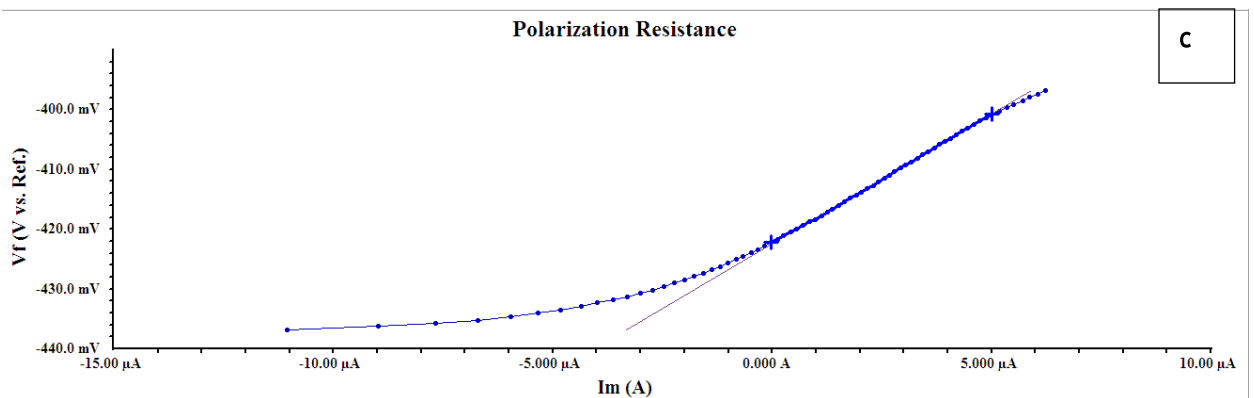


## 30CrMnSiA 0.3bar $N_2$



**Figure 4.26:Polarization resistance of30CrMnSiASteel (a) Ar melted (b) 0.1 bar $N_2$ (c) 0.3 bar $N_2$in NaHCO₃ electrolyte**

**Table 23: Ecorr, Icorr and Corrosion rates of316SS Steelsamples in NaHCO₃ electrolyte**

| Sample<br><br>316SS | $E_{corr}$(mV) | $I_{corr}$(nA) | Polarization resistance(Rp) kohm | Corrosion rate (mpy) | Corrosion rate (μmpy) |
|---|---|---|---|---|---|
| Ar melted | -230.4 | 162.0 | 160.8 | 0.105 | 2.667 |
| 0.1 bar $N_2$ | -249.1 | 118.8 | 219.2 | 0.075 | 1.905 |
| 0.3 bar $N_2$ | -221.0 | 82.92 | 314.2 | 0.057 | 1.447 |

## 316SS Ar melted
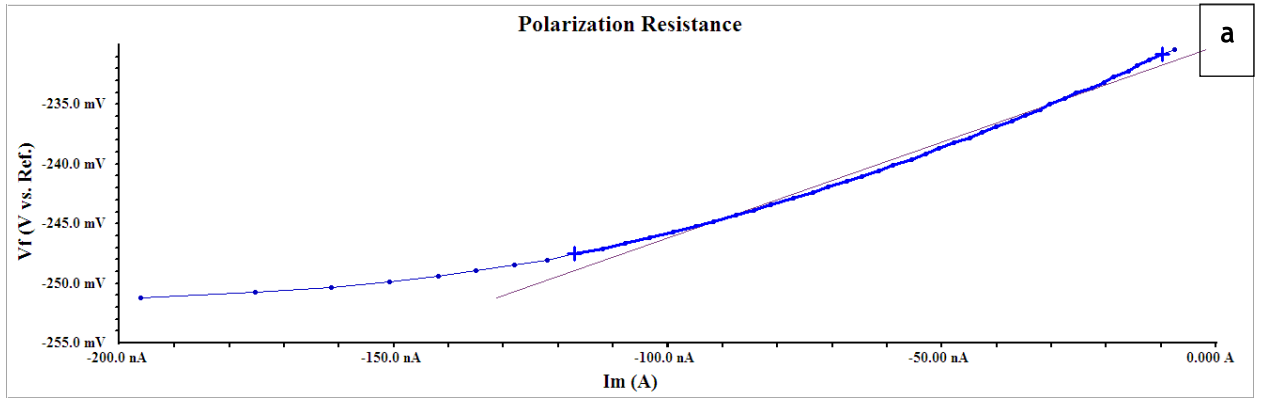


## 316SS 0.1 bar N$_2$
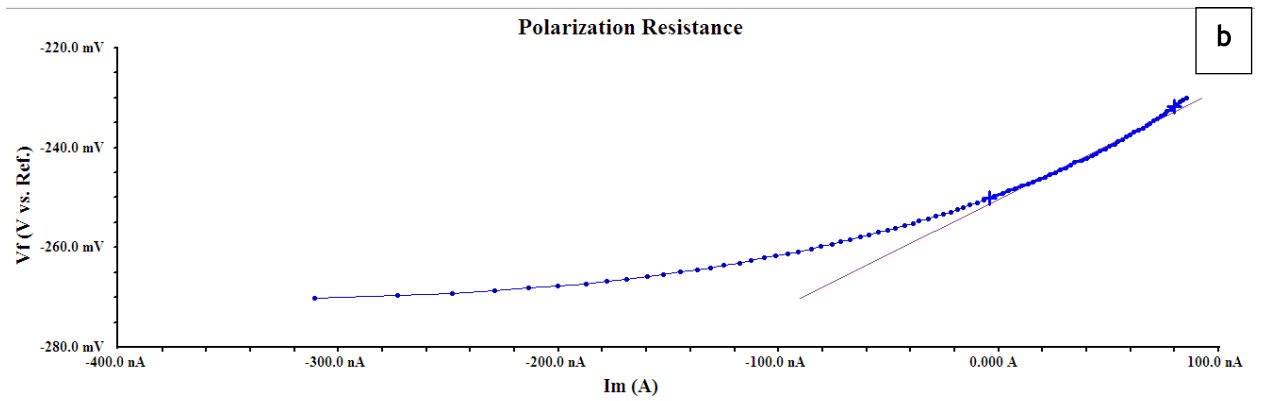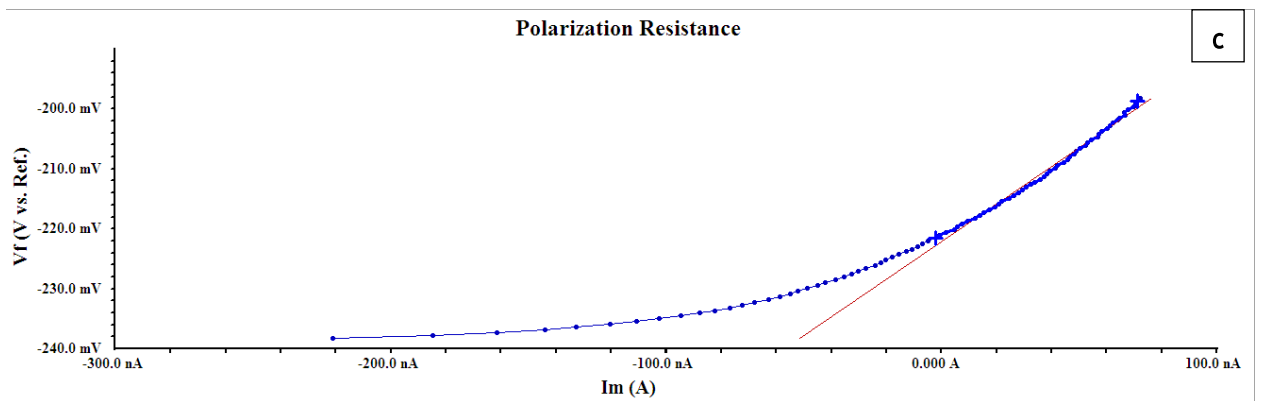


## 316SS 0.3 bar N$_2$



**Figure 4.27:Polarization resistance of316SS Steel (a) Ar melted (b) 0.1 bar N$_2$ (c) 0.3 bar N$_2$in NaHCO$_3$ electrolyte**

## 4.6 Conclusion

In this work, Arc melting of 30CrMnSiA and 316SS was performed in different condition such as melted in presence of Ar, 0.1bar $N_2$ pressure and 0.3bar$N_2$ pressure. Microstructural analysis, mechanical and corrosion resistance properties were examined. Summarized results of this study are as below:

1. Microstructural analysis showed that the addition of nitrogen results in grain boundaries alignment and a eutectic net was observed with high nitrogen content(0.3bar$N_2$) steel sample. Optical micrographs showed that with the increase of nitrogen content grain boundaries became more spherical and regular

2. EDX analysis confirmed the presence of nitrogen. No nitrogen was observed in the steel sample meted in the presence of Ar while 0.68 and4.37wt% nitrogen was confirmed for 30CrMnSiA steel for 0.1bar and 0.3bar $N_2$ respectively. And for 316SS nitrogen content ranges from 1.93 to 2.06 wt% $N_2$ respectively.

3. Average Vickers microhardness was increased to 514.86HV in the steel sample incorporated with maximum nitrogen (0.3bar) as compared to the untreated steel 244.10HV for 30CrMnSiA. For 316SS hardness ranges from 158.18HV to 345.76HV for untreated and 0.3bar$N_2$ respectively.

4. Based on the corrosion rate measurement it was observed that corrosion resistance property was greatly enhanced by the incorporation of nitrogen as compared to argon melted steel samples of 30CrMnSiA and 316SS in various acidic and basic media.

# References

| [1] | W. Adams and J. B. Dirlam, "Big steel, invention, and innovation," The Quarterly Journal of Economics, pp. 167-189, 1966. |
|---|---|
| [2] | R. Lula, J. Parr, and A. Hanson, "Stainless Steel, American Society for Metals," Metals Park, Ohio, 1986. |
| [3] | M. Venkatraman, K. Pavitra, V. Jana, and T. Kachwala, "Manufacturing and Critical Applications of Stainless Steel–An Overview," in Advanced Materials Research, 2013, pp. 163-173. |
| [4] | U. R. Evans, "Stress corrosion: its relation to other types of corrosion," Corrosion, vol. 7, pp. 238-244, 1951. |
| [5] | M. Eckert, "Max von Laue and the discovery of X‑ray diffraction in 1912," Annalen der Physik, vol. 524, pp. A83-A85, 2012. |
| [6] | J. R. Connolly, "Elementary crystallography for X-ray diffraction," EPS400-002, 2012. |
| [7] | M. Rasel Das, E. Ali, and S. B. A. Hamid, "CURRENT APPLICATIONS OF X-RAY POWDER," Rev. Adv. Mater. Sci, vol. 38, pp. 95-109, 2014. |
| [8] | H. Determann, E. Leitz, and F. Lepusch, The microscope and its applications: E. Leitz, 1982. |
| [9] | D. Stokes, Principles and Practice of Variable Pressure/Environmental Scanning Electron Microscopy (VPÂ?-ESEM): John Wiley & Sons, 2008. |
| [10] | J. I. Goldstein, D. E. Newbury, J. R. Michael, N. W. Ritchie, J. H. J. Scott, and D. C. Joy, Scanning electron microscopy and X-ray microanalysis: Springer, 2017. |
| [11] | A. J. Nozik, G. Conibeer, and M. C. Beard, Advanced concepts in photovoltaics: Royal Society of Chemistry, 2014. |
| [12] | R. L. Smith and G. Sandly, "An accurate method of determining the hardness of metals, with particular reference to those of a high degree of hardness," Proceedings of the Institution of Mechanical Engineers, vol. 102, pp. 623-641, 1922. |
| [13] | P. J. Blau, "Methods and Applications of Microindentation Hardness Testing," in Applied Metallography, ed: Springer, 1986, pp. 123-138. |
| [14] | R. Holland, "Corrosion testing by potentiodynamic polarization in various electrolytes," Dental Materials, vol. 8, pp. 241-245, 1992. |
| [15] | S. Munir, M. H. Pelletier, and W. R. Walsh, "Potentiodynamic corrosion testing," Journal of visualized experiments: JoVE, 2016. |
| [16] | E. McCafferty, "Validation of corrosion rates measured by the Tafel extrapolation method," Corrosion science, vol. 47, pp. 3202-3215, 2005. |
| [17] | R. Dahm and R. Latham, "The potentiostat and its applications," Transactions of the IMF, vol. 71, pp. 77-79, 1993. |
| [18] | C. Örnhagen, J. O. Nilsson, and H. Vannevik, "Characterization of a nitrogen‑rich austenitic stainless steel used for osteosynthesis devices," Journal of Biomedical Materials Research: An Official Journal of The Society for Biomaterials and The Japanese Society for Biomaterials, vol. 31, pp. 97-103, 1996. |
| [19] | Y. S. Lim, J. S. Kim, S. J. Ahn, H. S. Kwon, and Y. Katada, "The influences of microstructure and nitrogen alloying on pitting corrosion of type 316L and 20 wt.% Mn-substituted type 316L stainless steels," Corrosion Science, vol. 43, pp. 53-68, 2001. |

| [20] | P. Levey and A. Van Bennekom, "A mechanistic study of the effects of nitrogen on the corrosion properties of stainless steels," Corrosion, vol. 51, pp. 911-921, 1995. |
|------|---|
| [21] | J. Rawers and M. Grujicic, "Effects of metal composition and temperature on the yield strength of nitrogen strengthened stainless steels," Materials Science and Engineering-A-Structural Materials, vol. 207, pp. 188-194, 1996. |
| [22] | A. Conde, I. García, and J. De Damborenea, "Pitting corrosion of 304 stainless steel after laser surface melting in argon and nitrogen atmospheres," Corrosion Science, vol. 43, pp. 817-828, 2001. |
| [23] | G. Balachandran, B. NB, and P. K. Rao, "Processing nickel free high nitrogen austenitic stainless steels through conventional electroslag remelting process," ISIJ international, vol. 40, pp. 478-483, 2000. |
| [24] | Y.-S. Song, J.-H. Lee, K.-H. Lee, and D. Y. Lee, "Corrosion properties of N-doped austenitic stainless steel films prepared by IBAD," Surface and Coatings Technology, vol. 195, pp. 227-233, 2005. |
| [25] | Y. Sun, "Enhancement in corrosion resistance of austenitic stainless steels by surface alloying with nitrogen and carbon," Materials Letters, vol. 59, pp. 3410-3413, 2005. |
| [26] | Y. Qiao, Y. Zheng, W. Ke, and P. Okafor, "Electrochemical behaviour of high nitrogen stainless steel in acidic solutions," Corrosion Science, vol. 51, pp. 979-986, 2009. |
| [27] | H. Li, Z. Jiang, H. Feng, S. Zhang, L. Li, P. Han, et al., "Microstructure, mechanical and corrosion properties of friction stir welded high nitrogen nickel-free austenitic stainless steel," Materials & Design, vol. 84, pp. 291-299, 2015. |
| [28] | H.-f. Xu, F. Yu, C. Wang, W.-l. Zhang, J. Li, and W.-q. Cao, "Comparison of microstructure and property of high chromium bearing steel with and without nitrogen addition," Journal of Iron and Steel Research, International, vol. 24, pp. 206-213, 2017. |
| [29] | F. Alresheedi and J. Krzanowski, "Structure and morphology of stainless steel coatings sputter-deposited in a nitrogen/argon atmosphere," Surface and Coatings Technology, vol. 314, pp. 105-112, 2017. |
| [30] | J. Y. Park, S.-J. Park, J.-Y. Kang, C.-H. Lee, H.-Y. Ha, J. Moon, et al., "Fatigue behaviors of high nitrogen stainless steels with different deformation modes," Materials Science and Engineering: A, vol. 682, pp. 622-628, 2017. |
| [31] | J. Simmons, "Overview: high-nitrogen alloying of stainless steels," Materials Science and Engineering: A, vol. 207, pp. 159-169, 1996. |
| [32] | J. Park, D.-J. Kim, Y.-K. Kim, K.-H. Lee, K.-H. Lee, H. Lee, et al., "Improvement of the biocompatibility and mechanical properties of surgical tools with TiN coating by PACVD," Thin Solid Films, vol. 435, pp. 102-107, 2003. |
| [33] | A. Schulz, V. Uhlenwinkel, C. Bertrand, R. Kohlmann, A. Kulmburg, A. Oldewurtel, et al., "Nitrogen pick-up during spray forming of high-alloyed steels and its influence on microstructure and properties of the final products," Materials Science and Engineering: A, vol. 383, pp. 58-68, 2004. |
| [34] | C. Duan, C. Chen, J. Zhang, Y. Shen, and X. Feng, "Nitriding of Fe–18Cr–8Mn stainless steel powders by mechanical alloying method with dual nitrogen source," Powder Technology, vol. 294, pp. 330-337, 2016. |
| [35] | A. Schulz, V. Uhlenwinkel, C. Bertrand, R. Kohlmann, A. Kulmburg, A. Oldewurtel, et al., "Nitrogen pick-up during spray forming of high-alloyed steels and its influence |

| | on microstructure and properties of the final products," Materials Science and Engineering: A, vol. 383, pp. 58-68, 2004. |
|---|---|
| [36] | V. Valasamudram, S. Selvamani, M. Vigneshwar, V. Balasubramanian, and D. Jayaperumal, "Tensile, Impact, Wear and Corrosion Behavior on Conventionally Melted Nitrogen Alloyed Martensitic Stainless Steel in hot forged, hardened and tempered conditions," Materials Today: Proceedings, vol. 5, pp. 8338-8347, 2018. |
| [37] | J. Simmons, "Overview: high-nitrogen alloying of stainless steels," Materials Science and Engineering: A, vol. 207, pp. 159-169, 1996. |
| [38] | J. Park, D.-J. Kim, Y.-K. Kim, K.-H. Lee, K.-H. Lee, H. Lee, et al., "Improvement of the biocompatibility and mechanical properties of surgical tools with TiN coating by PACVD," Thin Solid Films, vol. 435, pp. 102-107, 2003. |
| [39] | J.-Y. Li, Y.-L. Chen, and J.-H. Huo, "Mechanism of improvement on strength and toughness of H13 die steel by nitrogen," Materials Science and Engineering: A, vol. 640, pp. 16-23, 2015. |
| [40] | L. Valentini, A. Di Schino, J. Kenny, Y. Gerbig, and H. Haefke, "Influence of grain size and film composition on wear resistance of ultra fine grained AISI 304 stainless steel coated with amorphous carbon films," Wear, vol. 253, pp. 458-464, 2002. |
| [41] | R. Presser and J. Silcock, "Aging behaviour of 18Mn–18Cr high nitrogen austenitic steel for end rings," Metal science, vol. 17, pp. 241-248, 1983. |
| [42] | G. Stein, J. Menzel, and M. Wagner, "N-Alloyed steels for retaining rings and other applications," in Proc. 2nd Int. Conf. on High Nitrogen Steels, 1990, p. 399. |
| [43] | H.-f. Xu, F. Yu, C. Wang, W.-l. Zhang, J. Li, and W.-q. Cao, "Comparison of microstructure and property of high chromium bearing steel with and without nitrogen addition," Journal of Iron and Steel Research, International, vol. 24, pp. 206-213, 2017. |
| [44] | I. KAMACHI MUDALI and S. Ningshen, "Unified mechanism for localised corrosion behaviour of nitrogen-alloyed steels and stainless steels," Transactions of the Indian Institute of Metals, vol. 55, pp. 461-472, 2002. |
| [45] | U. K. Mudali and B. Raj, High nitrogen steels and stainless steels: manufacturing, properties and applications: Alpha Science International, 2004. |
| [46] | X. Changsheng, S. Peizhen, and Z. Jansheng, "An approach to developing a hot-work die steel for high-temperature application," Materials Science and Engineering: A, vol. 124, pp. 203-209, 1990. |
| [47] | I. KAMACHI MUDALI and S. Ningshen, "Unified mechanism for localised corrosion behaviour of nitrogen-alloyed steels and stainless steels," Transactions of the Indian Institute of Metals, vol. 55, pp. 461-472, 2002. |
| [48] | S. Ningshen, U. K. Mudali, V. Mittal, and H. Khatak, "Semiconducting and passive film properties of nitrogen-containing type 316LN stainless steels," Corrosion science, vol. 49, pp. 481-496, 2007. |
| [49] | C.-O. Olsson and D. Landolt, "Passive films on stainless steels—chemistry, structure and growth," Electrochimica acta, vol. 48, pp. 1093-1104, 2003. |
| [50] | M. Metikoš-Huković, R. Babić, Z. Grubač, Ž. Petrović, and N. Lajçi, "High corrosion resistance of austenitic stainless steel alloyed with nitrogen in an acid solution," Corrosion science, vol. 53, pp. 2176-2183, 2011. |
| [51] | M. Pujar, U. K. Mudali, and S. S. Singh, "Electrochemical noise studies of the effect of nitrogen on pitting corrosion resistance of high nitrogen austenitic stainless steels," |

| | Corrosion Science, vol. 53, pp. 4178-4186, 2011. |
|---|---|
| [52] | P. Behjati, A. Kermanpur, and A. Najafizadeh, "Influence of nitrogen alloying on properties of Fe318Cr312Mn3XN austenitic stainless steels," Materials Science and Engineering: A, vol. 588, pp. 43-48, 2013. |
| [53] | U. K. Mudali and B. Raj, High nitrogen steels and stainless steels: manufacturing, properties and applications: Alpha Science International, 2004. |
| [54] | H. C. B. Hansen, C. B. Koch, H. Nancke-Krogh, O. K. Borggaard, and J. Sørensen, "Abiotic nitrate reduction to ammonium: key role of green rust," Environmental Science & Technology, vol. 30, pp. 2053-2056, 1996. |
| [55] | S.-L. Chou, M.-J. Tsai, W.-T. Tsai, and J.-T. Lee, "Effect of nitrogen on the electrochemical behavior of 301LN stainless steel in H2SO4 solutions," Materials chemistry and physics, vol. 51, pp. 97-101, 1997. |
| [56] | C. C. Huang, W. T. Tsai, and J. T. Lee, "Laser Cladded High Chromium‐Nitrogen Alloys on Carbon Steel," Journal of the Electrochemical Society, vol. 142, pp. 1221-1225, 1995. |
| [57] | F. F. Eliyan and A. Alfantazi, "Mechanisms of corrosion and electrochemical significance of metallurgy and environment with corrosion of iron and steel in bicarbonate and carbonate solutions—A review," Corrosion, vol. 70, pp. 880-898, 2014. |